SPECTRA-STRUCTURE CORRELATION IN CERTAIN MONOSUBSTITUTED BENZENES

A Thesis Submitted
In Partial Fulfilment of the Requirements
for the Degree of
DOCTOR OF PHILOSOPHY

BY
VISHNU NARAIN

to the

DEPARTMENT OF PHYSICS
INDIAN INSTITUTE OF TECHNOLOGY KANPUR
DECEMBER 1970

CERTIFICATE

This is to certify that the work presented in this thesis has been carried out by Shri Vishnu Narain under my supervision and has not been submitted elsewhere for a degree.

H.D. Bist

(H.D. Bist)
Department of Physics
Indian Institute of Technology
Kanpur, India

ACKNOWLEDGEMENTS

I wish to express my deep sense of gratitude to Dr. H.D. Bist for his inspiring guidance and many valuable suggestions during the course of these investigations.

I am grateful to Professor P. Venkateswarlu for giving me the initial impetus and encouragement to carry out research and to Professor J. Mahanty for his benevolence throughout the course of this work.

I am thankful to Professor D.P. Khandelwal and Dr. S.D. Pandey for useful discussions and valuable suggestions.

It gives me great pleasure to acknowledge the cooperation and help from Drs. G.C. Upreti, K. Kumar, K.V. Subbaram, V.S. Tomar, Shri Y.S. Jain and M.M. Rai.

The facilities provided by Professor J.C.D. Brand and the Director, Indian Institute of Technology Delhi, for recording some of the spectra are gratefully acknowledged.

Thanks are due to Shri S.L. Rathore for typing the thesis and to Shri Lallu Singh for cyclostyling the same.

VISHNU NARAIN

CONTENTS

SYNOPSIS

Inspite of the availability of commercial far infrared spectrophotometers, accurate vibrational data for large molecules in gaseous phase are not always available due primarily to difficult experimental techniques required for such work. Consequently, the earlier assignments of low frequency vibrations of monosubstituted benzenes are ambiguous. Low temperature infrared studies in crystalline state are also not available in the complete range for correlation purposes.

In the present work infrared and Raman spectral studies of chlorobenzene (PhCl), benzaldehyde (BzH), phenol (PhOH) and two deuterated species of phenol have been made with special emphasis on infrared vapour phase band contours. Solid phase infrared spectra of PhCl, BzH and PhOH have also been studied at liquid nitrogen temperature. Accurate vapour phase vibrational data have been correlated with the available electronic emission and absorption studies. Earlier vibrational data for these molecules have been reexamined and suitable modifications are suggested on the basis of present more precise data. The thesis consists of six chapters. Related figures, tables, references and appendices have been inserted at the end of each chapter.

Various aspects of infrared and Raman spectroscopy which are of relevance to the present investigations have been briefly reviewed in Chapter I.

Chapter II contains details of the experimental set up and techniques used. This includes the descriptions of (i) the modified low temperature cell fabricated for these

experiments, and (ii) the vacuum line specially designed for the study of samples in vapour and solid phases.

The infrared data in all phases and the Raman data in the liquid phase for PhCl, BzH and PhOH have been reported in Chapters III, IV and V respectively. The assignments for PhCl and BzH have been mainly suggested on the basis of vapour phase infrared band contours and the Raman polarization data. In case of PhCl these have been further confirmed by electronic spectral data. The vapour phase forbidden transitions of PhCl, BzH and PhOH have been obtained from the solid phase spectra. The observed changes in peak positions, intensities and half band widths of infrared bands on going from vapour to liquid and then to solid phase at liquid nitrogen temperature have been discussed, as also the splittings observed for the first time in the solid phase at low temperature. Hydrogen bonding effects have been looked into carefully in the different phases of phenol.

In PhCl the isotopic splitting due to the presence of ^{35}Cl and ^{37}Cl which should occur invariably in all the X-sensitive modes has been detected for the first time. The suggested presence of dimers in vapour phase PhCl and the occurrence of Fermi doublets in the regions 1400-1600 cm^{-1} and 1000-1100 cm^{-1} have been closely examined and found to be untenable.

In BzH the unperturbed positions of the vibrational levels of the aldehydic CH stretch and overtone of CHO valence angle deformation have been calculated from the observed Fermi doublet in that region. The infrared vapour phase vibrational data have been found to support the

triplet-singlet hypothesis proposed earlier to explain the anomalies in absorption and fluorescence spectra of BzH.

From the observed overtones the anharmonicities associated with the fundamental bands have been calculated for all the molecules. The bands observed in the infrared spectra of condensed phases of phenol in the range 2000-3000 cm^{-1} have been assigned to the binary combinations of OH deformation mode with the internal vibrations of the phenoxy-ring.

All the related results reported in Chapters III, IV and V have been compared and discussed further at the end of Chapter V.

Thermodynamic properties like specific heat at constant pressure, enthalpy, Gibbs energy, entropy, enthalpy of formation, Gibbs energy of formation and logarithm of the standard equilibrium constant of PhCl, BzH and PhOH have been calculated using vapour phase spectroscopic data and applying isotopic and gas imperfection corrections. These values are given at the end of corresponding chapters and compared with the earlier data wherever available.

In Chapter VI the special features of the vapour phase infrared band contours such as the PR separation and the relative intensity of Q branch with respect to that of the whole band have been calculated and compared with the observed values in PhCl, BzH, PhOH and two of its deuterated species (C_6H_5OD and C_6D_5OH). In most of the cases the agreement is good. The empirical relation for calculating PR separation of hybrid bands has been modified and the general applicability of the infrared band contour method for deducing the molecular parameters is critically examined.

CHAPTER I

INTRODUCTION

A. GENERAL

The commercial production of high resolution automatic recording infrared spectrophotometers has within last two decades rendered infrared method as one of the most popular ones in the determination of the structure of organic compounds. The recent developments in the automatic recording Raman spectrophotometers, particularly those fitted with laser sources have made Raman spectroscopy an equally important tool, especially in molecules of high symmetry where the information obtained is complimentary to that of the infrared method. Some salient aspects of these methods which are relevant to the present study have been concisely reviewed in the following sections.

B. TOTAL ENERGY

The total energy T (in cm^{-1}) of a molecule, neglecting the nuclear spin and magnetic interactions and taking Born-Oppenheimer approximation, can be expressed as:

$$T = T_e + G + F \qquad (1.1)$$

In this expression T_e, G, and F have been used to denote the term values of the pure electronic, vibrational and rotational contributions, respectively; and the translational contribution to the total energy is neglected.

C. ROTATIONAL CONTRIBUTION

In accordance with Mulliken convention (2) I_A, I_B and I_C are used to represent the three principal moments of inertia of a molecule with $I_A \leq I_B \leq I_C$; and A, B and C are used to denote the corresponding rotational constants, where $A=h/(8\pi^2 I_A c)$ cm^{-1}, etc. Depending on relative magnitudes of A,B,& C all molecules are classified into four general categories, with rotational energy structure as given below:

Linear and Spherical Top Molecules: For linear ($A_v=0$, $B_v=C_v$) and for spherical top ($A_v=B_v=C_v$) molecules the term value can be given by:

$$F_v(J) = B_v J (J+1) - D_v J^2 (J+1)^2 \qquad (1.2)$$

with usual notations (3-4).

Symmetric Top Molecules: For a rigid prolate symmetric top molecule ($A_v < B_v = C_v$), the term value is given by

$$F_v(J,K) = B_v J (J+1) + (A_v-B_v) K^2 \qquad (1.3)$$

The quantum number K represents the component of the total angular momentum J about the figure axis of the molecule (4). For an oblate symmetric top molecule ($A_v = B_v < C_v$), the term value is:

$$F_v(J,K) = B_v J (J+1) + (C_v-B_v) K^2 \qquad (1.4)$$

Asymmetric Top Molecules: The rotational energy pattern of asymmetric top molecules is complicated and has been discussed in Chapter VI.

D. VIBRATIONAL CONTRIBUTION

Normal Modes: In a non-linear polyatomic molecule having N atoms there occur 3N-6 normal modes of vibration (3N-5 for a linear molecule). In a given mode, to a first approximation, all the nuclei move in phase and execute simple harmonic motions with a common frequency about their equilibrium positions. Thus each normal vibration may be considered by taking a normal coordinate Q which in fact is a mass weighted cartesian displacement coordinate and simplifies the expressions for the kinetic and potential energies (5).

A very general expression for potential energy, U_Q measured from the bottom of the potential well may be written as a series expansion (about Q = 0) as:

$$U_Q = \frac{1}{2!}\left(\frac{d^2U}{dQ^2}\right)_{Q=0} Q^2 + \frac{1}{3!}\left(\frac{d^3U}{dQ^3}\right)_{Q=0} Q^3 + \ldots \qquad (1.5)$$

The quadratic term which is predominant for small oscillations, gives the usual harmonic oscillator energy levels. However, when the whole expression is used to deduce the energy levels, the additional terms appear in the energy expression. Thus:

$$G(v) = w_e(v+\tfrac{1}{2}) - w_e x_e (v+\tfrac{1}{2})^2 + w_e y_e (v+\tfrac{1}{2})^3 + \ldots \qquad (1.6)$$

where w_e is the harmonic oscillator frequency and $w_e x_e$ and $w_e y_e$ are the anharmonicity constants. However, $w_e y_e << w_e x_e << w_e$.

The Electrical Anharmonicity: In general the instantaneous dipole moment 'M_Q' for an oscillating molecule may be expressed by a Maclaurin series about $Q = 0$ as:

$$M_Q = (M)_{Q=0} + \left(\frac{dM}{dQ}\right)_{Q=0} Q + \frac{1}{2!}\left(\frac{d^2M}{dQ^2}\right)_{Q=0} Q^2 + \ldots \qquad (1.7)$$

The first term in the expansion gives the permanent dipole moment which is responsible only for the pure rotational infrared spectrum; the second term is responsible for the appearance of vibrational infrared spectrum, while the quadratic and higher terms are effective in providing intensity to overtones and combination bands.

Evaluation of Anharmonicity Constants: From the expression (1.6) we can calculate the separation of two successive vibrational levels:

$$\begin{aligned} \Delta G_{(v+\frac{1}{2})} &= G(v+1) - G(v) \\ &= w_e - 2w_e x_e - 2w_e x_e v \end{aligned} \qquad (1.8)$$

Likewise the second difference is:

$$\begin{aligned} \Delta G_{(v+1)} &= \Delta G_{(v+3/2)} - \Delta G_{(v+\frac{1}{2})} \\ &= -2w_e x_e \end{aligned} \qquad (1.9)$$

However, often we have situations where only the fundamental and the first overtone are available. In such cases the procedure

is to express the vibrational term value in terms of the lowest level (v = 0) as zero, i.e.:

$$G_o(v) = w_o v - w_o x_o v^2 \qquad (1.10)$$

Hence

$$G_o(1) = w_o - w_o x_o \qquad (1.11)$$

and

$$G_o(2) = 2w_o - 4w_o x_o \qquad (1.12)$$

Here $G_o(1)$ and $G_o(2)$ are the actual observed fundamental and the first overtone respectively. From these both w_o and $w_o x_o$ can be obtained.

Combination Bands: Some overtones and combination bands may occur both in the infrared and Raman spectrum. The vibrational bands for which the total change in the vibrational quantum number is 2 or 3 are called binary or ternary combinations, respectively. Binary combinations can occur by the quantum number v changing by two units or by two different ones v_i and v_k changing by one unit each. The occurrence of ternary combinations can be explained in a similar way.

The selection rules for the combination bands can be evaluated from the character table of the point group of the molecule. The direct product of the characters of the species to which the vibrations w_i and w_k belong is found and the product thus obtained represents the species of the combination $w_i + w_k$.

Symmetry Species of a Vibration: If a molecule has a number of symmetry elements the normal vibrations are classified into

various species (5) according to the number and the kind of symmetry elements preserved during a vibration. Using group theory the distribution of the vibrations into different species of a point group, for all the known point groups, has been discussed by Herzberg (6) in detail. Knowing the point group and its character table the activity of the vibrations belonging to different species are directly known; e.g., for molecules belonging to C_{2v} point group the vibrations of A_2 species are forbidden in their vapour phase infrared spectra.

E. ABSORPTION INTENSITY

The intrinsic absorption corresponding to a transition from the ground state m to an excited state n may be expressed in terms of transition probability coefficient B_{mn} by the expression

$$\Delta I = - hc w_{mn} B_{mn} \ell_{mn} N_m \Delta x \qquad (1.13)$$

where $c \ell_{mn} = I$ gives the intensity of the incident beam, ΔI is the amount absorbed in traversing a layer of thickness Δx, N_m is the number of molecules per unit volume in state m, and population N_n is considered negligibly small.

The Einstein coefficient B_{mn} is related with the matrix element R_{mn} of the electric moment M_Q between the states m and n. We have:

$$R_{mn} \equiv \int \psi_n^* M_Q \psi_m \, d\tau \qquad (1.14)$$

and then B_{mn} is given (3) by:

$$B_{mn} = \frac{8 \pi^3}{3ch^2} \left| R_{mn} \right|^2 \qquad (1.15)$$

The matrix element R_{mn} is also called the transition moment between the given states m and n. For an allowed transition R_{mn} is non-zero.

Formula (1.14) may be used to determine the interaction of electromagnetic wave with (a) electric dipole moment, (b) magnetic dipole moment, (c) quadrupole or higher moments, (d) induced dipole moments (in case of Raman scattering), etc. by substituting the appropriate moment in place of M_Q. In particular R_{mn} turns out to be zero for all cases where the product of the two wave functions involved does not have the symmetry of one of the components of M_Q.

When M_Q, given by equation (1.7), is substituted in (1.14) the integral corresponding to the permanent dipole moment $(M)_{Q=0}$ becomes zero in view of orthogonality of ψ functions, and R_{mn} comes out to be

$$R_{mn} = \frac{1}{\sqrt{2\alpha}} \left(\frac{dM}{dQ}\right)_{Q=0} \tag{1.16}$$

with the well known relations:

$$\alpha = \frac{2\pi (\mu k)^{\frac{1}{2}}}{h} \tag{1.17}$$

and

$$\frac{1}{2\pi c} \left(\frac{k}{\mu}\right)^{\frac{1}{2}} = w_{mn} \tag{1.18}$$

The extinction coefficient A' is given by

$$A' \equiv -\frac{1}{\Delta x} \frac{\Delta I}{I} = h w_{mn} B_{mn} N_m \tag{1.19}$$

and using relations (1.13), & (1.15) to (1.18) one gets:

$$A' = \frac{\pi N}{3c^2\mu}\left(\frac{dM}{dQ}\right)^2 \qquad (1.20)$$

where N_m is put equal to N as a close approximation.

Relation with Experimental Measurements: In actual experiments if L cm path of a solution containing C gm-moles of absorbing sample per litre transmits intensity I out of incident intensity I_o, we have

$$A' = \frac{1}{L}\log_e \frac{I_o}{I} \quad \text{and} \quad N = \frac{CN_o}{1000} \qquad (1.21)$$

where N_o is Avogadro's number. Substitution in (1.20) gives the molar extinction coefficient

$$A' \equiv \frac{1}{LC}\log_e \frac{I_o}{I} = \frac{\pi}{3c^2\mu}\,\frac{N_o}{1000}\left(\frac{dM}{dQ}\right)^2 \qquad (1.22)$$

Actually the transition $m \rightarrow n$ is not a sharp transition. Apart from the natural width in gases the absorption band spreads due to Doppler and pressure broadening. In liquids various other physicochemical effects make the bands very broad. Added to these is the effect of finite slit width of the spectrophotometer. Hence in using relation (1.22) to deduce (dM/dQ) one must obtain integrated absorption coefficient $\bar{A}$ over the complete band corresponding to the given transition $m \rightarrow n$. If A_ν is the molecular extinction coefficient of frequency ν in an absorption band, we define $\bar{A}$ by:

$$\bar{A} = \int_{\text{entire band}} A_\nu \, d\nu \qquad (1.23)$$

Experimentally a graph between A_ν against ν is plotted. Subsequently either the squares on the graph paper are counted or the paper profile is weighed or the band areas are evaluated by using a planimeter to obtain the quantity $\bar{A}$.

F. SPECTRA IN DIFFERENT STATES

Vapour State: In the vapour phase spectra of simple light molecules the individual rotational lines can be identified in a rotation-vibration band. If the vapour pressure is small at ambient temperature better structure is obtained because of low pressure-broadening, but the path lengths have to be large. Often to overcome instrumental limitations pressure broadening is induced by introducing a non-absorbing gas. This smears out the detailed structure, but the integrated intensity is not altered. On the other hand if the pressure of the absorbing gas itself is increased smaller path length may be used, but the structure will again be smeared out, until at large enough pressures when gas density approaches that of the liquid state, the rotational structure coalesces to give a broad band with a pronounced maximum at the band centre.

In the heavier polyatomic molecules, even at low pressures, only band contours with P,Q and R branch maxima are obtained, that too in favourable cases only (cf. chapter VI).

Liquid State: In the liquid state the molecules in general do not exhibit quantized free rotations. Consequently, the vibrational Raman and infrared bands do not show any rotational fine structure. In fact, in pure liquids and solutions the vibrational

bands possess a comparatively simple form, usually consisting of a single maximum at the appropriate vibrational frequency. The shape of the curve may be approximated by a Lorentzian curve of the form

$$P = \frac{a}{(\nu - \nu_o)^2 + b^2} \qquad (1.24)$$

where P is the value of absorbance of frequency ν (section E) having its maximum value P_o equal to a/b^2 at the band centre ($\nu = \nu_o$); 'a' and 'b' are constants. The band half-width, defined as the full width of the absorption band at half the maximum absorbance value is given by

$$\Delta\nu = 2b \qquad (1.25)$$

The above formulae hold if the instrumental inadequacies are ignored. In practice the bands in the liquid state have half-width in the range of 5 to 10 cm^{-1}.

In the condensed state some new bands which are not present in the vapour state may appear either due to the formation of new species (e.g. polymers or associated complexes) or due to resulting change of symmetry which allows the vapour phase infrared or Raman inactive vibrations.

Solid State: In the solid phase, due to absence of rotations and homogeneity of environment the vibrational bands may be quite narrow. Some changes may also occur in the band positions and their relative intensities with respect to vapour phase

values. The magnitude of frequency changes are small, usually not above 5.0 percent except in cases where hydrogen bonding is involved. It is noteworthy that different vibrations of a particular molecule may show very different relative shifts, which may be with opposite sign.

In crystalline state another important phenomenon is the splitting in the bands. The splittings may be classified as: (a) the site symmetry splitting and (b) the factor-group splitting. The former type of splitting occurs simply because in several cases the site symmetry in the crystal may be lower than the molecular symmetry and the selection rules are altered to suit the crystal symmetry. Consequently, these equilibrium crystal field effects may result in the appearance of frequencies which are unexpected for free molecules. Further, the degenerate vibrations may also show splitting due to site-symmetry effects. However, if a crystal contains 'n' molecules per unit cell, each non-degenerate vibration of the molecules may split into 'n' components due to the possible resonance-interaction; and the phenomena is commonly known as factor - group or exciton splitting (8-10). If the splittings are small, only broadening of bands near peak positions will be observed.

In addition to the above two types of splittings, some new bands may occur due to lattice vibrations. Combination of lattice vibrations with the fundamental internal modes of a molecule may lead to some additional bands in their vibrational finger print region.

Phase transformations resulting due to change of temperature in solid state may create additional complexities in the vibrational spectra. However, in molecules exhibiting rotational isomerism in free state the solid phase spectra are sometimes simpler than the gas phase spectra if out of the several possible conformations one isomer gets stabilized at low temperature.

G. RAMAN EFFECT

Induced Dipole Moment: For a Raman active mode corresponding to a normal coordinate Q_k, there must occur a change in the 'induced' dipole moment M' resulting from a change in the polarizability tensor α during vibration in an electric field $\underline{E}$. In accordance with the rules for the matrix multiplication, one may write:

$$M' = \alpha \cdot \underline{E} \tag{1.26}$$

Expansion of Polarizability: For molecules executing small vibrations, a component α_i of the polarizability may be expanded in terms of the normal coordinates:

$$\alpha_i = \alpha_i^o + \sum_{k=1}^{3N-6} \left(\frac{\partial \alpha_i}{\partial Q_k}\right)_o \cdot Q_k + \text{higher terms} \tag{1.27}$$

where α_i^o is the equilibrium polarizability and determines the Rayleigh intensities, whereas $\left(\frac{\partial \alpha_i}{\partial Q_k}\right)_o$ determines the Raman intensities of fundamental bands. The higher terms account for the appearance of the overtone and combination bands.

Intensities of Raman Shifts: The intensity of a fundamental Raman band (11) is given by

$$I_{rn} = \text{const.} \frac{N(\nu_o - \nu_{rn})^4 (45\alpha'^2 + 13\beta'^2)}{1 - \exp(-h\nu_{rn}/kT)} \frac{h}{8\pi^2\nu_{rn}} \qquad (1.28)$$

where N is the number of molecules in the initial energy state n, α' represents the average of the derivatives of the three principal polarizabilities and β' is the magnitude of the derivative of anisotropy part of the polarizability of the molecule. The constants 45 and 13 arise in the averaging over all configurations in the experimental arrangement when the scattered light is observed per unit solid angle at right angles to the incident direction; and r denotes higher energy state.

Polarization of Raman Lines: The degree of polarization depends on the anisotropic character of the molecules. Experimentally it has been established that normally the polarized Raman lines are sharp and intense, whereas depolarized lines are diffuse and of weak intensity.

The state of polarization of the Raman lines is studied by measuring the depolarization ratio D which is defined as:

$$D = \frac{6\beta'^2}{45\alpha'^2 + 7\beta'^2} \qquad (1.29)$$

and for the polarized incident radiation the depolarization ratio, D'_p is given by:

$$D'_p = \frac{3\beta'^2}{45\alpha'^2 + 4\beta'^2} \qquad (1.30)$$

For totally asymmetric vibration $\alpha' = 0$, the scattered light is totally unpolarized and $D = \frac{6}{7}$ and $D_p' = \frac{3}{4}$. However, the symmetric vibrations are polarized and the depolarization ratio lies between 0 and $\frac{6}{7}$ for unpolarized incident radiation, and between 0 and $\frac{3}{4}$ for polarized incident radiation.

Thus, the polarization studies of the Raman lines provide additional information for the correct assignment of the vibrational frequencies.

H. GROUP FREQUENCIES

It has been found empirically that certain groups when present in a molecule give rise to the absorption bands in the same spectral region. These are called the characteristic group frequencies (12). The changes in these group frequencies in different molecules may be better understood if the interaction between the groups and the environment is specifically considered.

Resonance Splitting: As a rule the vibrations of different symmetries (e.g. the in-plane and out-of-plane vibrations in a planar molecule) do not interact with each other. However, when each of the two bond oscillators with a common atom have nearly the same individual frequency, they interact very strongly. The resulting frequencies are displaced from their original positions, depending on the relative phasing and coupling of the two oscillators.

Mass Distribution: A change in the mass distribution in a group of a molecule alters the form as well as the frequency of vibration; an increase in mass usually causes a decrease in the frequency (cf. section I).

Electronegativity: The intrinsic power of an atom to attract electrons within the molecule is defined as its electronegativity. For example, a covalent bond between C and F develops an ionic character, because a partial negative charge at F and equivalent positive charge on C are produced due to higher electronegativity of F than C. The Coulombic attraction between opposite charges makes the bond stronger than a purely covalent one. Thus the position and the intensity of the corresponding band in the spectrum will be affected due to the ionic character of the bond.

The Inductive Effect: The action of one group of a molecule to affect electrostatically the electron distribution in the other groups is described as the inductive effect. Due to the change in the charge distribution in the molecule, the force constants (and hence the frequencies) of many bonds may be altered.

Conjugation in Aromatic Molecules: A fundamental contribution of wave-mechanics to the theory of molecular structure is the concept of resonance or electron exchange. It can be shown mathematically that, when an electron exchange is possible (and does take place), the energy of the resonating structures

is less than that of the molecule without exchange. Thus the exchange or resonance energy leads to an increase in the stability of the resulting structures. Resonance, may arise from oscillations of electrons from one position in the molecule to another. This is what happens in the case of benzaldehyde or phenol and we get resonance structures.

In benzaldehyde, the exchange of π-electrons takes place between a carbonyl bond and the benzene ring and we call it by the name of conjugation. For the effective conjugation, the two parts should be planar or nearly planar (13,14).

Hydrogen Bonding: When a proton attached to a more electronegative atom X (e.g. Cl, O etc.) forms a partial bond with a neighbouring electronegative atom Y (e.g. Cl, O, etc.) or a π - bond (e.g. C = O, C = C, aromatic ring etc.), it is termed as hydrogen bonding. The hydrogen bonding may be both intramolecular or inter-molecular; the former being stronger than the latter. Strongest hydrogen bonds are formed when the atomic centers X, H and Y are collinear. The energy of a hydrogen bond is of the order of few kilo-calories; weaker by a factor of 10 than the covalent bond between atoms and stronger by almost the same factor than the van der Waals' bond.

All these factors affect the characteristic group frequencies to different extent and considerable experience is required to assign a particular band unequivocally in an unknown spectrum.

I. ASSIGNMENTS

Selection Rules: In large molecules the assignment of 3N-6 normal vibrations, their overtones, combinations and difference

bands becomes fairly complicated. However, if the point group for the molecule in vapour phase is known by any other method, the vibrations can be divided into various symmetry species of the group. The selection rules available from the character table will provide information about the allowed and forbidden transitions which will ultimately help in the vibrational assignments.

Group Frequencies: The knowledge of group frequencies is another useful aid to identify a vibrational band (Section H). It is now a well established assumption that for a particular bond, the stretching vibration has larger frequency than its in-plane bending mode. Likewise, the out-of-plane bending vibration involving the bond is to be expected in even lower frequency range.

Band Contours: The infrared vapour phase band contours whenever available as distinct A-, B- or C-type envelopes also provide a very good and reliable criterion for band assignments (Chapter VI).

Raman Effect: The activity and intensity of a Raman line, and especially its polarization character helps to a great extent in attributing the particular vibration to a known species of a point group (section G).

Polarized Infrared: In case of single crystals, polarized infrared spectra can reveal information about the direction of

the change in dipole moment of the unit cell as a result of molecular vibrations. If the molecular orientation in the crystalline sample is known, the polarized infrared spectrum can be of help in making the band assignments.

Isotope Effect: If one assumes that the isotopic molecules have the same electronic distribution and their potential energies (consequently the force constants) remain unaltered to a very high degree of approximation; the shifts in frequencies observed due to the substitution of an atom by its isotope can be attributed principally to the mass effect. The frequency (taking diatomic approximation) would be inversely proportional to the square root of the mass. In case of mixed modes selective deuteration can usually indicate the contribution made by component vibrations.

A quantitative relation known as the Teller-Redlich product rule can be used to verify the assignments of a given symmetry type if the geometry of the molecule and all the zero order frequencies of that type for both the isotopic species are known.

The extra frequencies observed for isotopic species provide additional data to verify the validity of the normal coordinate analysis in a molecule. Once the vibrational bands corresponding to different isotopic species are identified, the isotopic abundance ratio can be calculated from the band intensities.

Care has to be taken to apply the Teller-Redlich product rule, if isotopic substitution results in lowering the symmetry of the molecule.

J. HINDERED INTERNAL ROTATION (HIR)

The phenomenon in which a 'part' of any molecule (e.g. OH in C_6H_5OH or CHO in C_6H_5CHO) can rotate about the bond connecting it to the rest of the parent molecule is termed as HIR if the force acting on the 'part' is dependent on and is also a periodic function of the angle φ of its rotation from any arbitrary position. The phenomenon is found to occur only in complex molecules containing six or more atoms. On the other hand, the rotation is called a free rotation if the force is independent of the angle φ.

Assuming that the potential energy of a molecule has the same symmetry as its equilibrium configuration and the potential barrier has a sinusoidal shape corresponding to the first term in its Fourier series expansion, one could represent the two fold hindering potential (V_φ) by the equation:

$$2V_\varphi = V_o(1 + \cos 2\varphi) \qquad (1.31)$$

where V_o is the barrier height. One can obtain the barrier height from the splitting observed in microwave spectra. The infrared studies provide completely independent data (i.e. the torsional fundamental frequencies and the molecular geometry) for such calculations; and the two techniques provide a mutual check on each other.

The use of benzene derivatives for the study of HIR has the advantage that the phenyl ring provides a heavy 'anchor' and all of its vibrations fall above 400 cm^{-1}. Benzaldehyde has the added advantage that there are no complications due

to intermolecular or intramolecular hydrogen bonding effects. Both phenol and benzaldehyde exhibit two fold barrier. If the barrier is sufficiently high ($\sim$1000 cm^{-1}) the rotation reduces to torsional oscillations. The torsional energy levels would be doubly degenerate if the tunnelling effect did not split them into two sublevels. The splitting becomes greater as the levels approach the top of the barrier and finally, well above the barrier, the levels go into those of freely rotating groups.

K. FERMI RESONANCE

When two unperturbed vibrational eigen functions Ψ_1 and Ψ_2 have almost the same energies and belong to the same symmetry species, the anharmonic terms in the vibrational potential function (equation 1.5) may shift them quite considerably. The resultant shifting and associated sharing of the absorption intensities between the two levels is known as Fermi-resonance.

Unperturbed Separation: The magnitude of repulsion between the states Ψ_1 and Ψ_2 depends on the value of the matrix element W_{12} of the perturbation function W, i.e.

$$W_{12} = \int \Psi_1 \, W \, \Psi_2^* \, d\tau \qquad (1.32)$$

If the resonance is close, the magnitude of the displacement Δ' of the levels from their original mean position, can be obtained by using the first order perturbation theory and is given by:

$$\Delta' = \left[|W_{12}|^2 + \left(\frac{\delta}{2}\right)^2 \right]^{\frac{1}{2}} \qquad (1.33)$$

Now $2\Delta'$ is the observed separation Δ and δ is the separation of the unperturbed states.

If δ is large, compared to $2W_{12}$, one can expand the equation (1.33) and obtain:

$$\Delta' = \frac{\delta}{2} + \frac{|W_{12}|^2}{\delta} \qquad (1.34)$$

a result which one would obtain from second-order perturbation theory applied to each level separately.

Observed Intensities: The wave functions Ψ_1' and Ψ_2' of the perturbed vibrational states can be expressed as orthogonal combinations of the functions Ψ_1 and Ψ_2, i.e.

$$\Psi_1' = a\,\Psi_1 + b\,\Psi_2 \qquad (1.35)$$

$$\Psi_2' = b\,\Psi_1 - a\,\Psi_2$$

where

$$a^2 + b^2 = 1$$

and

$$a = \left[\frac{\Delta + \delta}{2\Delta}\right]^{\frac{1}{2}}, \quad b = \left[\frac{\Delta - \delta}{2\Delta}\right]^{\frac{1}{2}} \qquad (1.36)$$

when $\delta = 0$ we obtain equal mixtures of Ψ_1 and Ψ_2; and when δ is very large $\Psi_1' \rightarrow \Psi_1$ and $\Psi_2' \rightarrow \Psi_2$.

An explicit expression for the ratio R of the intensities of the observed (perturbed) transitions I_1' and I_2' from the ground vibrational level to the splitted levels has been given by Bertran et. al. (15) in terms of the intensities of the unperturbed transitions I_1 and I_2:

$$G^{\circ} = E_o^{\circ} - RT \ln \frac{Q}{N} \tag{1.39}$$

$$H^{\circ} = E_o^{\circ} - RT^2 \left[\frac{d}{dT} (\ln Q) \right] + RT \tag{1.40}$$

$$C_p^{\circ} = \frac{d}{dT} \left[RT^2 \frac{d}{dT} (\ln Q) \right] + R \tag{1.41}$$

$$S^{\circ} = \frac{H^{\circ} - G^{\circ}}{T} \tag{1.42}$$

Here R is the gas constant, E_o° is the zero point energy, T is absolute temperature of molecular system and Q is the total partition function which is given under well known approximations by:

$$Q = Q_{tr} \cdot Q_{rot} \cdot Q_{vib} \tag{1.43}$$

where tr, rot and vib denote the translational, rotational and vibrational contributions, respectively. Each of the above Q's can be expressed as:

$$Q_{tr} = V\left(\frac{2\pi m\, k\, T}{h^2}\right)^{3/2} \tag{1.44}$$

where V is the total volume of the system, m is the molecular weight (in grams) and other symbols have their usual meanings. Likewise:

$$Q_{rot} = \frac{(\pi I_A\, I_B\, I_C)^{1/2}}{\sigma} \left(\frac{8\pi^2\, k\, T}{h^2}\right)^{3/2} \tag{1.45}$$

Here σ is the symmetry factor and I_A, I_B and I_C are the three principal moments of inertia. Similarly,

$$Q_{vib} = \prod_i \left[1 - \exp(-hcw_i/kT) \right]^{-d_i} \tag{1.46}$$

In the above expression w_i stands for i^{th} vibrational frequency (in cm^{-1}) and d_i denotes its degeneracy.

For the purpose of actual calculations the thermodynamic functions may be arranged in the following form:

$$\frac{G^o - E_o^o}{T} = -R\left[\ln\left\{\left(\frac{4kT}{h^2}\right)^3 \pi^5 m^{3/2} (I_A I_B I_C)^{\frac{1}{2}} \frac{1}{\sigma} \frac{V}{N}\right\}\right.$$

$$\left. - \sum_i d_i \left\{\ln\left[1 - \exp(-x_i)\right\}\right]\right] \qquad (1.47)$$

$$\frac{H^o - E_o^o}{T} = \left[4 + \sum_i d_i x_i/(e^{x_i} - 1)^2\right] R \qquad (1.48)$$

$$C_p^o = R\left[4 + \sum_i \frac{d_i (x_i)^2 \exp x_i}{(\exp x_i - 1)^2}\right] \qquad (1.49)$$

where

$$x_i = \frac{hcw_i}{kT} = \frac{1.4388 w_i}{T} \qquad (1.50)$$

Substituting the values of various constants (16) for an ideal gas at one atmospheric pressure, equation (1.47) may be simplified as:

$$\frac{G^o - E_o^o}{T} = -\left[R - 8.2866 + 4 \ln T + 1.5 \ln M + 0.5 \ln(I_A I_B I_C) - \ln \sigma - \right.$$

$$\left. \sum_i d_i \ln\left\{1 - \exp(-1.4388 w_i/T)\right\}\right] \qquad (1.51)$$

where M is the mass of the molecule in amu and I_A, I_B and I_C are the principal moments of inertia in amu . A^{o2}.

Internal Rotation: In case of large barrier height V_o (cf. sec. J) the internal rotational motion is treated as torsional vibration

and its contribution is added to the thermodynamic functions. On the other hand, if V_o is small, the torsional frequency is dropped out and the partition function Q is modified, multiplying by a factor Q_f which is known as the partition function for free rotation and given by

$$Q_f = \frac{(8 \pi^3 \bar{I} k T)^{\frac{1}{2}}}{h \sigma_r} = \frac{2.7935 \times 10^{19} (\bar{I} T)^{\frac{1}{2}}}{\sigma_r} \qquad (1.52)$$

Here $\bar{I}$ is the reduced moment of inertia about the axis of internal rotation, σ_r is the number of potential maxima occurring in one revolution of the rotating group.

If the potential barrier is of significant height the tables given by Pitzer et. al. (17) may be used to obtain more accurate results.

Isotopic Species: If the system contains isotopically substituted molecules, then the thermodynamic functions for mixtures are calculated using the formula

$$K = \sum_i N_i K_i \qquad (1.53)$$

where K is any one of the thermodynamic functions for the mixture, N_i represents the mole fraction for the i^{th} species for which the value of the function is K_i .

Entropy and Free Energy of Mixing: According to Schottkey and Wagner (18) the entropy and free energy changes due to mixing of non-interacting ideal gases (for a total of 1 mole of the mixture of ideal gases) are given by

$$\Delta S^{\circ} = - R \sum_{i} N_i \ln N_i \qquad (1.54)$$

$$\frac{\Delta G^{\circ}}{T} = R \sum_{i} N_i \ln N_i \qquad (1.55)$$

where N_i is the mole fraction of i^{th} species.

Heat, Free Energy and Equilibrium Constant of Formation: The calculated thermodynamic functions, the experimental heat of formation $\Delta Hf^{\circ}_{298.16}$ and the thermodynamic functions of C(graphite), H_2(gas), O_2(gas) and Cl_2(gas) (16) may be used to compute values of ΔHf°, ΔGf° and $\log_{10} K_p$ at the desired temperatures using the following relations:

$$\Delta Hf^{\circ}_T = \Delta Hf^{\circ}_{298.16} + (H^{\circ}_T - H^{\circ}_{298.16}) \text{ compound} - \Sigma (H^{\circ}_T - H^{\circ}_{298.16}) \text{ elements} \qquad (1.56)$$

$$\Delta Gf^{\circ}_T = \Delta Hf^{\circ}_T - T \Delta Sf^{\circ}_T \qquad (1.57)$$

where

$$\Delta Sf^{\circ}_T = S^{\circ}_T \text{ (compound)} - \Sigma S^{\circ}_T \text{ (elements)}$$

$$\log_{10} K_p = \frac{- \Delta Gf^{\circ}_T}{0.004575845T} \qquad (1.58)$$

ΔHf°_T and ΔGf°_T are the heat of formation and Gibbs energy (or Free energy) of formation of the molecule respectively; $\log_{10} K_p$ is the equilibrium constant in terms of pressure and ΔSf°_T is the entropy change for the formation of the molecule.

M. NUMBERING OF NORMAL MODES

The vibrational modes of the phenyl ring in the mono-substituted benzenes are numbered after those of benzene (4,5).

As there are more than one convention for denoting the vibrations of benzene itself (4,5,19), we have followed the Wilson's method (19). Wilson has arranged the symmetry species of D_{6h} benzene in the order A_{1g} , A_{2g} , B_{1g} , B_{2g} , E_{2g} , E_{1g} , A_{1u} , A_{2u} , B_{1u} , B_{2u} , E_{2u} and E_{1u} . Subsequently, the frequencies are arranged in the increasing order of their magnitudes in each of the above species. Thus, each of the vibrations has been denoted by a number running from 1 through 20 in benzene. A very significant point to understand Wilson's numbering is the following: Normal coordinates of the vibrational modes are expressed in terms of the generalized coordinates of carbon and hydrogen; and for the modes involving similar expressions for normal coordinates, those involving carbon coordinates are given lower number than those involving hydrogen coordinates in any of the above species.

In Table 1.1 Wilson's numbering (19) has been compared with those given by Herzberg (4) and by Whiffen (20). Subscripts 'a' and 'b' with the Wilson's numbering have been used to denote the two components of the degenerate vibrations of benzene which split in the monosubstituted benzenes having C_{2v} point group. The symmetry classes of the vibrational modes, in the last column of Table 1.1, are denoted after Mulliken (2).

N. REFERENCES

1. M. Born and R. Oppenheimer, Ann. Physik 84, 457 (1927).

2. R.S. Mulliken, J. Chem. Phys. 23, 1997 (1955).

3. G. Herzberg, "Molecular Spectra and Molecular Structure, Vol. I", D. Van Nostrand Co. Inc. Princeton (1950).

4. G. Herzberg, "Molecular Spectra and Molecular Structure, Vol. II", D. Van Nostrand Co. Inc., Princeton, (1945).

5. E.B. Wilson Jr, J.C. Decius and P.C. Cross, "Molecular Vibrations", McGraw-Hill Book Co., Inc. New York (1955).

6. G. Herzberg, "Molecular Spectra and Molecular Structure, Vol. III, Electronic Spectra and Electronic Structure of Polyatomic Molecules", D. Van Nostrand Co. Inc. Princeton, New Jersey, (1966).

7. J. Morcills, J. Herranz and J.F. Biarge, Spectrochim. Acta 15, 110 (1959).

8. S. Bhagvantam and T. Venkatarayudu, Proc. Ind. Acad. Sci. 9A, 224 (1939).

9. R.S. Halford, J. Chem. Phys. 14, 8 (1946).

10. D.F. Hornig, J. Chem. Phys. 16, 1063 (1953).

11. B.P. Stoicheff in "Methods of Experimental Physics, Vol. 3, Molecular Physics", edited by D. Williams, Academic Press, New York (1962).

12. L.J. Bellamy, "Advances in Infrared Group Frequencies", Methuen and Co., Ltd., (1968).

13. N.B. Colthup, L.H. Daly and S.E. Wiberlay, "Introduction to Infrared and Raman Spectroscopy", Academic Press, New York (1964).

14. C.N.R. Rao, "Chemical Applications of Infrared Spectroscopy", Academic Press, New York (1963).

15. J.F. Bertran, L. Ballester, L. Dobrihalova, N. Sanchez and R. Arrieta, Spectrochim, Acta 24A, 1765 (1968).

16. D.R. Stull, I. Carr, J. Chao, T.E. Dergazarian, L.A. du Plessis R.E. Josted, S. Levine, F.L. Oetting, R.V. Petrella, H. Prophet and G.C. Sinke, JANAF Thermochemical Tables, Clearing-house for Federal Scientific and Technical Information Springfield, Va. (1966).

17. K.S. Pitzer and L. Brewer, Thermodynamics (by G.M. Lewis and M. Randell), Ind. Ed. McGraw-Hill New York (1961).

18. W. Schottky and C. Wagner, cited by W. Schottky, H. Ulich and C. Wagner, Thermodynamik, Springer-Verlag, Berlin, (1929) p. 377.

19. E.B. Wilson, Jr. Phys. Rev. 45, 706 (1934).

20. D.H. Whiffen, J. Chem. Soc. 1350 (1956).

TABLE 1.1

Comparison of Systems of Notations for Monosubstituted Benzenes

Vibrational species of Benzene	Description[a]	Wilsons' Number	Herzberg's Number	Whiffen's Symbols	Species of C_{2v} symmetry
A_{1g}	ν CC	1	2	p	A_1
A_{1g}	ν CH	2	1	z_1	A_1
A_{2g}	βCH	3	3	e	B_2
B_{2g}	δCC	4	8	v	B_1
B_{2g}	γCH	5	7	j	B_1
E_{2g}	αCCC	6a	18'	t	A_1
		6b	18	s	B_2
E_{2g}	νCH	7a	15'	q	A_1
		7b	15	z_5	B_2
E_{2g}	νCC	8a	16'	k	A_1
		8b	16	l	B_2
E_{2g}	βCH	9a	17'	a	A_1
		9b	17	c	B_2
E_{1g}	γCH	10a	11	g	A_2
		10b	11'	i	B_1
A_{2u}	γCH	11	4	f	B_1
B_{1u}	αCCC	12	6	r	A_1
B_{1u}	ν CH	13	5	z_2	A_1
B_{2u}	ν CC	14	9	o	B_2
B_{2u}	βCH	15	10	d	B_2
E_{2u}	δCC	16a	20	w	A_2
		16b	20'	x	B_1

Contd...

E_{2u}	γCH	17a 17b	19 19'	h y	A_2 B_1
E_{1u}	βCH	18a 18b	14 14'	b u	A_1 B_2
E_{1u}	νCC	19a 19b	13 13'	m n	A_1 B_2
E_{1u}	νCH	20a 20b	12 12'	z_3 z_4	A_1 B_2

(a) In these notations, ν, α, β, γ and δ denote bond stretching, angle deformation, in plane bending, out-of-plane bending, and torsional deformation or twist of the bonds or angles between the atoms written after each symbol, respectively.

CHAPTER II

EXPERIMENTAL DETAILS

A. SPECTROPHOTOMETERS

The infrared spectra in the solid and liquid phases were recorded on the Perkin-Elmer Model 521 spectrophotometer and on Carl Zeiss UR-10 spectrophotometer (Cf. Chapter V). The vapour phase spectra were primarily recorded on the Perkin-Elmer Model 621. Both the Perkin Elmer models are self-recording, high performance double beam grating spectrophotometers with the only difference that the Model 521 covers the spectral region from 4000 to 250 cm^{-1} and the Model 621 covers from 4000 to 200 cm^{-1}.

In the P-E 521 spectrophotometer (1) the monochromator has two gratings fixed back to back with 100 lines/mm and 25 lines/mm. The first grating is used in the first order (630 to 2000 cm^{-1}) and also in the second order (2000 to 4000 cm^{-1}); and the second grating is used only in the first order in the region 250 to 630 cm^{-1}. Suitable interference filters are used in the instrument to eliminate higher spectral orders of radiation from the gratings. A resolution of about 0.3 cm^{-1} is obtained at 1000 cm^{-1} with slit widths of about 70 microns. The accuracy is $\pm$ 0.5 cm^{-1} over the entire range with a reproducibility of $\pm$ 0.25 cm^{-1}. The P-E 621 instrument is of similar design.

The frequency marker accessory has been used for high resolution studies with P-E 621 instrument. This accessory

facilitates the exact measurement of band positions and enables the frequency calibration of the machine to be utilized fully, independent of the recording paper. The direct marking can be set at an interval of 0.2, 0.5, 1.0, 2.0, 5.0 or 10.0 cm^{-1}. We used 2.0 cm^{-1} marking-interval while recording the vapour spectra.

The P-E spectrophotometers have been provided with a wide range of adjustments for scanning the spectrum of a sample. To obtain a well resolved spectrum of a sample a suitable adjustment of the slit width, gain, signal to noise ratio and the scanning speed are of vital importance; a proper combination of the above parameters was chosen after enough experience with each instrument.

B. LOW TEMPERATURE CELL

The spectra of the samples in solid state were recorded using the low temperature cell shown in Figure 2.1. The cell as fabricated by us is slightly different from the conventional Wagner-Hornig type cell (2). The cone-socket joint to connect the cell-jacket with the dewar has been replaced in our design by a ball-socket joint which provided the required flexibility essential to connect the cell assembly directly to the vacuum system. Further, in place of copper to glass House-keeper seal we have used a glass-to-kovar seal which has worked very satisfactorily. The copper block to hold the halide window in the cold finger has been replaced by an annular copper frame with an exactly fitting copper cold finger top. The advantage of this modified cold finger is that it allowed easy deposition of the sample onto the cooled CsBr plate (40 mm x 20 mm).

The low temperature cell can directly be inserted in the sample-beam of the infrared spectrophotometer without any material change in the optical path. Prior to cooling, the assembled cell was evacuated to a pressure of about 10^{-5} cm of Hg and then the liquid nitrogen was poured in the dewar. After some time the copper frame and the cesuim bromide plate in the cold finger attained the temperature of the refrigerant.

A thin film of the sample was obtained by slowly depositing vapour from the vacuum system onto cooled cesium bromide plate. To avoid the glassy state of the material, the temperature of the sample was cycled above and below the melting point, until well resolved spectrum was obtained at liquid nitrogen temperature (LNT). To minimize the scattering of the infrared radiation the thickness of the deposited sample should be thin and uniform. To get such a sample was one of the difficult parts of the experiment because the process had to be repeated several times to get a suitable deposition. The distinction between glassy and crystalline deposition could be made visually and finally confirmed from the spectrum. The infrared spectrum due to glassy deposition resembled the liquid phase spectrum.

The outer metallic parts of the kovar seal and the cold finger block had to be insulated with a cello-tape to facilitate the deposition of thin crystalline film onto the cold cesium bromide plate, especially so in case of the substances having relatively higher vapour pressure. As the cell, made of thick pyrex glass, was big enough and the inside pressure

was maintained at about 10^{-4} cm of Hg, the exterior CsBr windows (i.e. the entrance and exit windows) of the cell were not cooled perceptibly. The numerals in Figure 2.1 indicate the various dimensions in mm.

The instrument was purged with dry air from compressed dry air cylinders to get rid of the unwanted atmospheric water vapour and CO_2 absorptions.

Fixing of External Windows: Although care was taken not to allow the corrosive materials to react with the adhesive (Araldite-CIBA, Ltd. Basle Switzerland) by thoroughly evacuating the cell just after use, even then the adhesive was slowly eaten away by some compounds and the cell started leaking. To remove the leak the windows were taken out (by dissolving the adhesive in dry chloroform) from the cell jacket, repolished (on a Perkin-Elmer Polishing kit) and fixed to the cell jacket with the adhesive.

The transmittance obtained with the low temperature assembly (without the sample on the cold finger window) was upto 50% which was good enough for all precision measurements.

Fatique in Kovar Seal: It has already been mentioned that for proper deposition of the sample on the window the temperature of the sample was cycled above and below its melting point several times in one experiment. This frequent cooling to liquid nitrogen temperature and warming the cell upto little below the room temperature, weakens the kovar seal and it cracks. So before removing the external windows we had to ascertain the place of the leakage in the assembly and then get it repaired.

C. MULTIPLE REFLECTION CELL

The vapour phase spectra of the samples were recorded on the P-E 621 spectrophotometer using a multiple reflection cell with an adjustable path length from 1.25 to 10 meters in steps of 1.25 meters. The optical system of this cell is shown in Figure 2.2.

After maintaining a hard vacuum in the multiple reflection cell for some time, the pressure of the sample and the path length of the cell were adjusted to obtain a good spectrum. As far as possible low pressures and full 10 meter path lengths were used to obtain the resolved band contours.

The transfer optics in the cell introduced in the sample beam an additional optical path which was not under vacuum. Therefore to eliminate this, the purging (with the dry air) of the instrument along with the multiple reflection cell was all the more essential. While recording the gas phase spectra, purging was achieved with dry air obtained from a high pressure line, after drying with a pneumatic air dryer.

D. VACUUM SYSTEM

A simple vacuum system illustrated in Figure 2.3 was fabricated for the triple purpose of (i) purifying the samples immediately before recording the spectrum (ii) filling the gas cell and (iii) obtaining thin solid films of samples at LNT.

As shown in the figure the piece of glass manifold from J_1 to J_5 could easily be detached from the rest of the vacuum

system. Although all the stopcocks, joints and connecting tubes were thoroughly cleaned before any new compound was introduced in the system; special care was always taken to leave no trace of earlier impurities inside the J_1 - J_5 piece. Traps T_1 and T_2 were cooled externally by liquid nitrogen to prevent the contamination of the Duo Seal forepump (model 1402 from Welch Scientific Company) and/or the single stage oil diffusion pump by the vapour of the samples used in the experiments. Three-liter capacity bulb B is a safety storage tank for the oil of the vacuum forepump in case of occasional breakdown of the power supply. S_{10} is a release valve for the forepump and F_1, F_2 and F_3 are the three flasks used to purify a sample. The system was capable of giving vacuum of the order of 10^{-5} cm of Hg inside the glass manifold S_1 - S_5.

Purification of Samples: The sample was kept in one of the flasks (say F_1) which was attached to the system through a joint (J_2). Initially, the whole system was evacuated except the flask F_1. Subsequently, S_3 and S_4 were closed and the flask F_1 was opened to the vacuum line for a small period, which depended on the vapour pressure of the sample. After a small portion of the sample evaporated from F_1, the stopcock S_2 was closed and the flask F_1 was cooled to liquid nitrogen temperature and again evacuated to obtain good vacuum. Subsequently, the inlet S_3 of another flask (say F_2) cooled to LNT was also opened to the vacuum system. After about half an hour the stopcock S_5 was closed and the coolant outside the flask F_1 was

removed. The flask F_1 gradually attained the room temperature and the sample evaporated and collected in the flask F_2. After collecting adequate amount of first portion of the sample in flask F_2 , the middle portion of the sample (which must be comparatively more pure) was collected in flask F_3 in a similar fashion. This process was repeated several times for all the compounds to obtain pure samples. Our original chemicals were of A.R. grade from Aldrich Co. and we purified them at least three times by the above process before filling them into the gas cell or depositing a thin film at LNT in low temperature cell.

Filling of the Cells: The vacuum system including the cell in question was evacuated to the desired pressure and then the stopcock S_5 was closed. Purified sample was evaporated into the gas cell till a required band intensity was obtained. In case of samples with low vapour pressure, the tube connecting the cell and the vacuum system was heated by wrapping a heating tape on it.

The vapour of a sample were evaporated into the low temperature cell in an identical fashion and there they were deposited on the cesium bromide plate in the cold finger as explained in section B of this chapter.

E. SPECTRA IN THE LIQUID PHASE

The liquid phase spectra were recorded by using fixed cells of different stratum thicknesses. For pure liquids CsBr cells of .05 and .025 mm stratum thickness were used, because

the cells with thickness (fixed) smaller than .025 mm were not available. In case of high absorption bands a little of the liquid sample was pressed between two CsBr plates without the spacing foils. If the absorption bands under investigation were still very strong, the sample liquid was dissolved in a suitable solvent and spectrum was recorded, as the solution method is comparatively simple for obtaining the required spectrum by varying the cell thickness and the concentration of the solution. Absorption bands due to solvents were eliminated by using an equivalent amount of solvent in the reference beam of the double beam instruments. In solutions, the spectra free from environmental effects were obtained by using inert, non-polar solvents. Purity of the solvents was always checked before use by recording their infrared spectra.

F. CALIBRATION IN INFRARED REGION

The wave number calibration of the spectrophotometers was made by recording the infrared spectra of H_2O, CO_2 and D_2O vapour under conditions identical to that of the spectrum to be investigated. The calibration data were taken from standard texts (3-4). In case of liquids indene bands were used for calibration (5).

G. RAMAN SPECTRA

For recording the Raman spectra of the liquids Coderg model PH-1 Raman spectrophotometer equipped with a Spectra-Physics Model 125 He-Ne laser source was used. The laser source has an output of about 50 milli-watt power at 6328 $\AA$. The

spectrophotometer has two monochromators with 600 and 300 mm focal lengths; the latter acts as a filter to get rid of stray light and eliminate ghost lines. The plane grating has 1200 lines/mm blazed at 7500 A^{o}. The maximum resolution of the instrument is 0.5 cm^{-1}.

For obtaining the Raman depolarization data a half wave plate is introduced in the path of the incident radiation. This half wave plate rotates the plane of polarization of the incident light. The spectra are recorded by using incident light polarized parallel and perpendicular to the slit which is kept vertical. This is attained by rotation of the half wave plate through 45^{o}.

Band intensity ratios have been evaluated by comparing the areas under the same band in the two spectra. The measured intensity ratio R is not simply equal to depolarization ratio D, but is a function of 'f' and is given by

$$R = D((1 + f)/(f + D))$$

where 'f' is defined as the ratio of the efficiency of monochromator and detector system for horizontally polarized light to that for vertically polarized light (6). This ratio can be easily measured and for the limiting value of f = 1, it has the value R = .86.

It has been found that accurate depolarization ratios are not obtained using coaxial or right angle laser excitation, from samples contained in a multipass capillary cell. This is because the inherent directional polarization of the laser beam

becomes disoriented when reflected from the walls of the cell. Therefore, theoretical band ratios cannot be expected in an experiment and only a semiquantitative information could be obtained. The Raman spectra of chlorobenzene were recorded using a sample holder of capacity 1 cc. The slit-width and the photomultiplier voltage were adjusted to obtain a proper spectrum. The Raman spectra of benzaldehyde were recorded on a Cary-81 spectrophotometer (Cf Chapter IV).

H. REFERENCES

1. Perkin-Elmer Corporation, Instruction Mannual for Model 521 Spectrophotometer, Norwalk, Connecticut, U.S.A. (July 1965).

2. E.W. Wagner and D.F. Hornig, J. Chem. Phys. 18, 296 (1950).

3. K.N. Rao, C.J. Humphreys and D.H. Rank, "Wave Length Standards in Infrared" Academic Press, New York (1966).

4. "Tables of Wave Numbers for the Calibration of Infrared Spectrometers", Butterworth, London (1961).

5. R.N. Jones, N.B.W. Jonathan, M.A. MacKenzie and A. Nadeau, Spectrochim. Acta 17, 77 (1961).

6. H.H. Claassen, H. Selig and J. Shamir, App. Spectry. 23, 8 (1969).

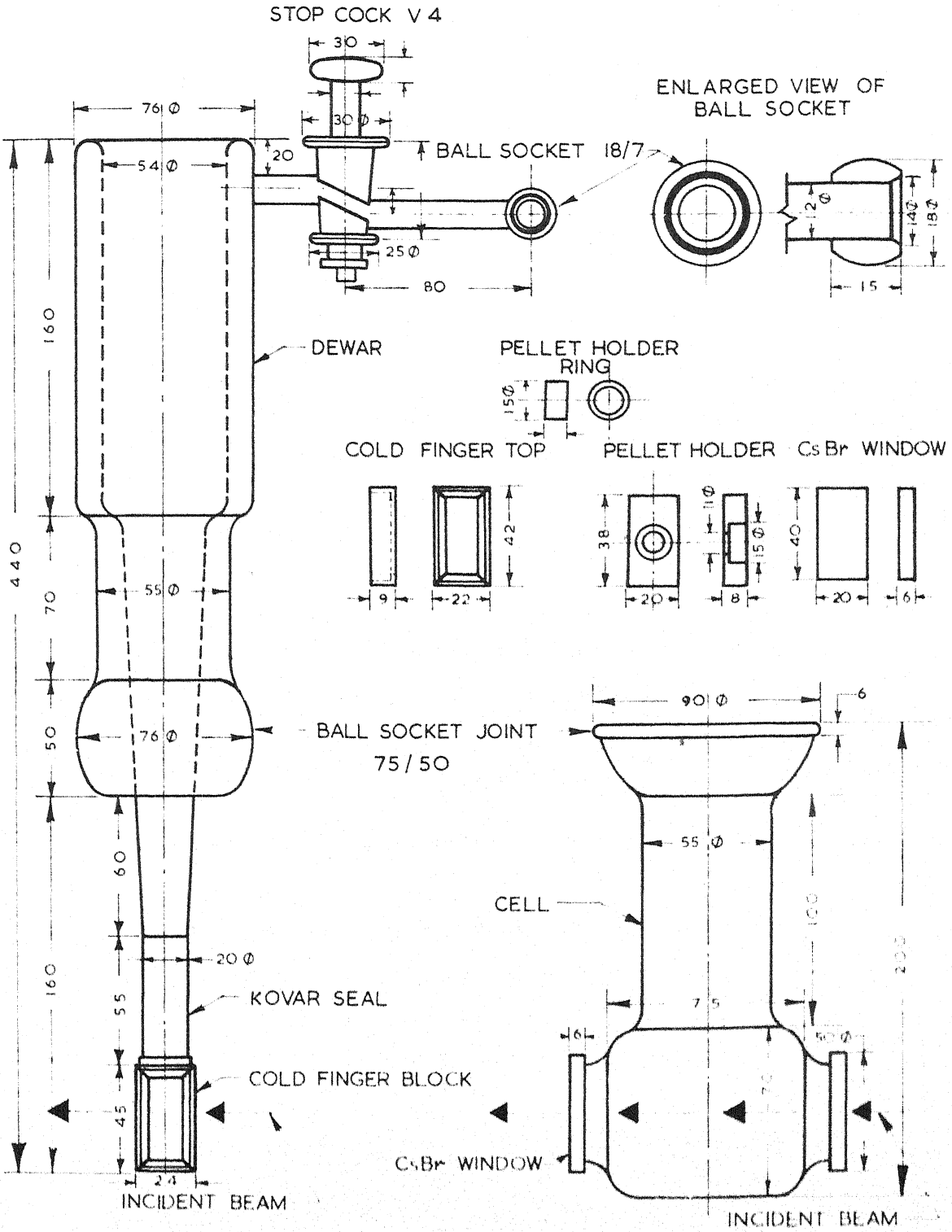

LOW TEMPERATURE CELL

Fig. 2.1

TEN-METER CELL OPTICAL SYSTEM

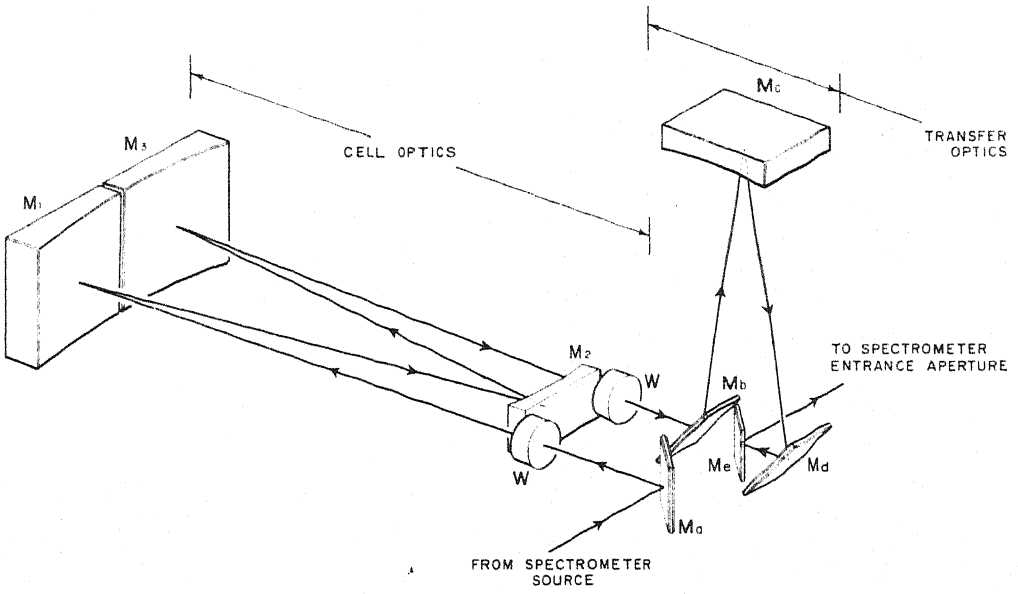

Mirrors: M_1, M_2 and M_3 and two windows W are inside the cell.

Mirrors: M_a, M_b, M_c, M_d and M_e are outside the cell.

Fig. 2.2

VACUUM SYSTEM

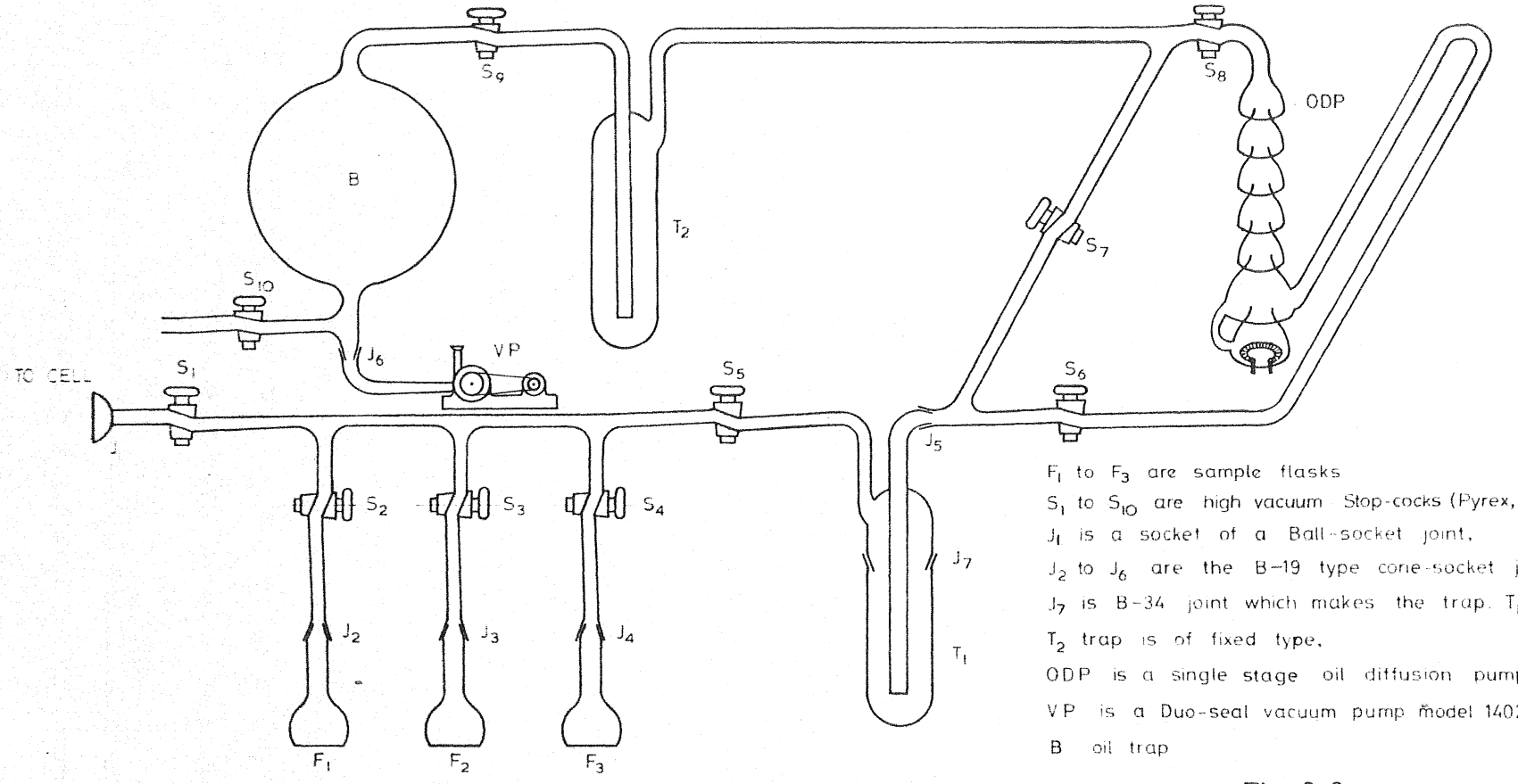

F_1 to F_3 are sample flasks

S_1 to S_{10} are high vacuum Stop-cocks (Pyrex, V-6),

J_1 is a socket of a Ball-socket joint,

J_2 to J_6 are the B-19 type cone-socket joint,

J_7 is B-34 joint which makes the trap. T_1,

T_2 trap is of fixed type,

ODP is a single stage oil diffusion pump,

VP is a Duo-seal vacuum pump model 1402

B oil trap

Fig. 2.3

CHAPTER III

SPECTRAL CORRELATION WITH STRUCTURES OF CHLOROBENZENE IN VAPOUR, LIQUID AND SOLID STATES*

ABSTRACT

An extensive study of the vibrational levels of chlorobenzene has been conducted in the vapour, liquid, solid (crystalline film at liquid nitrogen temperature - LNT) phases and also in solutions. A combined analysis of high resolution vapour phase electronic spectra and infrared absorption spectra has provided accurate vibrational data for the ground state fundamentals. Isotope effect has been detected invariably in all the X-sensitive modes due to the presence of ^{35}Cl and ^{37}Cl species. The vibrational constants w_e and $w_e x_e$ for a few of the fundamentals have been evaluated. A ground-state geometry of the molecules with a stronger C-Cl bond is suggested. The relative changes in the intensities of the bands and the fractional changes in the positions of the well established fundamentals, on going from one phase to another and splitting of bands in the solid state (LNT), are discussed. An increase in the ionic character of chlorobenzene is suggested on going from vapour to solid state at LNT. Earlier vibrational studies and assignments have been thoroughly reexamined. The existence of dimers and few Fermi interactions stipulated in vapour phase has been shown to be untenable. The thermodynamic quantities have been calculated using the present spectroscopic data.

A paper based on this Chapter has appeared in Spectrochim. Acta, 26A, 841 (1970).

A. INTRODUCTION

The infrared data for chlorobenzene (PhCl) are available under low resolution in the rock salt region (1-18). Recently the studies have also been extended to 700-20 cm^{-1} range (19-26). The Raman shifts in the vapour (27), liquid (with depolarization ratios) (28-32) and solid (33-36) phases have been recorded to make the assignments. Stimulated Raman scattering (37) and microwave studies (38-39) have also been performed. Normal coordinate calculations have been tried by various workers (40-51) and the dipole moment of the compound has been estimated (52-54). In all these studies chlorobenzene forms only a part of large number of substituted benzenes that have been studied by each worker.

Inspite of recent availability of commercial high resolution far infrared spectrophotometers, the accurate vibrational data for large molecules in gaseous state are not always available, mainly due to difficult experimental techniques required for such work. Consequently, the assignments of low frequency vibrations of PhCl are ambiguous (24). Bist and coworkers (55-57) have developed a method to obtain accurate and complete vibrational data from an analysis of high resolution electronic spectrum, especially for low lying fundamental vibrations of phenol. Analogous analysis, based on the two types of electronic and three types of infrared band contours is not available for PhCl; although its electronic spectrum on medium dispersion (58-59) and infrared on low resolution (4,5) have been reported. In the present study we have collected accurate data on directly

observable low lying planar vibrations in the ground state based, especially, on the identification of A_e- and B_e-type band contours in the high resolution electronic spectrum of PhCl. Our analysis (60) is consistent with the information now available from electronic band contour analysis (61) and is in agreement with those of earlier workers (49,51) based on infrared (4,5) and Raman (31) spectral studies.

In this chapter we present an extensive study of the vibrational spectra in the vapour, liquid and solid phases of PhCl. Complete assignments of all the fundamental modes, observed combinations and overtones have been made on the basis of combined study of the infrared, Raman and high resolution electronic spectra. The infrared study at liquid nitrogen temperature (LNT) has helped in locating the vapour phase forbidden bands and also in confirming the splitting due to the presence of ^{35}Cl and ^{37}Cl isotopic species. The thermodynamic quantities have been obtained using the accurate vapour phase data and have been compared with the earlier results (4).

B. EXPERIMENTAL

The chlorobenzene (PhCl) sample used throughout the experimental work was Aldrich, A.R. grade, purified to a high degree by repeated fractional distillation under vacuum (cf. Chapter II).

The infrared spectra in the vapour, liquid and solid (LNT) phases, and the Raman spectra of the PhCl liquid and its

solution in CS_2 were recorded as described in Chapter II. The accuracy in the vapour phase data is better than ± 0.5 cm^{-1}, while in liquid and solid phases accuracy may be limited to $\pm$ 1 cm^{-1}.

While recording the vapour phase spectrum the scan speed was kept nearly 0.3 cm^{-1}/min, the slit width and pen response were adjusted to provide well resolved spectrum. The wavelength abscissa was expanded 12.5 fold, so as to record a band profile as wide as possible on a chart paper in order to estimate the contours and intensities accurately.

For recording the infrared spectra in the liquid and solid phases of PhCl, the scan speed was kept nearly 6 cm^{-1}/min. The slit width and the pen response were suitably adjusted to obtain a well resolved spectrum.

The Raman spectra and depolarization ratio of most of the Raman shifts of PhCl liquid and its solution in CS_2 were recorded on Coderg PH-1 spectrophotometer (Cf. Chapter II).

The high resolution electronic spectra were photographed in 19 - 22 order of 3.4 m Jarrell-Ash Ebert spectrograph fitted with a 57000 line Harrison grating (55).

C. RESULTS

The infrared spectra of PhCl in all the three phases i.e. vapour, liquid and solid (LNT) are shown in Figure 3.1. Well resolved infrared vapour phase band contours are given in Figure 3.2 (A,B,C). The Raman spectra of pure liquid (PhCl) and its solution in CS_2, obtained by using polarized incident

radiation and then changing its plane of polarization by 90°, (Cf. Chapter II) are presented in Figure 3.3 (A,B).

The vapour phase infrared band positions, type of band contours, relative peak heights and the assignments of all the observed bands are listed in Appendix 3.1. Liquid and solid phase infrared band positions with their assignments are contained in Appendix 3.2. In the last column of this Appendix, the possible explanation for the observed splitting of bands in the solid phase (LNT) is mentioned.

The Raman spectral data of PhCl like: liquid phase Raman shifts, their values in CS_2 solution, depolarization ratio of most of the bands and the comparison with earlier (31) similar data are given in Appendix 3.3, assignments are also suggested in the last column.

D. MOLECULAR GEOMETRY

The PhCl molecule is planar in its ground ($\underline{e}A_1$) state as suggested by (i) its definite A-, B- and C-type vapour phase infrared band contours (Cf. section F), (ii) the $A_{\underline{e}}$- and $B_{\underline{e}}$-type envelopes of the 'hot' bands observed in the electronic spectrum (Cf. section G), (iii) the Raman polarization data (Cf. section H), and (iv) the smallness of inertial defect observed from the microwave studies (38). An unequivocal determination of the geometry from microwave data requires at least six suitably chosen isotopic species. However, considerable progress can be made by starting with a plausible model and then improving it in the light of further experimental evidence.

Assuming a planar regular hexagonal phenyl ring with all equivalent CH bond lengths of 1.084 A^{o} (62) and neglecting the centrifugal distortion effects; we have illustrated in Figure 3.4 the most probable and the simplest conceivable geometry of PhCl in its ground state as computed on IBM 7044 computer. The computed parameters are corresponding to the best fit of the observed rotational constants (38). We have also mentioned the coordinates of all the atoms in the center of mass system for better understanding. The CC bond distance which is primarily fixed by the moment of inertia about Z axis comes out to be slightly higher in PhCl than in benzene. According to Badger's rule this would suggest a lower value for the vibrational ring breathing mode in PhCl, while actually it is higher than in benzene. This could mean that the Badger's rule cannot be applied in its simplest form to the complex modes of vibration.

E. SELECTION RULES

Assuming a planar configuration and C_{2v} point group symmetry for both the ground and first singlet excited state ($\overset{e}{=}B_2$); the 30 normal modes of PhCl in each state divide into symmetry classes as shown in Table 3.1. The vibrations a_1 and b_2 are planar and are directly observed as A- and B-type band contours (Chapter VI) in vapour phase infrared spectrum. However, in electronic spectrum the vibrations belonging to a_1 and b_2 species appear with $B_{\underline{e}}$- and $A_{\underline{e}}$- type contours respectively (Cf. section G). The six vibrations of b_1 class (observed as C-type contours) and three of a_2 class (forbidden in infrared)

are perpendicular to the plane of the ring. The detailed characteristics of all the fundamental modes of PhCl in the infrared, Raman and electronic spectra have been described in Table 3.1.

F. INFRARED BAND CONTOURS

PhCl being an asymmetric top molecule the vapour phase infrared band contours corresponding to the vibrations for which the change of dipole moment is along the axis of least moment of inertia (Z aix here) appear as A-type and correspond to the totally symmetric a_1 species of C_{2v} point group. The vibrations for which the change of dipole moment is parallel to the axis of intermediate and maximum moments of inertia (along Y- and X-axes respectively) appear as B-type (corresponding to b_2 species) and C-type (corresponding to b_1 species) envelopes respectively. The characteristic shapes of contours and the relative intensity of Q branch with respect to whole band depend on the relative values of moments of inertia and are used for identification of bands of the same species. The details of the infrared band contour analysis have been described in Chapter VI.

G. ELECTRONIC BAND CONTOURS

The $\underline{a}_1$ and $\underline{b}_2$ species are directly observed in the electronic spectrum with $B_{\underline{e}}$- and $A_{\underline{e}}$-type contours respectively. Under C_{2v} point group, to which PhCl belongs, the $B_{\underline{e}}$ type contours are vibronically allowed, with transition moment in the molecular plane along a direction perpendicular to the C-Cl

bond (60). The A_e-type bands correspond to the "forbidden" part with transition moment along C-Cl bond. The intensity in the "forbidden" part is borrowed from the other locally excited and charge-transfer states of the molecule due to mixing of their wave functions with those of the two states involved in this transition (56). The C_e-type contours have not been observed in the monosubstituted benzenes (56,57).

On comparison with the observed and calculated B_e- and A_e-type band contours of phenol (56,57) it was easy to identify the analogous bands in PhCl. In fact now electronic band contour analysis is also available for PhCl (61). The (0,0) band, all the totally symmetric a_1 fundamentals, the even combinations and overtones of all the non-totally symmetric modes have B_e-type contour showing a prominent sharp peak in the middle with a very weak hump on its high frequency side and a relatively weaker broader component on its low frequency side as shown in Figure 3.5A. The inplane non-totally symmetric b_2 vibrations, or the combinations having net b_2 symmetry show A_e-type contour with only one sharp peak (Figure 3.5B).

In order to analyse the electronic spectrum, some approximate information on the ground state fundamentals is helpful. The accurate frequencies for the a_1 and b_2 modes are subsequently obtained from an analysis of the electronic spectrum towards the longer wave length side of the (0, 0) band, based on the two types of contours mentioned above. The middle peak for the B_e-type contours and the single peak for A_e-type contours have been measured. The data given in Appendix 3.4

have been used to obtain the consistent values of wave numbers for the fundamental modes in the ground state by subtracting the measured values from (0,0 origin) band position. Likewise, the data given in Appendix 3.5 have been used to deduce the out-of-plane fundamentals in the ground state.

H. THE RAMAN POLARIZATION DATA

Most of the single bands in the Raman spectra were of Lorentzian shape, while asymmetry in the envelopes at the edges was due to overlapping of neighbouring bands (Figure 3.3A). The intensity measurements for the individual Raman shifts were made by finding the product of peak height and the half width (full width at half the peak height). Thus, it provided better estimates of the intensities than the visual estimation. The Raman data and their assignments are listed in Appendix 3.3.

The Raman shifts and their depolarization ratio for pure liquid and its solution in CS_2 have nearly the same values, which suggests that there is no appreciable association in the PhCl molecules in the liquid state. The depolarization ratios for almost all observed Raman shifts have been calculated, which resemble well with those reported earlier (28-32). The polarized Raman lines support the assignments of a_1 modes.

I. FUNDAMENTAL VIBRATIONS

The assignments of the fundamental vibrations of PhCl have been made on the basis of the data obtained by us and compared with earlier studies (Tables 3.2 - 3.5). Some of the striking features in the infrared spectra, vibrational

frequencies whose assignments have been changed and the assignments of the infrared vapour phase inactive vibrations have been discussed in the following pages.

Class - a_1: Out of eleven modes expected in this class nine have been observed as A-type contours in the vapour phase infrared spectrum of PhCl. Vibrational mode 2 at 3054 cm^{-1} being mixed with other bands in such a way that the band contour is not separable, but for mode 12 at 706 cm^{-1} the band envelope is asymmetric due to the bands of two isotopic species, while modes, 1 at 1003.3 cm^{-1} and 18a at 1025.4 cm^{-1}, are resolved from a composite band (Figure 6.4 iii). The vibrational modes, 9a at 1153 cm^{-1} and 8a at 1586 cm^{-1}, have been assigned in place of 1174 and 1580 cm^{-1}, respectively, on the basis of infrared band contours. The values of the vibrational frequencies are in good agreement with the electronic data except for CH stretching vibrations because the electronic spectrum in this region is complex. The Raman depolarization ratio for most of the bands given in Appendix 3.3 have confirmed the assignments. Our data are better than those of Whiffen (4) given in Table 3.2.

Class - b_2: Out of ten vibrations of this class, seven are recognized by their characteristic B-type band contours and are listed in Table 3.3. The CH stretching vibrations (3067 and 3096 cm^{-1}) and CC stretching vibration (1598 cm^{-1}) do not show recognizable contours. But all the band positions except that of CH stretching vibrations agree well with the electronic spectral results. For most of the vibrations our results

agree with Whiffen's data within the limits of accuracy of the instruments used. But the assignments of 9b at 1296.3 cm^{-1} and 8b at 1598 cm^{-1} in place of 1157 and 1580 cm^{-1}, respectively, have been made on the basis of present detailed spectral study of PhCl. The asymmetry in B-type band enevelope of the X-sensitive mode at 294.8 cm^{-1} has been attributed to the overlap of two isotopic bands. They have been resolved by graphical method and the respective positions are 294.8 cm^{-1} and 288.4 cm^{-1} (Appendix 3.1). The band contours of the modes 6b at 614.8 cm^{-1}, and 19b at 1448 cm^{-1} are affected by the vibrational bands (16a + 11) at 605.2 cm^{-1} and (6a + 11) at 620.2 cm^{-1} and (10a + 6b) at 1446.1 cm^{-1} (Figure 6.4 (ii)) respectively.

Class - b_1: Out of six vibrations of this class four are recognized in the vapour phase infrared spectrum by their C-type contour, where Q branch is medium to very strong. The vibration at 197.5 cm^{-1} is beyond the range of our instrument and the mode 5 at 981 cm^{-1} has weak intensity. The mode 4 at 684.6 cm^{-1} is overlapped by (16a + 18b) at 692.0 cm^{-1} and the mode 17b at 902.3 cm^{-1} is overlapped by (12 + 11) at 897.5 cm^{-1}. All these vibrational frequencies are in agreement with the electronic spectral results and Whiffen's data collected in Table 3.4.

Class - a_2 : In Table 3.5 the three vibrational frequencies of this class have been listed on the basis of observed sequences, cross sequences, combinations and overtones in the electronic vapour phase spectra; and combinations and overtones in vapour phase and solid (LNT) phase infrared spectra. The electronic spectral

frequency of the mode 16a at 403.4 cm^{-1} could not be observed in the Raman and liquid phase infrared spectrum of PhCl. This vibration should lie near to benzene frequency at 405 cm^{-1} as it is not substituent sensitive and has been observed at 408.9 cm^{-1} in the solid phase infrared spectrum. So the value is unambiguously decided at 403.4 cm^{-1} as its overtone in the vapour phase infrared spectrum has been observed at 806 cm^{-1} with A-type band contour. The mode 10a has been estimated from the observed difference band (10a - 18b) at 536.8 cm^{-1} and overtone of 10a at 1662.6 cm^{-1}, these values are in accordance with the electronic results. We have observed in the infrared vapour phase spectrum combinations (17a + 16a) at 1364 cm^{-1}, (17a + 17b) at 1862 cm^{-1}, a difference band (17a - 16a) at 559 cm^{-1} and the overtone of 17a at 1920 cm^{-1} (Appendix 3.1). Thus the value of 17a mode found from the above observations is in agreement with electronic results. In this way, the three infrared inactive modes have been unambiguously decided.

J. RELATIVE INTENSITIES

The relative peak heights of the observed bands in the Raman spectrum of PhCl (liquid) and in the infrared spectra of vapour, liquid and solid (at LNT) phases have been collected in the Appendices 3.1 to 3.3. In every spectrum, the peak height of the most intense band has been arbitrarily fixed as 100 and the peak heights of other bands have been normalized with respect to this band. These peak heights (which may denote band intensity in a semiquantitative way) have been

illustrated in Figure 3.6 for the Raman and the infrared spectra of the sample. The vibrations belonging to a_1, b_2, b_1 and a_2 classes have been shown by different lines in the figure. The approximate description of different modes has also been given. The following points have been noted:

(1) The vibrations belonging to b_1 class share most of the intensity in the infrared absorption spectra and out of these, the CH out-of-plane bending mode near 740 cm^{-1} invariably appears with maximum intensity in all the three phases.

(2) The intensity of vibrations belonging to a_1 class is next to those belonging to b_1 class. In class a_1 the x-sensitive vibrations and the vibrations involving mainly CC stretch and CH in-plane bending contributions are stronger compared to the others. However, the ring breathing vibration at 1003 cm^{-1} and the CH in-plane bending vibration at 1153 cm^{-1}, are weak in the vapour phase but, are relatively stronger in the liquid and the solid phases.

(3) Most of the b_2 class vibrations have low intensity in vapour phase infrared but they progressively gain in intensity on going to liquid and then to solid phase. The weak vibrations of this class become relatively intense in their solid phase spectrum and vice versa. The vibrations which have gained intensity are mostly bending ones or those associated with the motion of the ring.

(4) The intensity of all the five CH stretching vibrations decreases considerably in infrared on going from vapour to solid phase (LNT).

(5) The a_2 class vibrations are not observed in vapour phase infrared spectrum as they are forbidden by symmetry selection rules. However, all the $3a_2$ modes appear as weak bands in the solid phase infrared spectrum of PhCl.

(6) In the Raman spectrum, the ring breathing mode appears with the maximum intensity while the remaining intensity is shared mostly by its neighbours (on the higher frequency side), the X-sensitive and the ring deformation modes. In general overtone and combination bands are weak in the Raman effect.

The factors affecting the absolute absorption intensity of infrared bands have been discussed in section E of Chapter I. Primarily, the intensity of a band depends on the change in the magnitude and direction of the electric dipole moment during the vibration if the thickness of the sample and its concentration are kept the same. The peak heights as reported here would be proportional to the absolute intensity only if the shapes of the bands are identical - too ideal an assumption in actual practice. Thus, the reported data could give qualitative picture regarding the transition moments for different vibrations.

The appearance of vapour phase infrared forbidden bands in the solid phase may suggest that the symmetry selection rules for C_{2v} point group for free PhCl molecule are changed in the solid phase (in solid phase due to association of molecules the symmetry is changed). Likewise, the large decrease in intensity of CH stretching vibrations may be due to the decrease in the amplitude of these modes in solid phase (LNT), while the gain in the intensity of the b_2 class vibrations in solid phase may be due to an increase in electric dipole moment of these vibrations due to intermolecular association.

The relative intensity and sharpness of bands in solid phase (LNT) infrared spectrum of PhCl depend on the manner of deposition of the sample onto the cold finger. For glassy film of PhCl obtained on rapid condensation of the sample vapour on the cold finger, the infrared bands resemble the corresponding ones in the liquid phase, and are relatively broad. Whereas for a properly deposited and annealed sample reproducible spectra could be obtained with sharper lines.

K. BINARY COMBINATIONS

The symmetry species of the binary combinations are given in Table 3.6. Among other things it shows that two out-of-plane fundamentals give a combination band with in-plane symmetry, though the reverse is not true. Various other combinations are also given in the table.

In the vapour and liquid phase spectra recorded at low resolution a characteristic pattern of five strong bands, with diminishing intensity toward lower wave numbers, has been reported earlier (11,12), in the range 1650-2000 cm^{-1}. But no mention has been made of other bands in this region, nor has a systematic study been made to obtain the anharmonicity constants for various fundamentals.

In the present study of the high resolution infrared spectra of PhCl in the vapour, liquid and solid phases, we have been able to resolve the complex structure of the bands in the region 1650-2000 cm^{-1} and have also explained all the binary combinations in the region 200-4000 cm^{-1} (listed in Appendices 3.1 and 3.2). It has been found that the out-of-plane fundamental vibrations of b_1 and a_2 symmetry, & inplane bending fundamentals of b_2 and a_1 symmetry, form most of the combinations that have been observed.

The most intense composite binary combination in the vapour phase is made of a C-type contour (10a + 18b) at 1126 cm^{-1} along with A-type contour (6a + 12) at 1119 cm^{-1}. The latter combination resulting from two X-sensitive fundamentals could derive its intensity in the vapour phase from another X-sensitive mode 7a which falls at 1092 cm^{-1}, possibly through Fermi-interaction (Chapter I, K). The intensities of the binary combinations, in different phases in general, have been found to be below 20% of the strongest band in the spectra. As the intensity of the combination bands is a complex function of mechanical and electrical anharmonicities (Chapter I, E), it is not possible to give an ab-initio explanation of the observed intensities.

L. ANHARMONIC EFFECTS

The differences between the calculated and observed wave number values of all the binary combinations are given in Appendices 3.1 and 3.2. These differences represent the anharmonicity constants $(w_e^i x_e^i + w_e^j x_e^j)$, where i and j represent the two vibrations involved in the combination. It is observed that the differences lie in the range -4.0 to +6.0 cm^{-1}, though in a few cases they are as high as 10 cm^{-1}. The anharmonicities in overtones are of great importance and are not known even for simple polyatomic molecules. Taking a diatomic approximation for each normal mode they can be easily calculated.

From the observed values of fundamental bands and their first overtones for PhCl molecule in vapour phase, approximate values of $2w_e x_e$ are obtained by subtracting the frequencies of the observed overtones from their harmonic values as shown in Table 3.7. From these values of $2w_e x_e$ the hypothetical values of w_e for all the vibrations for which overtones have been observed are calculated.

The observations reported in Table 3.7 include the data from electronic as well as infrared high resolution vapour phase spectra. The following important features have been observed:

(i) Most of the vibrations have small anharmonicities except 19a, 19b and 3. In case of vibrational mode 3 it is as high as 13.6 cm^{-1}. Some of the vibrations i.e. 8a, 10a, 4 and 17b show negative anharmonicities.

(ii) There is no definite order in which the anharmonicities change from one class of vibrations to another or from higher to lower frequencies and vice versa. Nevertheless overtones of b_1 fundamentals show low anharmonicities compared to the fundamentals of other classes.

(iii) Overtones which appear as strong bands in infrared spectrum of PhCl, show A-type contours and their PR separations are analogous to those of the A-type fundamentals (Chapter VI). This suggests the validity of our assignments of the overtones.

It is interesting to note that, in general, the anharmonicity effects are small and so from the allowed overtones in electronic and infrared spectra, if observed, the estimate of forbidden transition can be made. This criterion has been applied in assigning the infrared inactive fundamental vibrational frequencies of class a_2 from infrared studies; and $\underline{a}_2$ and $\underline{b}_1$ electronically forbidden fundamentals in the electronic spectrum.

M. ISOTOPE EFFECT

No data on isotopic substitution other than that of deuterium are available in literature. This is primarily due to the smallness of the expected isotopic shift and comparatively large inherent band widths in the infrared spectra of both the gaseous and condensed states at ambient temperatures.

We have now been able to detect the effect of the natural abundance of the two isotopic species of chlorine (^{35}Cl and ^{37}Cl) in most of the X-sensitive modes of the molecule on the basis of combined electronic and infrared studies in the vapour phase and infrared studies of their solid films at LNT. The low temperature studies are especially helpful, as due to the reduced half widths of the bands the isotopic splittings are clearly observable. However, for reported ^{13}C isotopic shifts (63-65) we could not draw any conclusive evidence inspite of these favourable conditions.

In Table 3.8 we have listed the observed infrared vapour phase frequencies assigned to ^{35}Cl and ^{37}Cl species. The values in the parentheses are the data from the analysis of the high resolution electronic absorption spectrum where all the planar X-sensitive fundamentals (i.e. 18b, 6a, 12 and 7a) corresponding to the less abundant ^{37}Cl species appear as satellites (with approximately one third the intensity) of the main bands corresponding to the ^{35}Cl species (60). The vapour phase electronic analysis, where bands even within one wave number could be distinguished and identified, was in fact the primary basis for the assignment of the bands due to two isotopic species.

Further corroborative evidence is obtained by extrapolating the expected shifts between ^{35}Cl and ^{37}Cl isotopic species from the known frequencies of the other monohalogenobenzenes (4). In Table 3.9 we have collected the data for all the X-sensitive modes as given by Whiffen (4). From the data, we have plotted a graph (shown in Figure 3.7) between the mass $'M_X'$ of the

substituent and the ratio ν_X / ν_I for each of the X-sensitive modes (where ν_X is the frequency of the substituent, 'X' being Cl, Br or I, and ν_I is the corresponding frequency of the iodobenzene). It is evident that the sensitivity for the X-substitution varies considerably from mode to mode. The extrapolated values (in column 5 of Table 3.8) have been deduced from Figure 3.7. The agreement between the extrapolated and observed shifts as shown in Table 3.8 is quite good. However, for mode 12 the observed shift (1.9 cm^{-1}) is considerably smaller than the extrapolated value (3.0 cm^{-1}). This may be due to the large contribution from phenyl ring modes in this vibration.

N. LOW TEMPERATURE STUDIES

Earlier low temperature infrared (16, 17, 25) and Raman (33,34) studies have been confined to the examination of the effect of phase transition on the CH stretching vibrations (17), determination of low lying fundamentals, lattice vibrations and librational modes (25, 33, 34), by cooling the sample to the desired temperature in the cell. With the changed technique of obtaining the sample at low temperature (Cf. Chapter II) we got either a glassy form or a crystalline form. Our discussion below is related to the crystalline form where we observed specific changes in the infrared spectra in the region 250 - 4000 cm^{-1}.

Half Intensity Band Width: Table 3.10 gives the half intensity band width of some distinct bands in infrared absorption of PhCl in vapour, liquid and solid phases. The half band width of

In the thick deposited films at LNT, certain bands have been observed which can be assigned as the weak combination bands.

Most of the lattice vibrations or librational modes have been reported earlier (33,34) at 49, 67, 86 and 105 cm^{-1} from the low temperature Raman studies of the sample. Although these vibrations do not lie in the range studied by us, a few of their combinations have been observed and are shown in Appendix 3.2.

The difference bands (10a - 16b) at 366.7, (10a - 18b) at 536.8 and (17a - 16a) at 559.1 have not been observed in solid phase (LNT), as there is no possibility of finding enough molecules in the vibrational excited states at LNT in accordance with the Boltzmann distribution.

The overtones of several low lying fundamental modes have not been observed. Those, which have appeared are very weak in intensity in the solid phase (LNT) spectrum.

Splitting of Bands: In PhCl molecule the solid phase splittings do occur in a few fundamental vibrational bands as shown in Appendix 3.2. The possibility of the site group splitting of the infrared bands may be ruled out because there are no degenerate modes of vibration in PhCl. But the factor group splitting may occur due to resonance interaction between inequivalent molecules in the unit cell. It may always be small in magnitude and depend on number of molecules per unit cell. As reported by Biswas et al. (66) and Henshaw (67) PhCl has an orthorhombic

crystal structure, with eight molecules per unit cell. In the two studies (66,67) the unit cell dimensions are fairly in agreement but there is a discrepancy in the suggested space groups. Since the structure is orthorhombic with eight molecules per unit cell, the splitting of the bands would be very complicated. We have observed some of the bands getting split into two. This suggests that the other components may be so close that they could not be resolved.

Relative Shifts: Generally, the difference between the observed vapour phase vibrational frequency (w_{vap}) and the modified frequency (w_{mod}) in other phase is called the shift in the band position. But the useful quantity is $\Delta w = (w_{vap} - w_{mod})/w_{vap}$, which can be used in discussion. From the data listed in Appendices 3.1 and 3.2 the quantity Δw for fundamental vibrational modes of PhCl both in liquid and solid phases (LNT) have been estimated and it is found that,

(i) All the totally symmetric a_1 class vibrations show shift in their band positions towards the low frequency side in going from vapour phase to the state of aggregation. However, the position of the x-sensitive mode at 416.8 cm^{-1} does not show any shift.

(ii) All the vibrations belonging to b_1 and a_2 classes show an increase in frequency, while b_2 class vibrations show a mixed character in the shifts of the band positions with the change of state from vapour to solid (LNT).

(iii) Comparatively larger shifts have been observed in the frequencies 3082 (CH stretch), 614.8 (ring deformation), 981 cm^{-1} (CH bend) and in all the a_2 class vibrations.

(iv) All the CH asymmetric and CH bending vibrations have shown an increase in frequency in the condensed phases.

All these changes may be attributed to the increased intermolecular interactions in the condensed phase and a decrease in the temperature of the sample. The decrease of CCl stretching frequency from 1092.0 cm^{-1} in vapour phase to 1083.7 cm^{-1} in the solid phase infrared spectrum may be indicative of an increased ionic character for CCl bond in PhCl on going from vapour to solid state. This observation supports the earlier studies (38) in vapour and solid states of PhCl.

0. PRESENCE OF MONOMER-DIMER SPECIES AND FERMI INTERACTION IN PhCl VAPOUR

Monomer-Dimer Species: Sirkar et al. (9) have assigned the asymmetry observed on the higher frequency side of the unresolved vapour phase infrared band contours in PhCl below 1600 cm^{-1} (on a low resolution instrument), which disappeared in the liquid phase spectrum, to a monomer-dimer mixture. They have further assumed that only dimers exist in the liquid phase. In the present study, the well resolved infrared band contours prove that their conjecture is untenable. The PhCl exists only as monomeric species in the vapour phase. In fact

the asymmetry of the band contours, which Sirkar et al. (9) have interpreted due to dimers, is only a part of the band envelope in the poorly resolved spectrum. Further, no other convincing evidence has been found for the dimer variety in the state of aggregation.

Fermi Interaction: Lisitsa et al. (68) have suggested Fermi interaction between the combination of mode 4 at 684.6 cm^{-1} and 16a at 403.4 cm^{-1} and the fundamental 15 at 1068 cm^{-1}. Both the combination and the fundamental would belong to b_2 symmetry species and should show B-type band contours. We, on the other hand, have observed one B- and one A-type band in this region, so their suggestion is untenable. Similarly, the Fermi interaction between the overtone of mode 10b at 740.6 cm^{-1} and the fundamental 19a at 1483 cm^{-1} reported earlier (69) could not be justified on the basis of present study.

P. THERMODYNAMIC PROPERTIES

Whiffen (4) used fundamental frequencies of liquid phase and moments of inertia determined by Erlandsson (73) to calculate the thermodynamic properties of PhCl. The spin contributions, isotopic mixing terms and gas imperfection correction were excluded in the computation. So it is worthwhile to recalculate the thermodynamic quantities using precisely determined vapour phase fundamental frequencies, the moments of inertia from the rotational constants determined by Poynter (38) and applying the corrections for isotopic mixing and gas imperfection.

For isotopic mixing the presence of two isotopes of chlorine ^{35}Cl and ^{37}Cl have been taken in the ratio 3:1. The gas imperfection correction has been estimated using the critical temperature and pressure from ref. (76). The symmetry number for over all rotation of the molecule is 2. Thus, the values computed (Cf. Chapter I, Section L) for 1 mole of gas at 1 atmospheric pressure in the temperature range 200 to 1000°K have been listed in Table 3.11.

The values given in columns 3 and 5 of Table 3.11 together with those (75) for C(graphite), H_2(gas), Cl_2(gas) and the experimental value of heat of formation of chlorobenzene gas (72) have been used to calculate ΔHf°_T, ΔGf°_T and $\log_{10} K_p$ for the reaction

$$6C(\text{graphite}) + \frac{5}{2}H_2(\text{gas}) + \frac{1}{2}Cl_2(\text{gas}) = C_6H_5Cl(\text{gas})$$

However the present computations though are slightly different from those of Whiffen (4) yet may be considered more reliable because we have applied the important corrections and used the accurate data.

Whiffen (4) used Stull's (70) calorimetric values of liquid phase entropies, Jones and Bowden's (71) values of latent heat of vapourization and values of vapour pressure from Stull's data (72) to calculate the gas state entropies for PhCl. The reported gas state calorimetric and calculated entropies are 71.8 cal/mole °K and 74.92 cal/mole °K, respectively, while the present computed value is 74.99 cal/mole °K. Whiffen's suggestions, that the Stull's (70) extrapolation

for entropy change in the range 0 - 91^{o}K and the errors in the values of vapour pressure and latent heats are responsible for this large difference between calculated and experimental values, gets further strong support from the present computations; and a direct determination of specific heats below 91^{o}K would be desirable.

Q. REFERENCES

1. J. Lecomte, J. Phys. Radium 8, 489 (1937)

2. R.R. Randle and D.H. Whiffen, Conference on Molecular Spectroscopy Institute of Petroleum, London, pp. 111-123, (1954).

3. R.D. Kross and V.A. Fassel, J. Am. Chem. Soc. 77, 5858 (1955)

4. D.H. Whiffen, J. Chem. Soc. 1350 (1956)

5. E.K. Plyler, H.C. Allen Jr. and E.D. Tidwell, J. Res. Natl. Bur. Std. (U.S.) 58, 255 (1957).

6. A.R. Katritzky and J.M. Lagowski, J. Chem. Soc. 4155 (1958).

7. L.A. Harrah, M.T. Ryan and C. Tamborski, Spectrochim. Acta. 18, 21 (1962).

8. I.N. Khalimonova, Optika i spektroskopia, 13, 791 (1962) Russ.

9. S.C. Sirkar, D.K. Mukherjee and P.K. Bishui, Indian J. Phys. 38, 610 (1964).

10. M.P. Lisitsa and I.N. Khalimonova, Optika i spektroskopia 11, 185 (1961).

11. C.W. Young, R.B. Duvall and N. Wright, Anal. Chem. 23, 709 (1951).

12. D.H. Whiffen, Spectrochim Acta 7, 253 (1955).

13. Y. Kakiuti, J. Chem. Phys. 25, 777 (1956)

14. A.R.H. Cole and A.J. Michell, Spectrochim Acta. 20, 747 (1964).

15. Y. Kakiuti, Y. Suzuki and M. Onda, J. Mol. Spectry. 27, 402 (1968).

16. H. Deslandres, Compt. Rend. 212, 28 (1941).

17. M.P. Lisitsa and I.N. Khalimonova, Optika i spektroskopia, 11, 332 (1961).

18. R. Mierzeki, Acta Phys. Polon. 25, 797 (1964).

19. E.K. Plyler, Discuss. Faraday Soc. 8-9, 100 (1950).

20. J.M. Lebas, J. Chemi. Phys. 59, 1072 (1962)

21. R.J. Jakobson and F.F. Bentley, Appl. spectry. 18, 88 (1964).

22. H.R. Wyss, R.D. Werder and Hs. H. Guenthard, Spectrochim. Acta. 20, 573 (1964).

23. D.H. Brown, Ali Mohammed and D.W.A. Sharp, Spectrochim Acta. 21, 659 (1965).

24. W.R. McWhinnie and R.C. Poller, Spectrochim. Acta. 22, 501 (1966).

25. P.R. Griffiths and H.W. Thomson, Proc. Roy. Soc. 298A, 51 (1967).

26. M. Davies, G.W.F. Parode, J.E. Chamberlain and H.A. Gebbie, Trans. Faraday Soc. 64, 847 (1968).

27. H. Sponer and J.S. Kirby Smith, J. Chem. Phys. 9, 667 (1941)

28. J.W. Murray and D.H. Andrews, J. Chem. Phys. 1, 406 (1933)

29. S. Venkateswaran, Phil. Mag. 15, 263 (1933).

30. R.A. Ananthakrishnan, Proc. Ind. Acad. Sci. 3A, 52 (1936).

31. K.W.F. Kohlrausch and H. Wittek, Monatsh Fur Chemie 74, 1 (1943).

32. D. Chanal, Ed. DeCamps, A. Hadni and H. Wendling, J. Phys. (Paris). 28, 165 (1967).

33. S.C. Sirkar and J. Gupta, Ind. J. Phys. 11, 55 (1937).

34. A.K. Ray, Ind. J. Phys. 24, 111 (1950).

35. K. Venkateswarlu, Proc. Ind. Acad. Sci. 16A, 45 (1942)

36. A.V. Sechkarev and N.I. Dvorovenko, Izv. Vysshikh Ucheb. Zavedenu, Fiz 8, 5(1965) ibid. 8, 13 (1965).

37. M.E. Movesyan, Zh. O. Ninoyan and L.T. Badalyan, Pokl. Akad. Nauk. Arm. S.S.R. 40, 205 (1965).

38. R.L. Poynter, J. Chem. Phys. 39, 1962 (1963).

39. E. Rosenthal, Dissertation Abstract, 24, 3559 (1964)

40. R.P. Bell, H.W. Thomson and E.E. Vago, Proc. Roy. Soc. A 192, 498 (1948).

41. A. Kahane and J. Paillous, Proc. Intern. Meeting, Mol. Spectry, 4th Bologna, 1, 237 (1959).

42. J.R. Scherer, Spectrochim Acta. 19, 601 (1963).

43. T. Shimanouchi, Y. Kakiuti and I. Gamo, J. Chem. Phys. 25, 1245 (1956).

44. Y. Kakiuti and T. Shimanouchi, J. Chem. Phys. 25, 1252 (1956).

45. J.K. Paillous, J. Chim. Phys. 57, 1048 (1960) (Fr.).

46. A.V. Sechkarev, Iav. Vysshikh, Ucheb Zavendenu Fiz, 3, 88 (1961).

47. J.R. Scherer, Spectrochim Acta. 24, 747 (1968).

48. Y. Kakiuti and N. Zasshi, J. Chem. Soc. Japan, pure chem. Sec. 80, 356 (1959).

49. J.R. Scherer, Spectrochim Acta 20, 345 (1964).

50. J.R. Scherer, Spectrochim Acta 23, 1489 (1967)

51. K. Radcliffe and D. Steele, Spectrochim. Acta 25, 597 (1969)

52. Th. G. Scholte, Physica. 15, 450 (1949).

53. A.R.H. Cole and A.J. Michell, Spectrochim Acta. 20, 739 (1964).

54. V.S. Griffiths and G.A.W. Derwish, J. Mol. Spectry, 13, 393 (1964).

55. H.D. Bist, J.C.D. Brand and D.R. Williams, J. Mol. Spectry, 21, 76 (1966).

56. H.D. Bist, J.C.D. Brand and D.R. Williams, J. Mol. Spectry, 24, 402 (1967).

57. H.D. Bist, J.C.D. Brand and D.R. Williams, J. Mol. Spectry, 24, 413 (1967).

58. K. Asagoe and Y. Ikemoto, Proc. Phys. Math. Soc. Japan, 22, 677 (1940).

59. H. Sponer and S.M. Wollman, J. Chem. Phys. 9, 816 (1941).

60. H.D. Bist, V.N. Sarin, A. Ojha and Y.S. Jain: Spectrochim. Acta 26A, 841 (1970).

61. T. Cvitas & J.M. Hollas, J. Mol. Phys. 18, 101 (1970).

62. B.P. Stoicheff, Can. J. Phys. 32, 339 (1954).

63. W. Gerlach, Sitz. Ber, Bay. Akad. Math. Nat. Kl. 39, No. 1 (1932).

64. H.C. Cheng, C.F. Hsueh and T.Y. Wu, J. Chem. Phys. 6, 8 (1938).

65. B.S.R. Rao, J. Chem. Phys. 6, 343 (1938).

66. S.G. Biswas, Acta. Cryst. 11, 882 (1958).

67. D.E. Henshaw, Acta. Cryst. 14, 1080 (1961).

68. M.P. Lisitsa and N.P. Kharchenko, Fix. Mat. Nauk. Sb. Statei 3, 232 (1967).

69. M.P. Lisitsa and N.E. Ralko, Optics and Spectroscopy 24, 284 (1968).

70. D.R. Stull, J. Am. Chem. Soc. 59, 2726 (1937).

71. W.J. Jones and S.T. Bowden, Phil. Mag. 37, 480 (1946)

72. D.R. Stull, Ind. Eng. Chem. 39, 517 (1947).

73. G.E. Erlandsson, Arkiv. Fys. 7, 189 (1953); 8, 341 (1954).

74. D.R. Stull, E.F. Westrum, Jr. and G.C. Sinke, "The Chemical Thermodynamics of Organic Compounds", John Willey and Sons Inc. N.Y. pp. 532.

75. D.R. Stull, I. Carr, J. Chao, T.E. Dergazarian, L.A. du Plessis, R.E. Josted, S. Levine, F.L. Oetting, R.V. Petrella, M. Prophet and G.C. Sinke "JANAF - Thermodynamical Tables", Clearinghouse for Federal Scientific and Technical Information, Springfield Va(1966).

76. "International Critical Tables, Vol 3"Edited by E.W. Washburn, McGraw-Hill Book Co. Inc. N.Y. (1933).

TABLE 3.1

Classification of 30 normal modes of chlorobenzene (assuming C_{2v} point group symmetry)

Symmetry species[a]	ACTIVITY[b]		
	Raman	Infrared	Electronic
11, a_1	R , P	IR, type-A	uv, $B_{\underline{e}}$-type (observed)
10, b_2	R , D	IR, type-B	xx, $A_{\underline{e}}$-type (observed)
3, a_2	R , D	xx	xx, $C_{\underline{e}}$-type (not observed)
6, b_1	R , D	IR, type-C	xx

(a) Nomenclature of species is after Mulliken (Chapter I, Reference 2).

(b) R = Raman active, P = polarized, D = depolarized, IR = infrared active, uv = active in electronic spectra, xx = forbidden, A, B, C, $A_{\underline{e}}$, $B_{\underline{e}}$ and $C_{\underline{e}}$ represent the type of band contour (see text).

TABLE 3.2

Totally symmetric, 'a_1' , fundamental frequencies (in cm^{-1})

Mode	T_o^{**} cm^{-1} Approximate description	37050.924 $^{35}ClC_6H_5$ u.v. 0-1 transition	Infrared		36351.870 OHC_6H_5(a) u.v. 0-1 transition	Infrared
6a	x-sensitive	416.8	416.8	(415)*	526.6	526
12	x-sensitive	706.5	706.0	(701)	823.2	823
1	Ring	1003.7	1003.3	(1003)	999.3	999
18a	CH bend	1025.7	1025.4	(1026)	1025.9	1025
7a	x-sensitive	1092.6	1092.0	(1085)	1261.5	1261
9a	CH bend	1153.0	1153	(1174)	1168.9	1168
19a	CC stretch	1482.3	1483.5	(1477)	-	1501
8a	CC stretch	1586.4	1586	(1580)	-	1603
13	CH stretch	-	3031	(3029)	-	3027
2	CH stretch	-	3054	(3050)	-	3068
20a	CH stretch	-	3082	(3071)	-	3087

** T_o denotes the position of observed 0,0 (origin) peak in the electronic spectrum.

(a) Data taken from Bist and coworkers (56).

* The data in parentheses are from Whiffen (4).

TABLE 3.3

Non-totally symmetric 'b_2' fundamental frequencies (in cm^{-1})

Mode	Approximate description	$^{35}ClC_6H_5$			OHC_6H_5 [a]	
		u.v. 0-1 transition	Infrared		u.v. 0-1 transition	Infrared
18b	x-sensitive	294.7	294.8	(297)*	403.1	403
6b	Ring deformation	614.9	614.8	(616)	618.7	619 [b]
15	CH bend	1067.6	1068	(1068)	1072.4	1070
9b	CH bend	1298.9	1296.3	(1157)	1150.7	1150
3	CH bend	1271.8	1270.5	(1271)	1277.4	-
14	CC stretch	1326.6	1324.8	(1326)	-	1343
19b	CC stretch	1447.2	1448	(1445)	-	1472
8b	CC stretch	1598.2	1598	(1580)	-	1610
7b	CH stretch	-	3067	(3052)	-	3049
20b	CH stretch	-	3096	(3071)	-	3070

[a] Data taken from Bist and coworkers (56).

*The data in parentheses are from Whiffen (4).

[b] Raman shift.

TABLE 3.4

Out of plane 'b_1' fundamental frequencies (in cm^{-1})

Mode	Approximate description	$^{35}ClC_6H_5$		OHC_6H_5[c]	
		Infrared Vapour	U.V. 0 - 1 Transition	Infrared Vapour	U.V. 0 - 1 Transition
11	x-sensitive	197.5[a] (196)*	197.5	244[b]	244.5
16b	x-sensitive	466.9 (467)	466.97	503	502.8
4	CC twist	684.6 (682)	684.51	686	685.9
10b	CH bend	740.5 (740)	740.90	751	750.6
17b	CH bend	902.3 (902)	902.14	881	881.0
5	CH bend	981 (985)	981.18	973	972.5

[a] Has not been observed directly in infrared.

[b] From Raman shift.

* Data in parentheses are from Whiffen (4).

[c] Data taken from Bist and coworkers (56)

TABLE 3.5

Out of plane infrared inactive 'a_2' fundamental frequencies (in cm^{-1})

Mode	Approximate description	$^{35}ClC_6H_5$				OHC_6H_5 [c]	
		U.V.	Infrared			U.V.	Infrared
			Liquid		Solid LNT		
16a	CC twist	403.40	-	(400)*	408.9	408.2	-
10a	CH bend	831.26	830	(830)	849.6	817.2	-
				(832)[b]			
17a	CH bend	961.77	963	(965)	971.7	995.2	-

*Data in parentheses are from Whiffen (4)

[b] Value from Raman Shift

[c] Data taken from Bist and coworkers (56)

TABLE 3.6

The symmetry species of binary combinations in C_{2v} point group

	a_1	b_2	b_1	a_2
a_1	a_1	b_2	b_1	a_2
b_2		a_1	a_2	b_1
b_1			a_1	b_2
a_2				a_1

In the first row and first column of the table the symbols a_1, b_2, b_1 and a_2 represent the species of C_{2v} point group. The symbols in the body of the table represent the symmetry species of the binary combinations.

TABLE 3.7

Overtones (observed and calculated) of fundamental vibrations, their anharmonicities and PR separations (in cm^{-1}) of $^{35}ClC_6H_5$

Mode	OBSERVED			CALCULATED		
	Fundamental	Overtone	PR Separation	Harmonic value of overtone	$2w_ex_e$	w_e
6a	416.8	829.2	-	833.6	4.4	421.2
	(416.8)*	(829.9)		833.6	3.7	420.5
12	(706.5)	(1412.5)	-	1413.0	0.5	707.0
1	(1003.8)	(2006.5)	-	2007.6	1.1	1004.9
7a	1092	2182	-	2184	2.0	1094.0
19a	1483	2955	-	2966	11.0	1494.0
8a	1586	3175	-	3172	-3.0	1583
18b	(294.7)	(588.1)	-	589.4	1.3	296.0
3	1271.8	2530	-	2543.6	13.6	1285.4
9b	1296.3	2590	-	2592.6	2.6	1298.9
19b	1448.0	2885	-	2896	11.0	1459.0
16a	(403.4)	(806.78)		806.8	0.02	403.4
		806	10.8		0.8	404.2
10a	(831.26)	(1664.7)		1662.52	-2.2	829.1
		1662.6	11.0		-0.1	831.1
17a	(961.77)	(1917.7)		1923.5	5.8	967.6
		1920	-	-	3.5	965.3
16b	466.9	932.8	10.5	933.8	1.0	468.0
		(932.9)	-		1.0	468.0
4	684.6	1368.3	10.5		0.9	685.5
		(1369.3)		1369.2	-0.1	684.5
10b	740.6	1480	10.8	1481.2	1.2	741.8
		(1480.53)			0.7	741.3
17b	902.3	1807.6	10.0	1804.6	-3.0	899.3
		(1803.9)			0.7	903.0
5	981.0	1960.8	10.0	1962	1.2	982.2

*Values in the parentheses are from high resolution electronic spectra.

TABLE 3.8

Isotopic shifts (in cm^{-1}) in X-sensitive infrared and ultraviolet absorption bands of chlorobenzene

Mode	Vapour phase				Solid phase LNT		
	Observed		Shifts		Observed		
	$^{35}ClC_6H_5$	$^{37}ClC_6H_5$	Observed	Extrapolated[b]	$^{35}ClC_6H_5$	$^{37}ClC_6H_5$	Shifts
11	-	-	-	1.8	-	-	-
18b	294.8	289	5.8	-	293	288	5.0
	(294.7)[a]	(290.8)	3.9	4.0	-	-	-
6a	416.8	-	-	-	416.8	412	4.8
	(416.8)	(410.0)	6.8	7.0	-	-	-
16b	466.9	-	-	1.5	471.4	466.4	5.0
12	706	704.8	1.2	-	702.5	700.9	1.6
	(706.5)	(704.6)	1.9	3.0	-	-	-
7a	1091.6	1090.2	1.4	-	1084.7	1082.9	1.8
	(1092.6)	(1090.5)	2.1	2.0	-	-	-

[a] Values in the parentheses are from U.V. absorption spectra.

[b] Extrapolated values are obtained by plotting graphs between the mass of the substituents and the corresponding frequencies for each of the modes (Cf. Figure 3.7).

'LNT' denotes liquid nitrogen temperature.

TABLE 3.9

Data from Whiffen (4) for mono-halogenobenzenes for extrapolating the corresponding ^{37}Cl frequency

Substituent with atomic weight[b]	X-sensitive modes and their frequencies (in cm^{-1})					
	11	18b	6a	16b	12	7a
F	241	406	520	501	806	1220
18.9984	(1.452)[a]	(1.845)	(1.955)	(1.118)	(1.232)	(1.151)
^{35}Cl	196	297	415	467	701	1085
34.96885	(1.181)	(1.350)	(1.560)	(1.042)	(1.072)	(1.023)
Br	181	254	314	458	669	1070
79.909	(1.090)	(1.154)	(1.180)	(1.022)	(1.023)	(1.009)
I	166	220	266	448	654	1060
126.9044	1	1	1	1	1	1

(a) Quantity in parentheses is the ratio of the frequency of a vibration and the corresponding mode of Iodine substituent.

(b) Atomic weights of halogens are in amu.

TABLE 3.10

Typical half band widths of some bands (in cm^{-1}) in infrared spectra of chlorobenzene in vapour liquid and solid phases

Mode	Vapour at 22°C		Liquid at 25°C		Solid at -190°C	
	Frequency	Half width	Frequency	Half width	Frequency	Half width
6a	416.8	23.0	416	16	416.8	2.6
1	1003	20.0	1001	4	1001.7	2.6
18a	1025	20.0	1021	5	1018.8	6.4
3	1270	20.0	1270	20	1276.6	2.2
9b	1296	24.0	1296	10	1302.7	1.9

TABLE 3.11

The molal thermodynamic properties of chlorobenzene in the ideal gas state

$T^{\circ}K$	C_p°	$(H^{\circ}-H_o^{\circ})/T$	$-(G^{\circ}-H_o^{\circ})/T$	S°	ΔHf_T°	ΔGf_T°	Log K_p
	Cal/mole $^{\circ}K$				K cal/mole		
200	17.51	10.15	56.13	66.28	13.39	20.27	-22.148
298.16	23.77	13.53	61.46	74.99	12.39	23.68	-17.357
400	30.75	17.04	66.07	83.11	11.48	27.62	-15.090
500	36.53	20.38	70.28	90.66	10.77	31.73	-13.869
600	41.45	23.47	74.30	97.77	10.21	35.94	-13.091
700	44.86	26.27	78.14	104.41	9.76	40.25	-12.566
800	47.87	28.79	81.82	110.61	9.46	44.64	-12.194
900	50.35	31.05	85.35	116.40	9.30	49.13	-11.930
1000	52.44	33.09	88.73	121.82	9.10	53.49	-11.690

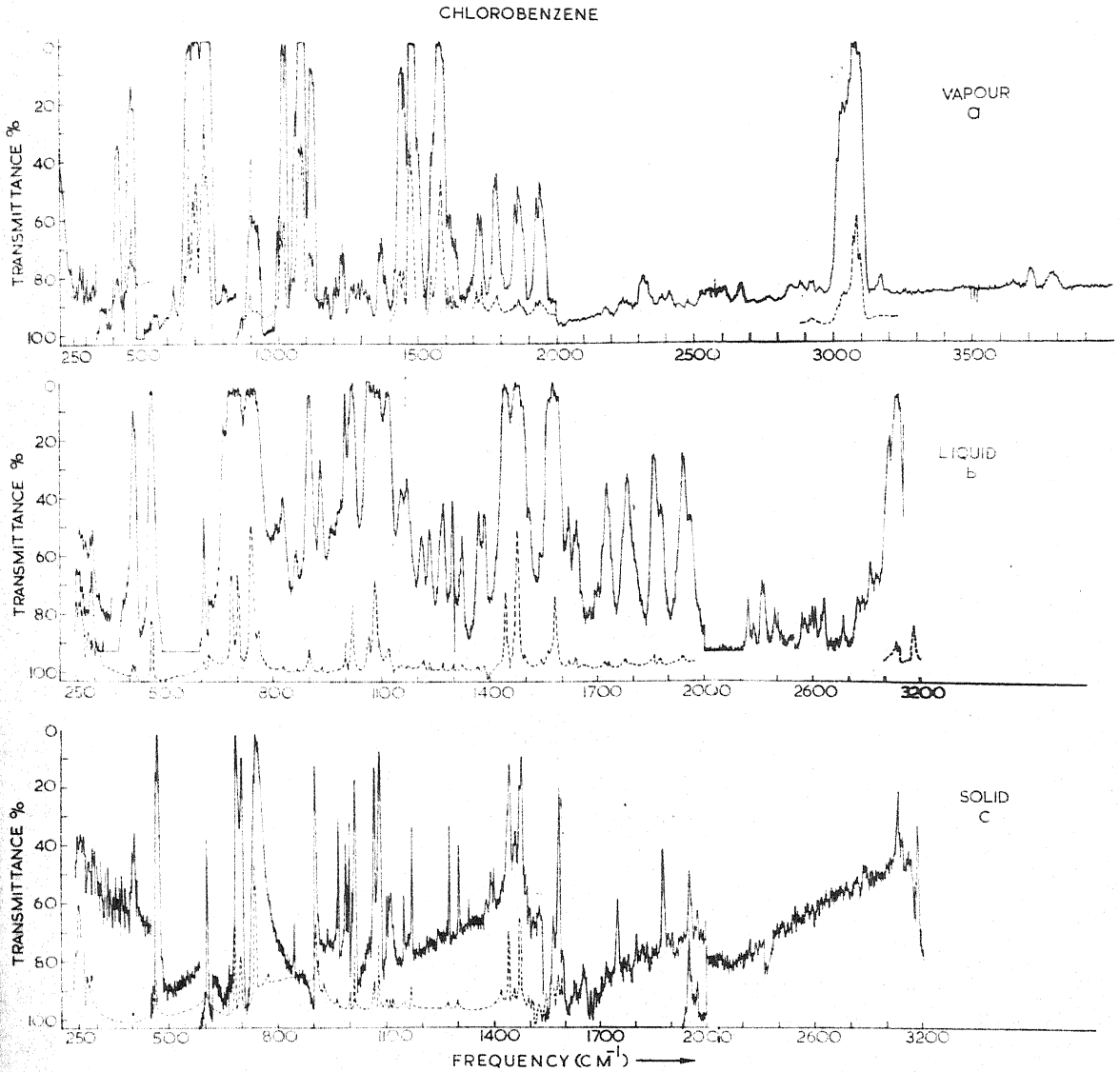

Fig. 3.1 The infrared spectra of chlorobenzene (a) vapour phase spectrum at 10 mm pressure and 1.25 meter path is denoted by_____ and at lower pressure by_____ (b) liquid phase spectrum using 0.05 mm cell is denoted by _____ and of thin film by_____ (c) solid phase spectrum of thick deposit (liquid nitrogen temperature) is denoted by_____ and of thin deposit by_____.

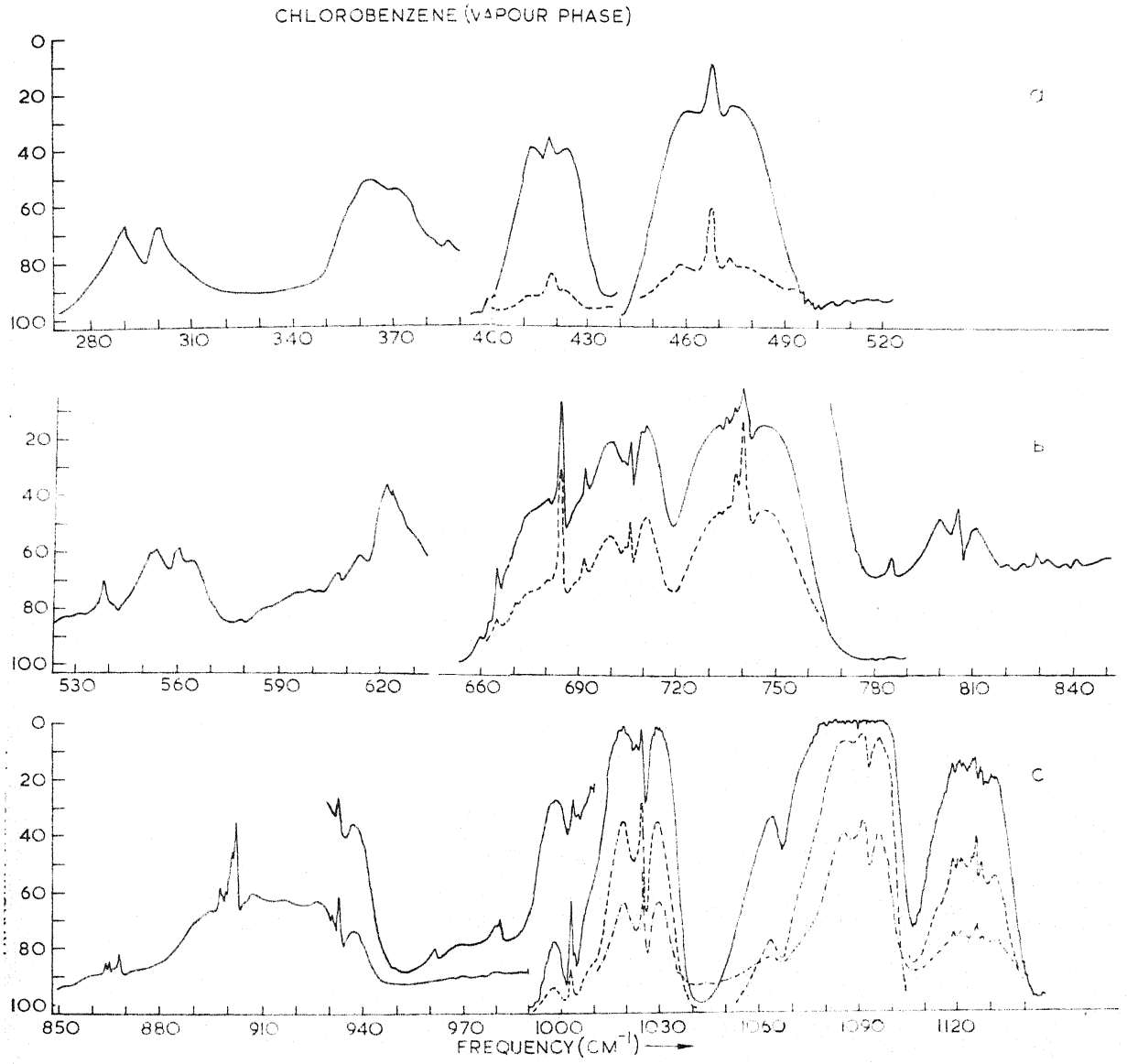

g. 3.2A The infrared spectra of chlorobenzene vapour (a) path length 1.25 meter and 10 mm pressure, below 270 Cm^{-1} the spectrum is ambiguous due to water absorption (b) path length 2.50 meter and 10 mm pressure (c) path length increased to 10 meters in the range 930 – 1010 Cm^{-1}. ____ denotes 10 mm pressure and ____ denotes lower pressure spectrum.

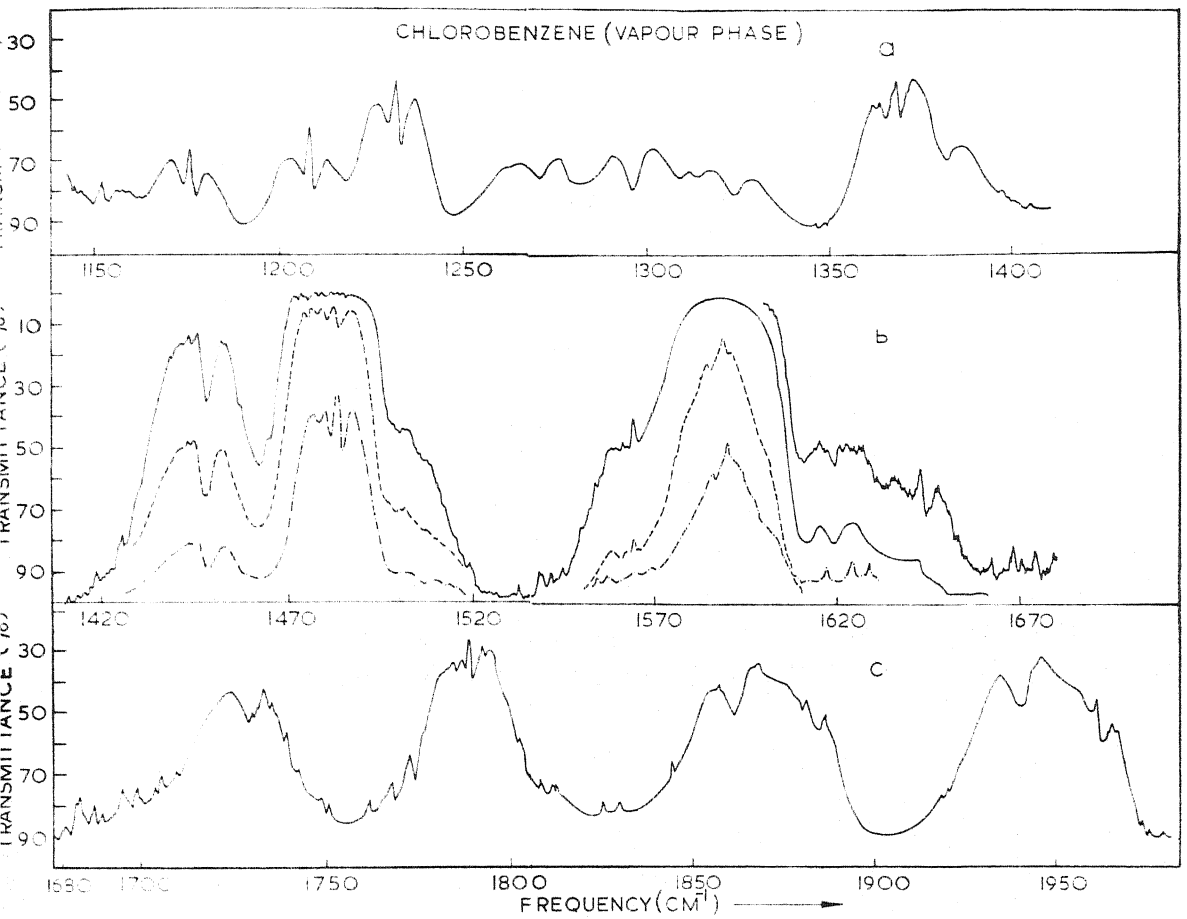

Fig. 3.2B The infrared spectra of chlorobenzene vapour (a) path length 3.75 meter and 10 mm pressure, (b) and (c) path length 1.25 meter and 10 mm pressure._____ denotes 10 mm pressure and___ lower pressure spectrum.

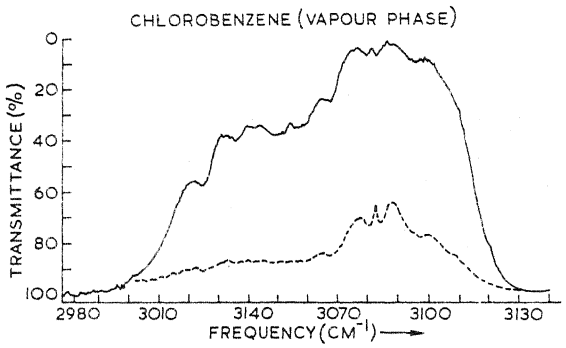

Fig. 3.2C The infrared spectra of chlorobenzene vapour with 1.25 meter path and at 10 mm pressure are denoted by ——— and at lower pressure by ----- .

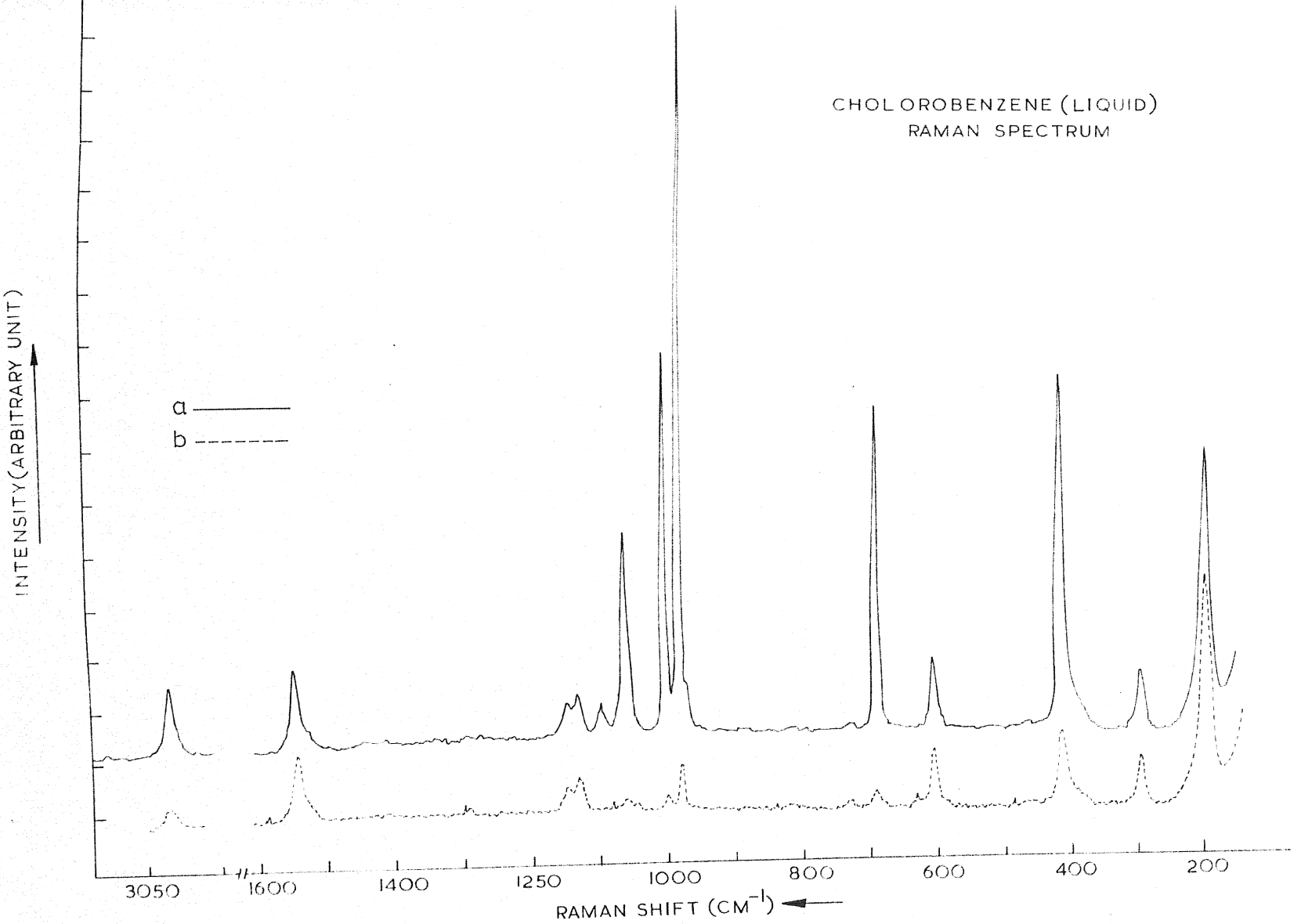

Fig. 3.3A: The Raman spectra of chlorobenzene liquid. 'a' incident light ⊥ to the slit and 'b' incident light ∥ to the slit.

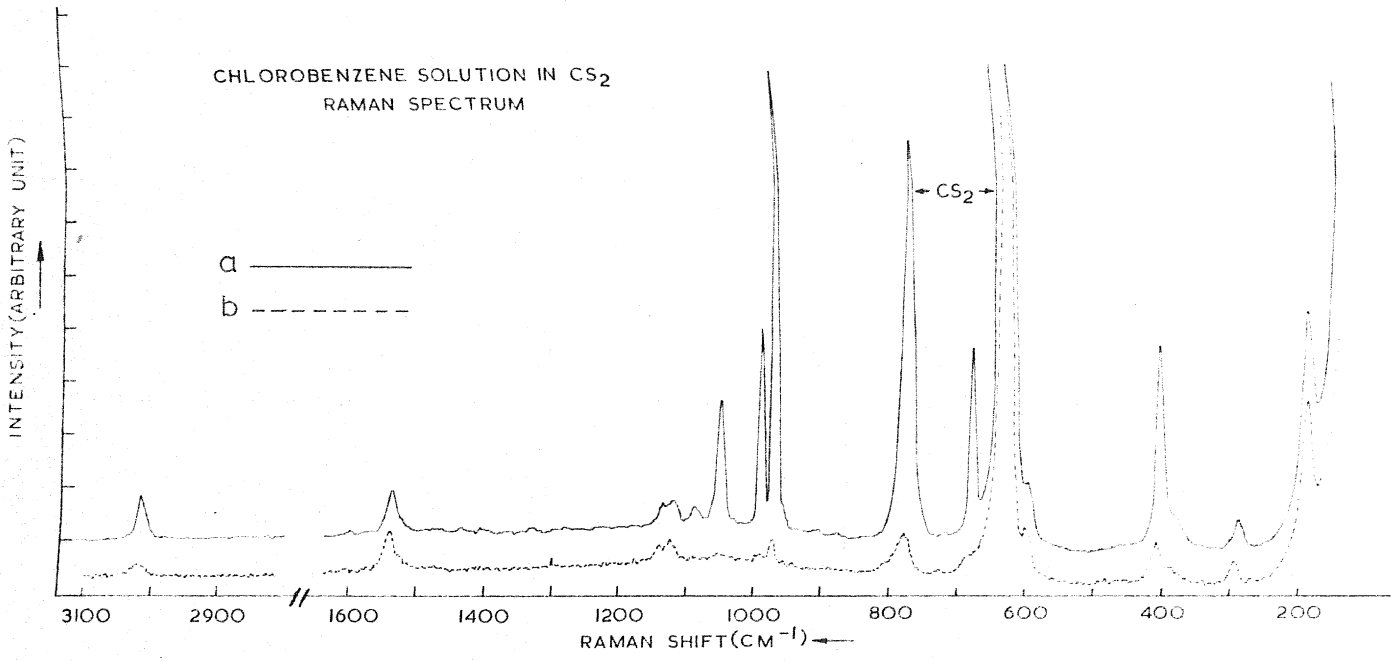

Fig. 3.3B: The Raman spectra of chlorobenzene in CS_2 solution. 'a' incident light polarized $\perp$ to the slit, 'b' incident light polarized $\parallel$ to the slit.

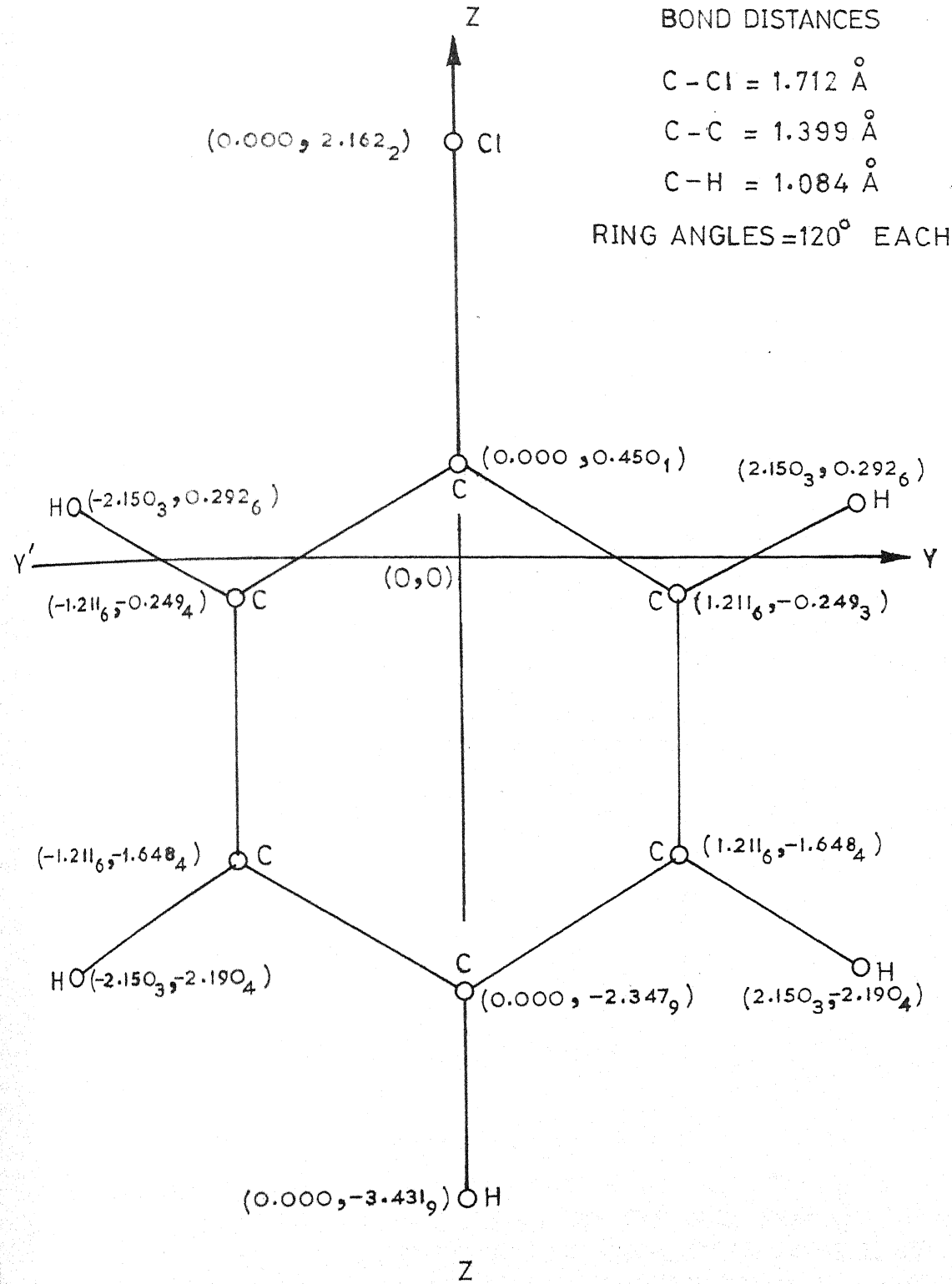

FIG. 3.4 VAPOUR PHASE GEOMETRY OF CHLOROBENZENE IN ITS GROUND STATE. THE NUMBERS IN PARENTHESES DENOTE THE Y,Z COORDINATES (IN Å UNITS) OF THE ATOMS WITH RESPECT TO THE ORIGIN (0,0) THE CENTRE OF MASS OF THE MOLECULE.

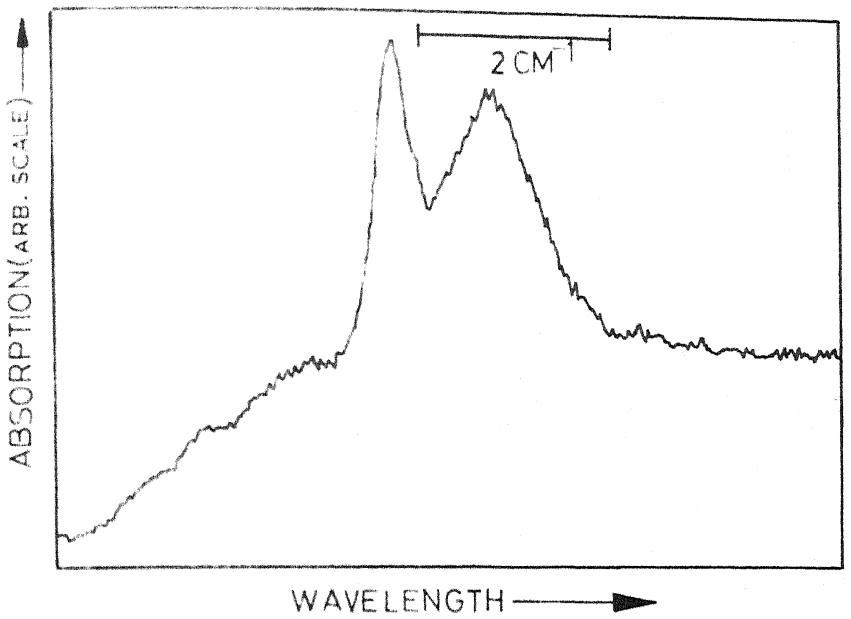

FIG. 3·5(A) THE ORIGIN BAND OF CHLOROBENZENE REPRESENTING A TYPICAL B_e-TYPE CONTOUR IN THE HIGH RESOLUTION ELECTRONIC SPECTRUM.

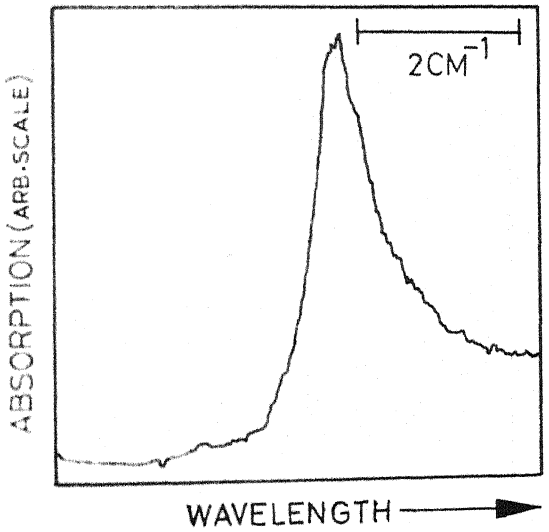

FIG. 3·5(B) REPRESENTATIVE A_e-TYPE BAND CONTOUR IN THE ELECTRONIC SPECTRUM OF CHLOROBENZENE. THIS BAND IS LOCATED TOWARDS SHORTER WAVELENGTH SIDE (BY 424.9 CM^{-1}) OF THE ORIGIN BAND AND IS A COMBINATION, $4_0^1 16a_0^1$, OF TWO OUT-OF-PLANE MODES (TO BE DISCUSSED SEPARATELY) WITH EFFECTIVE b_2 VIBRATIONAL SYMMETRY.

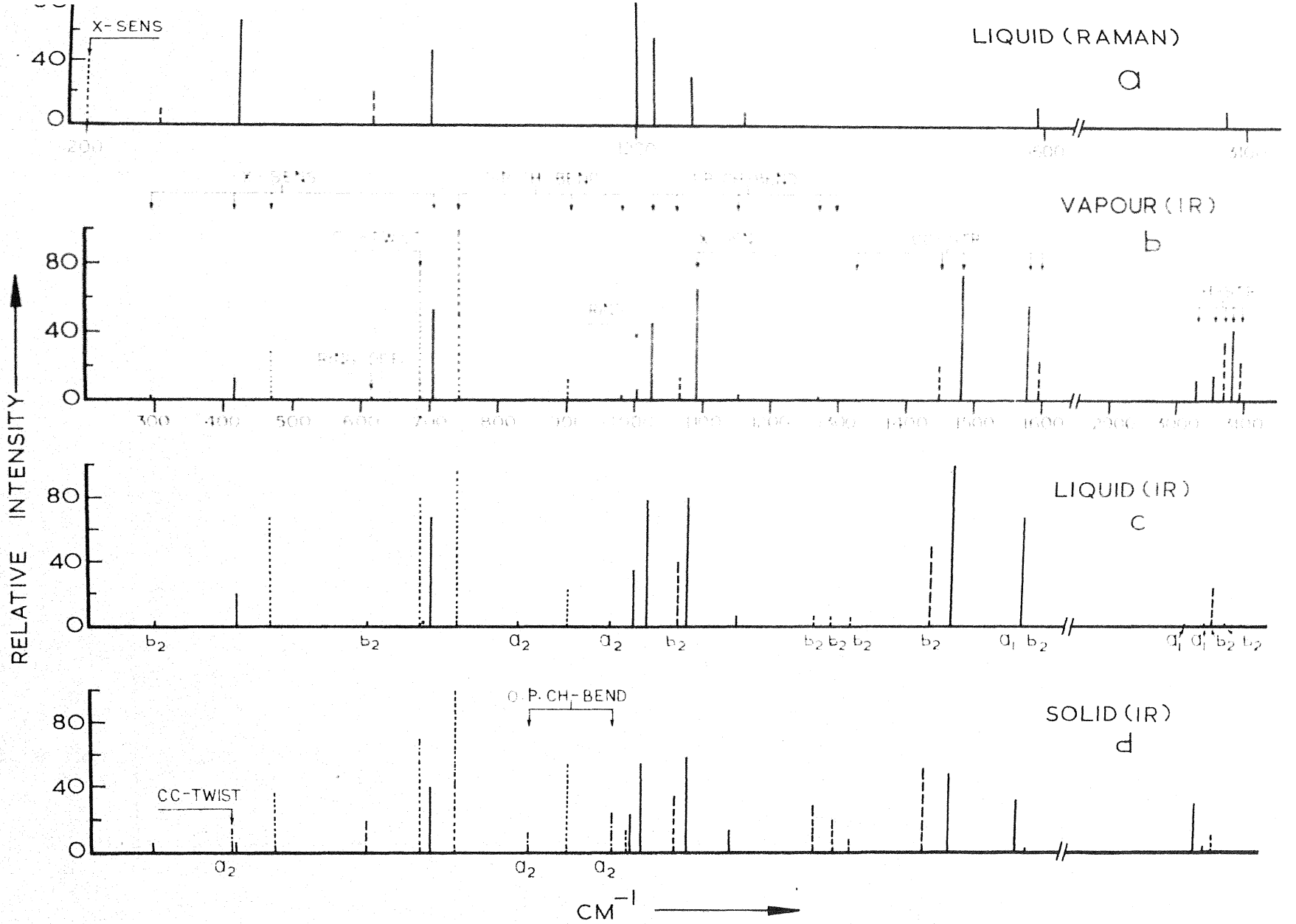

FIG. 3.6 RELATIVE INTENSITIES OF THE VIBRATIONAL MODES OF CHLOROBENZENE: a_1 ———, b_2 – – – – – –, b_1 ····· AND a_2 — — — SPECIES AND RAMAN SHIFTS (IN FIG. a)

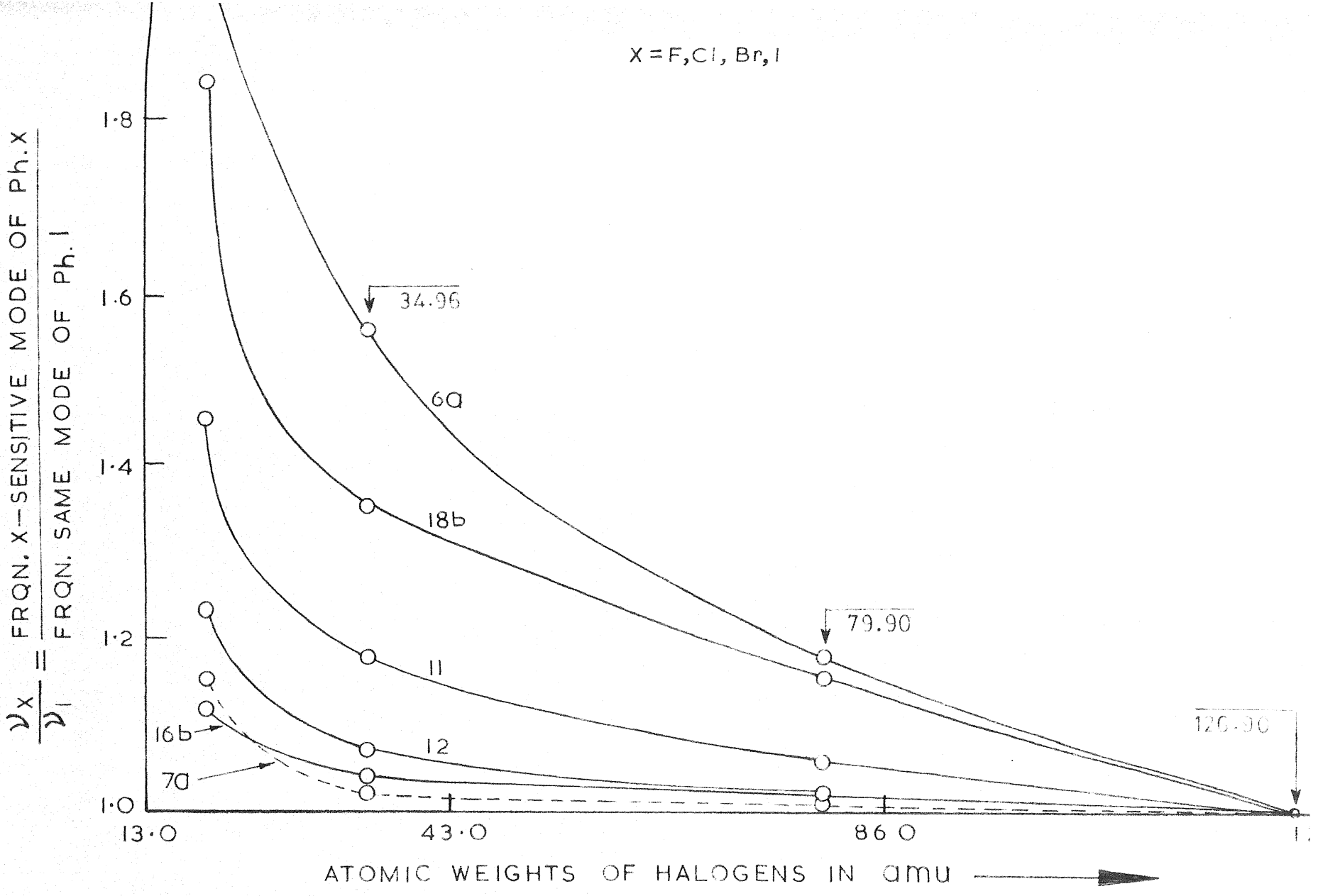

Fig. 3·7 Graphs between ν_X/ν_I and the atomic weights of the halogens for all the X - sensitive modes to extrapolate the isotopic shift due to the presence of ^{35}Cl and ^{37}Cl species in chlorobenzene.

APPENDIX 3.1

Infrared Absorption spectrum of chlorobenzene in vapour phase at 22°C

Frequency in cm^{-1}			Type of contour and PR separation in cm^{-1}	Assignments	Anharmonicity
1			2	3	4
281.5	P				
(288.4)[a]		(7)*	B, 11.0	18b, X-sensitive ^{37}Cl,	
292.4	R			fundamental	
289.4	P				
(294.8)		(15)	B, 10.0	18b, X sensitive ^{35}Cl.	
299.4	R			Fundamental	
361.2	P				
(366.7)		(7)	B, 9.1	10a-16b; 831.3-466.9=364.4 cm^{-1}	-2.3
370.3	R			(may be two B-type contours)	
411.8	P				
416.8	Q	(26)	A, 10.4	6a, X-sensitive Fundamental	
422.2	R				
459	P				
466.9	Q	(50)	C, 15	16b, X-sensitive Fundamental	
474	R				
536.8			C	10a-18b; 831.3-294.8=536.5 cm^{-1}	-0.3
552.3	P				
559.1	Q	(1)	A, 10.50	17a-16a, 961.8-403.4=558.4 cm^{-1}	-0.7
562.8	R				
605.2				16a+11, 403.4+197.5 = 600.9	-4.3
612.2	P				
(614.8)			B, 6.6	6b, ring Fundamental	
618.8	R				
620.2			C	6a+11, 416.8+197.5=614.3	-5.9
664.8		(64)		16b+11, 466.9+197.5=664.4	-0.4
676	P				
684.6	Q	(96)	C, 14	4, CC twist Fundamental	
690	R				
692		(88)	C	16a+18b, 403.4+294.8=698.2	6.2
699.5	P				
703.8				12, X-sensitive Fundamental ^{37}Cl	
706.0	Q	(92)	A, 11.0	12, X-sensitive Fundamental ^{35}Cl	
710.5	R				

Contd. ...

1		2		3	4
732	P				
738				9a-6a; 1153-416.8=736.2 cm^{-1}	-1.8
740.6	Q (100)	C,	15	10b, CH bend fundamental	
747.0	R				
785				?	
800	P				
806	Q (3)	A,	10.6	Overtone of 16a, 2(403.4)=806.8 cm^{-1}	0.8
810.6	R				
825	P				
829.2	Q	A,	7.8	Overtone of 6a, 2(416.8)=833.6 cm^{-1}	4.4
832.8	R				
840.6				?	
864	P				
868	Q (6)	A,	10.0	4+11, 684.6+197.5=882.1 cm^{-1}	14.1
874	R				
897.5	(29)			12+11, 706+197.5=903.5 cm^{-1}	6.0
902.3	(13)	C,		17b, CH bend Fundamental	
926.5	P				
931.0				Overtone of 16b ^{37}Cl	
932.8	Q (11)	A,	10.5	Overtone of 16b ^{35}Cl, 2(466.9)	1.0
937.0	R			? =933.8 cm^{-1}	
961				?	
968				?	
979.2					
981		C,		5,CH bend Fundamental	
998	P				
1003.3	Q (11)	A	10.4	1, ring Fundamental	
1008.4	R				
1019.4	P				
1025.4	Q (67)	A	10.6	18a, CH bend Fundamental	
1030.0	R				
1064	P				
(1068)	(21)	B	8.5	15,CH bend Fundamental	
1072.5	R				
1085.4	P				
1092.0	Q (83)	A	10.8	7a, CCl Stretch Fundamental	
1096.2	R				

Contd. ...

1		2		3	4
1119				10a+18b, 831.3+294.8=1126.1	7.1
1121	P				
1126	Q	(44)	A, 10.5	6a+12, 416.8+706=1222.8	-3.2
1131.5	R				
(1146)					
1153	Q	(2)	A, 11.0	9a, CH bend Fundamental	
1157	R				
1170.5	P				
1175.5	Q	(2)	A, 9.8	5+11, 981+197.5=1178.5 cm^{-1}	3.0
1180.3	R				
1202	P				
1208	Q	(2)	A, 10.0	10b+16b, 740.5+466.9 = 1207.5 cm^{-1}	-0.6
1212	R				
1226	P				
1232	Q	(6)	A, 11.0	10a+16a, 831.3+403.4=1234.7 or	2.7
1237	R				
1265	P				
(1270.5)		(2)	B, 10.0	3, CH bend Fundamental	
1275	R				
1291	P				
(1296.3)		(2)	B, 11.0	9b, CH bend Fundamental	
1302	R				
1312		(1)		?	
1318	P				
(1324.8)		(1)	B, 11.3	14, CC stretch Fundamental	
1329.3	R				
1362.5	P				
1364		(8)		17a+16a, 961.8 + 403.4=1365.2 cm^{-1}	1.2
1368.3	Q	(1)	A, 10.5	Overtone of 4, 2(684.6)=1369.2 cm^{-1}	0.9
1373.0	R				
1385.4				7a+18b, 1092+294.8=1386.8 cm^{-1}	4.8
1442.0	P				
1443.5					
1445.5				10a+6b, 831.3+614.8=1446.1 cm^{-1}	-1.9
(1448)		(42)	B, 10.5	19b, CC stretch Fundamental	
1452.5	R				

Contd. ...

1	2			3	4
1477	P				
1480				Overtone of 10b, 2(740.6)=1481.2 cm^{-1}	1.2
1483	Q	(70)	A, 10.8	19a, CC stretch Fundamental	
1487.8	R				
1558.6	P				
1564.4	Q	(19)	A, 10.8	9a+6a, 1153+416.8=1569.8 cm^{-1}	5.4
1569.4	R				
1581	P				
1586	Q	(70)	A, 9.0	8a, CC stretch Fundamental	
1590	R				
1594	P				
(1598)		(72)	B, 8.0	8b, CC stretch Fundamental	
1602	R				
1616.4	P				
1623.2	Q	(4)	A, 11.2	18b+14,294.8+1326=1620.8 cm^{-1}	-2.4
1627.6	R				
1636	P				
1643	Q	(4)	A, 11.5	10b+17b, 740.6+902.3=1642.9 cm^{-1}	-0.1
1647.5	R				
(1657)					
1662.6	Q		A, 11.0	Overtone of 10a, 2(831.3)=1662.6	0.0
1666	R				
1668.4	P				
1671				3+16a, 1270.5+403.4=1673.9 cm^{-1}	2.9
1674.4	Q	(5)	A, 11.2	15+6b, 1068+614.8=1682.8 cm^{-1}	8.4
1679.6	R			(composite band)	
1683.6		(4)	C,	19a+11; 1483+197.5=1680.5 cm^{-1}	-3.1
1687.4		(4)	C,	5+12, 981+706=1687 cm^{-1}	-0.4
1689.3	P				
1694.8	Q	(4)	C, 14.7	18a+4, 1025.4+684.6=1710 cm^{-1}	15.2
1699.0	P				
1404	R				
1708	Q	(8)	A, 11.0	12+1; 706+1003.3=1709.3 cm^{-1}	1.3
1710	R				
1723.6	P				
(1729)		(9)	B, 9.4	10a+17b, 831.3+902.3=1733.6 cm^{-1}	4.6
1733	R				

Contd. ...

1		2		3	4
1739	P				
1748.6	Q		A, 11.8	19b+18b, 1448+294.8=1742.8 cm^{-1}	-5.8
1750.8	R				
1761.8	P				
1767.6	Q	(3)	C, 10.4	10b+18a, 740.5+1025.4=1765.9 cm^{-1}	-1.7
1772.2	R				
1784	P				
1788.4	Q	(13)	A, 10.2	17a+10a, 961.77+831.3=1793.07 cm^{-1}	4.7
1794.2	R				
1802.2	P				
1807.6	Q		A, 9.8	Overtone of 17b, 2(902.3)=1804.6 cm^{-1}	-3.0
1812.0	R				
1825	P				
1830	Q		A, 9.0	2(6a)+1; 833.6+1003.3=1836.9	6.9
1834	R				
1844.4		(6)	C,	19b+16a; 1448+403.4=1851.4	7.0
1856	P				
(1862)		(11)	B, 11.6	17a+17b, 961.77+902.3=1864.1 cm^{-1}	2.1
1867.6	R				
(1876)	P				
1882	Q	(6)	A, 10.8	17b+5, 902.3+981=1883.3 cm^{-1}	1.3
1886.8	R				
1920			A,	Overtone of 17a, 2(961.77)=1923.5 cm^{-1}	3.5
1934.4	P				
(1940.8)		(11)	B, 11.2	5+17a, 981+961.77=1942.8 cm^{-1}	2.0
1945.6	R				
1955	P				
1960.8	Q	(6)	A, 10.0	Overtone of 5, 2(981)=1962 cm^{-1}	1.2
1965	R				
1980				1+5, 1003.3+981=1984.3 cm^{-1}	4.3
2182				Overtone of 7a, 2(1092)=2184 cm^{-1}	2.0
2245				9b+17a, 1296.3+961.77=2258.1 cm^{-1}	13.0
2260				8a+4, 1586+684.6=2270.6 cm^{-1}	10.6
2325				8a+10b, 1586+740.6=2326.6 cm^{-1}	1.6
2353		(15)		15+9b; 1068+1296.3=2364.3 cm^{-1}	11.3
2390		(18)		14+15. 1326+1068=2394 cm^{-1}	4.0
2418				17a+19b, 961.77+1448=2409.7 cm^{-1}	-8.3

contd. ...

1		2		3	4
2480				19a+1, 1483+1003.3=2486.3 cm^{-1}	6.3
2530				Overtone of 3, 2(1270.5)=2541.0 cm^{-1}	11.0
2560				8b+17a, 1598+961.77=2559.77 cm^{-1}	-0.3
2590				8a+1, 1586+1003.3=2589.3 cm^{-1}	-0.7
2610				8a+18a, 1586+1025.4=2611.4 cm^{-1}	1.4
2672				8a+7a, 1586+1092=2678 cm^{-1}	6.0
2772				19a+9b, 1483+1296.3=2779.3 cm^{-1}	7.3
2845				8a+3, 1586+1270.5=2856.5 cm^{-1}	11.5
2885				Overtone of 19b, 2(1448)=2896 cm^{-1}	11.0
2918				8b+14, 1598+1326=2924 cm^{-1}	6.0
2930				19a+19b, 1483+1448=2931 cm^{-1}	1.0
2955				Overtone of 19a, 2(1483)=2966	11.0
3022				8a+19b; 1586+1448=3034 cm^{-1}	12.0
3031		(12)		13a, CH stretch Fundamental	
3034	P				
3039	Q	(12)	A, 10.0	8b+19b, 1598+1448=3046 cm^{-1}	7.0
3044	R				
3054.0		(15)	A	2, CH stretch Fundamental	
3065	P				
(3067)		(35)	B, 9.0	7b, CH stretch Fundamental	
3074	R				
3077	P				
3082	Q	(43)	A, 11.0	20a, CH stretch Fundamental	
3088	R				
(3096)		(23)	B	20b, CH stretch Fundamental	
3099	R			(overlapped band)	
3175				Overtone of 8a; 2(1586)=3172 cm^{-1}	-3.0
3650				13a+6b, 3031+614.8=3645.8 cm^{-1}	-4.2
3708				13a+4, 3031+684.6=3715.6 cm^{-1}	7.6
3790				20a+12, 3082+706=3788 cm^{-1}	-2.0

*Number in parentheses indicates relative peak height of the absorption band.

aFrequency in parentheses indicates minimum in case of B-type contour or graphically resolved arm of A- or C-type contours in overlapped bands.

A, B and C denote the type of band contours observed and are discussed in section (F).

APPENDIX 3.2

Infrared Absorption spectrum of chlorobenzene in liquid (25°C) and solid (-190°C) phases

Liquid phase frequency cm^{-1}		Solid phase frequency cm^{-1}		Assignments	Remarks**
1		2		3	4
		281	(5)*	11+85 (Libration), 197.5+85 = 282.5 cm^{-1}	1.5
		288		18b, X-sensitive, ^{37}Cl	
294	(2)	293	(5)	18b, X-sensitive, ^{35}Cl Fundamental	Isotopic
		403.2	Sh		Crystal
		408.9	(15)	16a, CC twist Fundamental	effect
		412.0		6a, X-sensitive, ^{37}Cl	
416	(20)	416.8	(7)	6a, X-sensitive, ^{35}Cl Fundamental	Isotopic
		466.4	Sh	16b, X-sensitive ^{37}Cl	
464	(68)	471.4	(36)	16b, X-sensitive ^{35}Cl Fundamental	Isotopic
		601.5	Sh		Crystal
608	(2)	607.6	(20)	6b, ring, Fundamental	effect
660	(1)	667.5	(5)	11+16b, 197.5+471.4=668.9 cm^{-1}	1.4
686.8	(80)	687.5	(70)	4CC twist, Fundamental	
		690.2	Sh	6b+85 (libration) 607.6+85=692.8	2.8
		700.9	Sh	12, X-sensitive ^{37}Cl Fundamental	Isotopic
702.2	(68)	702.5	(40)	12, X-sensitive ^{35}Cl Fundamental	
		739.8	Sh	4+49 libration, 687.5+49=736.5	Crystal
		741.9	Sh		effect
738.2	(97)	747.3	(100)	10b, CH bend Fundamental	
746.3				2(6b)-16b, 1212-464=748	1.7
758.3				16b+18b, 464+294=758	-0.3
811.2				6b+11, 608+199=807	-4.2
831.5	(3)	849.7	(12)	10a, CH bend Fundamental	
867.3				16b+6a, 464+416=880	12.7
902.6	(23)	907.1	(55)	17b, CH bend Fundamental	
		909.1	Sh	6b+18b, 607.6+293=900.6	-8.5
		917.2		10a+67 (libration), 849.7+67=916.7	Thick film
935.6	(6)	932.2		Overtone of 16b, 2(466.4)=932.8	0.6
		940.6	(3)	Overtone of 16b, 2(471.4)=942.8	2.2
		966.9	(8)	18b+4, 288+687.5=975.5	8.6
964.2	(1)	971.8	(30)	17a, CH bend, Fundamental	
		992	(22)	18b+12, 293+702.5=995.5	3.5
		995.3	(12)	5CH bend Fundamental	
1000.8	(35)	1001.7	(25)	1, Ring, Fundamental	
		1009	Sh	17b+102 libration, 907.1+102=1009.1	0.1
1020.7	(78)	1017	(55)	18a, CH bend, Fundamental	
		1055	(4)	17a+85 libration, 971.8+85=1056.8	1.8
		1068	Sh		Crystal
1067.9	(41)	1070	(35)	15, CH bend, Fundamental	effect

Contd. ...

1		2		3	4
1083	(80)	1082.9	Sh		} Crystal
		1084.7	(58)	7a, CCl stretch Fundamental	} effect
		1103.8	(15)	6a+4, 416.8+687.5=1104.3 cm^{-1}	0.5
		1110	Sh	412+700.9=1112.8 cm^{-1}	2.8
		1116.7	(16)	6a+12, 416.8+702.4=1119.2 cm^{-1}	3.5
1156	(5)	1149.6	(12)	9a, CH bend Fundamental	} Crystal
		1151	Sh		} effect
		1171.5	Sh	11+17a, 197.5+966.9=1164.4 cm^{-1}	-7.1
1170	(5)	1173.4	(25)	11+17a, 197.5+971.8=1169.3 cm^{-1}	-4.1
1212	(2)	1213	(3)	Overtone of (6b), 2(607.6)=1215.2	2.2
1233	(5)	1243	(4)	2(16b)+18b, 942.8+293=1235.8	-7.2
1271.6	(6)	1271.3	Sh	11+7a, 197.5+1084.6=1282.1	10.8
		1277.6	(28)	3, CH bend Fundamental	
		1303.7	Sh	9b, CH bend Fundamental	
1323.6	(5)	1333.2	(8)	14, CC stretch Fundamental	
1368.8	(6)			?	
1384.2	(6)	1380.2	(4)	Overtone of 4, 2(687.5)=1375.0	-4.8
		1392.4	(7)	6a+17a, 416.8+971.8=1388.6	-3.8
		1394.4	Sh	412+971.8=1383.8	-10.6
		1400.3	(8)	Overtone of 12, 2(702.5)=1403	2.7
		1403.4	Sh	Overtone of 12, 2(700.8)=1401.6	-1.8
		1435.8		6a+18a, 416.8+1017.4=1434.2	-1.6
		1438.6		6a+18a, 412+1017.4=1429.4	-9.2
1443.6	(50)	1443.3	(52)	19b, CC stretch Fundamental	
		1458.4	(6)	10a+6b, 849.7+607.6=1457.3	1.1
		1471.7	Sh		} Crystal
		1474.7	Sh		} effect
1476.7	(100)	1478.5	(47)	19a, CC stretch Fundamental	
		1484.2		2(739.8)=1479.6	-4.6
		1490.7		Overtone of 10b, 2(741.9)=1483.8	-6.9
1492.2	W	1495.5		Overtone of 10b, 2(747.3)=1494.6	-0.9
1512.3	W	1526.4	W	2(6a)+12, 833.6+702.4=1536.0	10.0
1556	W	1554.2	W	10a+12, 849.7+702.4=1552.1	-2.1
1564.6	W	1565.7	(10)	6a+9a, 416.8+1149.6=1566.4	0.7
		1567	Sh	6a+9a, 416.8+1151=1567.8	0.8
1582.5	(68)	1580.2	(32)	8a, CC stretch Fundamental	
		1594	Sh	8b, CC stretch Fundamental	
1620.6	(3)	1629.1	(4)	18b+14, 293+1333.2=1622	-2.9
1641	(4)	1647.8	(8)	10b+17b, 747.3+907.1=1654.4	6.6
		1684	(3)	4+5, 687.5+992=1679.5	-4.5
		1704	(3)	Overtone of 10a, 2(849.7)=1699.4	-4.6
1724	(8)	1718	(5)	6a+9b, 416.8+1304.2=1721.0	3.0
1740	Sh	1748	(12)	10a+17b, 849.7+907.1=1756.8	8.8
		1750	Sh	10a+17b, 849.7+909.1=1758.8	8.8
1785	(9)			12+7a, 702.2+1083=1785.2	0.2
1800		1802.6	(6)	Overtone of 17b, 2(907.1)=1814.2	11.6
		1818	(5)	10a+17a, 849.7+971.8=1821.5	3.5
		1830	(4)	10b+7a, 747.3+1084.6=1831.9	1.9
1857	(9)	1866.4	(5)	18b+8a, 293+1580.2=1873.2	6.8
1878		1877.7	(16)	17b+17a, 907.1+971.8=1878.9	1.2

APPENDIX 3.3

The Raman spectral data of chlorobenzene

PRESENT DATA				KOHLRAUSCH et. al.[b]		Assignment
Liquid		Solution in CS_2		Liquid		
Frequency (cm^{-1})	Dp. ratio	Frequency (cm^{-1})	Dp. ratio	Frequency (cm^{-1})	Dp. ratio	
199(40)[a]	0.87	198(50)	0.77	196(150)	0.66	11, X-sensitive
277(.07)	–	–	–	–	–	–
298(9)	0.83	298(6)	0.83	297(23)	0.72	18b, X-sensitive
328(0.7)	–	–	–	–	–	
396(5)	0.30	397(7)		382(00)	–	16a
419(50)	0.23	420(44)	0.10	418(77)	0.28	6a, X-sensitive
469(0.7)	–	–	–	467(0)		16b, X-sensitive
598(1.5)	1.0					16a+11
615(11)	0.80	616(15)	0.80	615(31)	0.74	6b, ring
700(47)	0.07	704(40)	0.11	702(60)	0.21	12, X-sensitive
740(0.7)	1.0	743(1)	–	741(7)	–	10b, CH bend
811(0.7)	0.0	–	–	–	–	Overtone, 16a
839(0.7)	0.0	–	–	832(8)	–	19b-6b
				934(0)		?
992(6)	0.11	994(6)	–	987(13)		12+18b
1004(100)	0.06	1005(100)	0.05	1002(225)	0.05	1, ring
				1013(0)		?
1025(59)	0.05	1025(41)	0.05	1024(121)	–	18a, CH bend
1072(2)	–	–	–	–	–	15, CH bend
1085(28)	0.05	1087(25)	0.03	1083(71)	0.10	7a, X-sensitive
1125(4)	0.01	1128(3)	–	1121(2)	–	6a+12
1161(6)	0.75	1162(4)	1.0	1157(3)	0.9	9a, CH bend
1177(5)	0.71	1178(4)	0.75	1174(1)	0.5	5+11
1270(0.7)	1.0	–	–	–	–	3, CH bend
				1294(00)		?
1310(0.7)	1.0	–	–	–	–	?
1332(0.7)	–	–	–	1322(0.5)	–	14, CC stretch
1377(0.7)	–	1374(1)	–	1372(0)	–	Overtone of 4
				1399(0)	–	
1455(0.7)	–	1458(1)	–	1443(1)	–	19b, CC stretch
1488(0.7)	–	–	–	1479(1)	–	19a, CC stretch
1569(3)	0.50			1563(1)		9a+6a
1592(12)	0.76	1594(9)	1.0	1582(50)	0.68	8a&8b CC stretch
				1614(00)		?
				2545(0)		?
				2562(0)		?
2686(0.7)	–	–	–	–	–	8a+7a
				3005(0.5)		?
				3024(0)		?
3038(0.7)				3051(4)	0.31	8b+19b
3078(9)	0.34	3082(9)	0.25	3068(10)	0.31	20a, CH stretch
				3132(0)		?
3175(1)		–	–	3163(1)	–	Overtone of 8a

a. Number in parentheses denotes the intensity of the Raman shift on an arbitrary scale. b. Data from Kohlrausch et.al. (31).

Band positions and relative intensities. The intensities (in parantheses) are relative to origin band (0,0) = 100 in the electronic spectrum

Assignments	Frequency (cm^{-1})	Assignments	Frequency (cm^{-1})
0,0(origin)	37050.92(100)	14_1^0	35724.36(.2)
$i_{18\underline{b}_1}{}^0$	36760.15(2)	$15_1^0\ 18\underline{b}_1{}^0$	35689.60(.2)
$18\underline{b}_1{}^0$	36756.22(6)	$7\underline{a}_1{}^0 18\underline{b}_1{}^0$	35664.80(.1)
$i_{6\underline{a}_1}{}^0$	36640.53(2)	12_2^0	35638.48(.3)
$6\underline{a}_1{}^0$	36634.13(8)	$1_1^0\ 6\underline{a}_1{}^0$	35630.54(.2)
$18\underline{b}_2{}^0$	36463.41(2)	$6\underline{a}_1{}^0\ 18\underline{a}_1{}^0$	35609.13(.06)
$6\underline{b}_1{}^0$	36436.02(9)	$19\underline{b}_1{}^0$	35603.09(.03)
$i_{12_1}{}^0$	36346.32(2)	$9\underline{a}_1{}^0\ 18\underline{b}_1{}^0$	35581.40(.02)
12_1^0	36344.44(8)	$19\underline{a}_1{}^0$	35568.64(.1)
$6\underline{a}_2{}^0$	36220.98(1)	$6\underline{a}_1{}^0\ 15_1^0$	35565.44(.03)
$12_1^0\ 18\underline{b}_1{}^0$	36051.52(.2)	$6\underline{a}_1{}^0\ 9\underline{b}_1{}^0$	35467.87(.05)
1_1^0	36047.13(3)	$8\underline{a}_1{}^0$	35464.48(.02)
$18\underline{a}_1{}^0$	36025.25(2.5)	$8\underline{b}_1{}^0$	35452.73(.05)
$6\underline{a}_1{}^0\ 6\underline{b}_1{}^0$	36017.50(1)	$1_1^0\ 6\underline{b}_1{}^0$	35431.08(.2)
15_1^0	35983.29(.5)	$6\underline{b}_1{}^0\ 18\underline{a}_1{}^0$	35410.48(.06)
$i_{7\underline{a}_1}{}^0$	35960.39(.3)	$3_1^0\ 6\underline{a}_1{}^0$	35362.98(.06)
$7\underline{a}_1{}^0$	35958.32(1.5)	$6\underline{b}_1{}^0\ 7\underline{a}_1{}^0$	35343.84(.1)
$6\underline{a}_1{}^0\ 12_1^0$	35927.54(.8)	$1_1^0\ 12_1^0$	35340.96(.1)
$9\underline{a}_1{}^0$	35897.90(1)	$12_1^0\ 18\underline{a}_1{}^0$	35319.76(.03)
$9\underline{b}_1{}^0$	35883.82(.3)	$12_1^0\ 15_1^0$	35276.09(.04)
$6\underline{b}_2{}^0$	35824.95(.5)	$6\underline{b}_1{}^0\ 9\underline{a}_1{}^0$	35258.97(.04)
3_1^0	35779.14(.2)	$7\underline{a}_1{}^0\ 12_1^0$	35250.11(.03)
$1_1^0\ 18\underline{b}_1{}^0$	35751.99(.5)	$6\underline{a}_1{}^0\ 19\underline{b}_1{}^0$	35184.78(.03)
$6\underline{b}_1{}^0\ 12_1^0$	35729.23(.5)	1_2^0	35044.42(.5)

(i) denotes the bands corresponding to species having ^{37}Cl.

APPENDIX 3.5

Positions and relative intensities of main bands used in deducing the out-of-plane modes. The intensities (in parentheses) are relative to origin band (0,0) = 100 in the electronic spectrum

Assignments	Frequency(cm^{-1})	Assignments	Frequency(cm^{-1})
$17\underline{a}_2^0$	35133.13(.02)	$10\underline{b}_1^1$	36865.30(10)
$17\underline{b}_2^0$	246.98(.02)	$16\underline{b}_1^1$	904.35(20)
$10\underline{a}_2^0$	391.76(.01)	$4_1^0\ 10\underline{b}_0^1$	922.54(2.5)
$10\underline{b}_2^0$	570.39(.02)	$10\underline{a}_1^0\ 17\underline{a}_0^1$	949.36(7.0)
4_2^0	681.62(1.1)	$10\underline{b}_1^0\ 17\underline{b}_0^1$	965.12(.5)
$16\underline{b}_2^0$	36116.32(.1)	11_1^1	990.90(50)
$16\underline{a}_2^0$	244.14(1.0)	$4_1^0\ 17\underline{b}_0^1$	37021.72(1.0)
$11_0^1\ 17\underline{b}_1^0$	286.89(.3)	0,0(origin)	37050.92(100)
$16\underline{a}_0^1\ 17\underline{a}_1^0$	292.54(.005)	$4_1^0\ 5_0^1$	066.12(.005)
$5_1^0\ 16\underline{b}_0^1$	390.26(.5)	$10\underline{b}_0^1\ 16\underline{b}_1^0$	139.42(.01)
$10\underline{a}_1^0\ 16\underline{a}_0^1$	422.87(.8)	$11_1^0\ 16\underline{b}_0^1$	173.89(.5)
$16\underline{b}_0^1\ 17\underline{b}_1^0$	469.08(.01)	$16\underline{b}_1^0\ 17\underline{b}_0^1$	238.54(8.0)
$4_0^1\ 17\underline{b}_1^0$	570.24(.005)	$10_0^1\ 16\underline{a}_1^0$	263.37(5.0)
$5_1^0\ 10\underline{b}_0^1$	624.16(.1)	$4_0^1\ 11_1^0$	275.68(1.0)
$10\underline{b}_1^0\ 16\underline{b}_0^1$	629.62(.02)	$5_0^1\ 16\underline{b}_1^0$	282.32(.005)
$4_1^0\ 16\underline{b}_0^1$	687.19(.1)	11_0^2	325.07(2.0)
$10\underline{a}_0^1\ 17\underline{a}_1^0$	705.57(.7)	$16\underline{a}_1^0\ 17\underline{a}_0^1$	377.37(2.5)
$5_1^0\ 10\underline{b}_0^1$	724.68(.1)	$10\underline{b}_0^1\ 11_1^0$	409.51(1.0)
$4_0^1\ 10\underline{b}_1^0$	732.16(.01)	$16\underline{a}_0^2$	459.50(6.0)
5_1^1	768.36(4.0)	$5_0^1\ 11_1^0$	552.33(.005)
4_1^1	789.25(20)	$16\underline{b}_0^2$	690.80(4.0)
$17\underline{b}_1^1$	803.22(10)	4_0^2	890.52(1.5)
$17\underline{a}_1^1$	818.24(1.0)	$10\underline{b}_0^2$	38163.81(1.0)
$10\underline{a}_1^1$	835.64(4.0)	$10\underline{a}_0^2$	279.11(2.0)
$16\underline{a}_1^1$	850.59(45)	$17\underline{b}_0^2$	360.24(.5)

CHAPTER IV

SPECTRAL CORRELATION WITH STRUCTURES OF BENZALDEHYDE IN VAPOUR, LIQUID AND SOLID STATES

ABSTRACT

The infrared spectrum of benzaldehyde in the vapour, liquid and solid (at liquid nitrogen temperature) phases and the Raman spectrum in the liquid phase have been recorded. The vibrational assignments have been made on the basis of infrared band contours and the Raman polarization data. The internal modes corresponding to CHO group are contained in the species of C_s point group, and those of C_6H_5C - group belong to C_{2v} symmetry, consistent with the infrared and Raman data. The fundamental vibrational modes which are not observable or forbidden in the vapour phase infrared spectrum are observed in the solid phase. Intensities (peak height x band width at half the height) have been plotted for the fundamental vibrations for all the three phases. The triplet-singlet hypothesis to explain the anomalies in absorption and fluorescence spectra of benzaldehyde is supported on the basis of vapour phase vibrational data. Some bands are found to show splitting at low temperature in the solid phase. Shifts in the peak positions have been observed in changing from the vapour phase to condensed phases, but no regularity has been found. No indication of hydrogen bonding and dimerization have been observed in any of the physical states. Unperturbed positions of the vibrational levels of the aldehydic CH scretch and the overtone of CHO valence angle deformation, which are perturbed due to Fermi interaction, have been determined. Thermodynamic properties have also been calculated at different temperatures using spectroscopic data.

A. INTRODUCTION

Benzaldehyde (hereafter referred to as BzH) has been studied practically in every field of spectroscopy. Low temperature nuclear magnetic resonance studies (1), electron spin resonance spectra (2-3 microwave data (4-6) and the torsional fundamental observed in the far infrared (7-15), have all been used to determine the barrier height to internal rotation of the CHO group about the C-C bond with respect to the heavy phenyl anchor (7). In addition to the use of infrared data in the solution of internal rotation problem, attempts have been made to determine in BzH: (a) the extinction coefficients of some of its infrared bands (16); (b) their partial vibrational assignments (17); (c) the variations in the carbonyl stretching and the ring CH stretching modes (18-24); (d) the doublet nature of the aldehydic CH stretching vibration (25-28); and (e) the characteristic combination bands near 4545 cm^{-1} (29). The liquid phase Raman data along with the qualitative polarization measurements have been used to verify the vibrational assignments (17-30).

In the electronic absorption spectra of BzH efforts have centered around: (a) the analysis of the various transitions observed in the range 1600 to 3500 A^{o} (31-35) and (b) the interpretation of these transitions on the basis of known interactions due to the substituent (CHO) in the benzene ring (36-40). Likewise, the emission spectra of BzH molecule have been studied by many workers (41-44). Stockburger (44) has attempted to show that the $n \rightarrow \pi^{*}$ absorption corresponds to a singlet-singlet (S-S') transition in the CO group while the emission originates from the triplet (T) state which is also localized in the CO group.

In the present investigations we have presented a combined study of the infrared spectra in vapour (RT)*, liquid (RT) and solid (LNT)** phase in the region 200 to 4000 cm^{-1}. On the basis of well resolved infrared band contours and Raman polarization data, consistent assignments have been made for all the vibrational fundamentals. A large number of overtones including those due to the lowest torsional mode have been observed and assigned. On the basis of these assignments, anharmonicities have been calculated for several fundamentals. The overtone of the CO stretching mode observed in the vapour phase infrared spectra lends a quantitative support to the triplet-singlet hypothesis put forth by Stockburger (44) to explain the anomalies in absorption and fluorescence spectra of BzH. The unperturbed levels of the vibrations in Fermi interaction have been found; and using the spectroscopic data thermodynamic properties, have been calculated for different temperatures, which have not been determined so far.

B. EXPERIMENTAL

Analytical grade (BDH)+ BzH was distilled three times in the vacuum system (Cf. Chapter II). The middle portion of the sample was always used for the experiment. All the vapour phase data were obtained with Perkin-Elmer 621 spectrophotometer, which was fitted with a multiple reflection gas cell and equipped with frequency marker accessory. The vapour of the BzH was collected in the gas

---

*RT denotes room temperature

**LNT stands for liquid nitrogen temperature

+BDH stands for British Drug House (India) Private Ltd.

cell from the vacuum system containing the sample. The vapour was kept at low pressure in the cell and longer path lengths ranging from 1.25 meter to 10 meter were used. Path length and the pressure of the vapour were varied to get a well resolved spectrum.

The liquid phase spectra of BzH were recorded on Perkin-Elmer 521 spectrophotometer using fixed cells of thickness .025 and .05 mm with CsBr windows. For recording high absorption peaks, the BzH sample was pressed between two CsBr windows to get a thin film and thus a weaker spectrum.

The solid phase spectra of BzH were recorded with P-E 521, using the low temperature cell (Cf. Chapter II). Care was taken to deposit a uniform, thin crystalline film of the sample (from the vacuum system) onto the CsBr plate in the cold-finger to obtain a good spectrum. This was achieved by repeating the process of deposition several times.

The frequency accuracy for the vapour phase spectrum may be taken to be better than $\pm$ 1 cm^{-1} and for liquid and solid phases about $\pm$ 2 cm^{-1}.

The Raman spectra of BzH have been recorded on Cary-81 and the polarization studies have also been made.

C. RESULTS

Figures 4.1 (a,b,c) illustrate the observed infrared bands of BzH in the vapour (200 to 4000 cm^{-1}), liquid and solid (250 to 4000 cm^{-1}) phases. In the Figures 4.2 A and 4.2 B, the infrared band contours in the region (200 to 1800 cm^{-1}) have been shown. The Raman spectra along with polarization studies have been illustrated in Figure 4.3.

All the observed infrared bands of BzH in the three phases, along with the liquid phase Raman shifts and depolarization data have been listed in Table 4.1. The probable assignments have also been suggested in the last column. Numbering of the vibrational frequencies has been done according to the scheme described by E.B. Wilson Jr. (45).

D. MOLECULAR GEOMETRY

Both the CHO group and the phenyl ring are coplanar in BzH molecule as suggested by: (i) the low value of the inertial defect found from microwave studies (4-6), (ii) the A-, B- and C-type infrared vapour phase contours (Cf. Section E), (iii) the Raman polarization data (Cf. Section G). Further, Braude et al. (46) has suggested that BzH is planar because of resonance interaction (47) of the type $I_a \leftrightarrow I_b$.

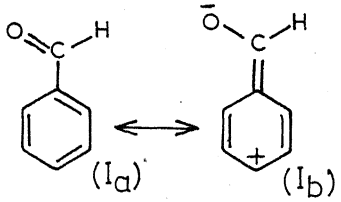

The exact determination of molecular geometry from microwave studies would require at least seven suitably chosen deuterated species of the molecule. However, one can get a suitable model for the molecule by assuming a planar structure and using the bond lengths and bond angles from the related compounds (13, 48-50).

The mean values of the three principal moments of inertia for BzH molecule, as calculated from the rotational constants determined by Kojima and coworkers (4-6) from microwave studies, are:

$I_A = 96.75_7$, $I_B = 323.20_2$ and $I_C = 419.96_0$ amu $\mathring{A}^2$.

To obtain the best fit with these values we have suggested in Figure 4.4, a reasonably satisfactory and most conceivable geometry of the molecule for which the computed values of the principal moments of inertia are: $I_A = 96.76_0$, $I_B = 323.10_6$ and $I_C = 419.31_9$ amu $\mathring{A}^2$. The coordinates of each atom in the center of mass system are also given in the figure.

E. SELECTION RULES

From the previous discussion it follows that BzH molecule belongs to C_s point group. The 36 normal vibrational modes will be distributed as (25 a' + 11 a'') (51). Both the a' and a'' modes are infrared and Raman active, but the a' modes would be polarized in the Raman spectrum.

If the substituent (CHO) is considered as a point mass 'X' centered on the symmetry axis of the phenyl ring, the C_6H_5 X fragment would belong to C_{2v} point group for which the 30 vibrations are comprised of $(11a_1 + 10b_2)$ planar and $(6b_1 + 3a_2)$ out-of-plane vibrations. The infrared and Raman activities of the various symmetry species in C_{2v} point group have already been given in Chapter III (Table 3.1). On the other hand, if the phenyl ring is considered as a heavy point mass 'X', the six modes of Y-CHO part (which belongs to C_s point group) would distribute as (5a' + 1a''). However, considering the BzH molecule as such (without any approximation) the 25a' vibrations consist of 21 vibrations for C_6H_5C- group and 4 for the CHO group; and likewise the 11 a'' vibrations consist of 9 for C_6H_5C-group and 2 for the

CHO group. The discrepancy in the total number of out-of-plane and in-plane vibrations occurs by taking separate groups. On considering the CHO group attached to benzene ring one planar vibration of a' species becomes redundant while one of a'' species (i.e. the torsional mode) is added to the sum given by different fragments.

F. INFRARED BAND CONTOURS

The Vibrations of C_6H_5C-Group: As described in the preceding section, the vibrations of this group belonging to a_1 , b_2 and b_1 classes should exhibit A-, B- and C-type infrared band contours, respectively; and a_2 modes should be inactive in the vapour phase infrared (Cf. Chapter III, Table 3.1).

The -CHO Group Vibrations: In addition to the valence stretching and bending modes, the CHO group when attached to the phenyl anchor, would give rise to three extra modes (i.e. wagging, twisting or torsion and rocking) shown in Figure 4.5. The contours of all these vibrations can be estimated on the following assumptions: the changes of dipole moment in the stretching vibrations are along the bonds; and in others they are along the direction of motion but always perpendicular to the bonds involved in the vibration. Thus, each of the CH and CO stretching, the valence angle (OCH) deformation and the CHO rocking modes should show an A/B hybrid character (Cf. Chapter VI) with different degrees of hybridization in the respective band contours. The wagging and twisting modes of CHO group should give rise to C-type band contours.

The details of three types of band contours to identify the various types of vibrations are given in Chapter VI.

G. THE RAMAN POLARIZATION DATA

It has been discussed for infrared band contours that the vibrational modes of C_6H_5C-group must primarily behave as those of C_{2v} point group and -CHO group modes as belonging to C_s point group. So the Raman shifts of BzH molecule should show polarization character according to these point groups i.e. a_1 class vibrations of C_{2v} point group and a' class vibrations of C_s point group should appear as polarized bands.

H. OVERLAPPING BANDS

Only a few distinct bands with no overlap by other bands are found in the infrared spectra of BzH. However, when two or more bands overlap, the components have to be resolved from the composite band. Representative cases of such graphical decomposition of the observed vapour phase bands are shown in Chapter VI; similar method is used for condensed phase bands. This procedure is helpful in correct identification of bands, especially in the vapour phase spectrum (Cf. Chapter VI).

I. FUNDAMENTAL VIBRATIONS OF C_6H_5C-GROUP

Using the information given in sections D to H and earlier experience on other monosubstituted benzenes (52-57) we have listed the fundamental vibrations of C_6H_5C- group in Tables 4.2 to 4.4.

The a_1 Modes: These vibrational modes show typical A-type contours with expected PR separation in the vapour phase spectrum

and are given in Table 4.2. In the CH stretching region (2950-3120 cm^{-1}) the positions of the bands are arrived at after resolving the complex structure and so the PR separations are not very certain. The bands near 3011 and 1489 cm^{-1} are too weak to give their contours but have been confirmed by the appropriate Raman polarization data. The X-sensitive '6a' mode is very weak and is overlapped by a stronger C-type band at 449.1 cm^{-1} and could not be observed in the vapour phase spectrum.

The b_2 Modes: The vibrations of this class show expected B-type contours and have been listed in Table 4.3. The two CC stretching modes (19b and 14) show polarized behaviour in the Raman spectrum (17). The observed PR separation is also somewhat larger, although greater discrepancies have been tolerated in case of the bands obtained after decomposition of a complex structure e.g. in bands at 3041 and 1591 cm^{-1}. The A/B hybrid nature and polarization character observed other than expected in a few bands may be due to the mixed character of the modes and overall symmetry of the molecule.

The b_1 and a_2 Modes: The observed data regarding these modes have been given in Table 4.4. Five out of six b_1 modes show clean C-type contours in the infrared and the observed Raman shifts are depolarized as expected. The vibrations of a_2 species have primarily been obtained from liquid and solid phase infrared spectra and also from liquid phase Raman spectrum.

J. SUBSTITUENT GROUP VIBRATIONS

All these vibrations have been listed in Table 4.5 and discussed individually as they are associated with special features.

Torsional Mode: We have been able to observe this frequency only in the liquid phase Raman spectrum. However, it has been studied earlier (10) in vapour phase and found to show C-type contour with its Q branch at 111 cm^{-1}. This frequency presents one of the unique examples where the ratio $(\nu_{liq} - \nu_{gas})/\nu_{gas}$ is as high as 20% (10). Using harmonic approximation, the value of barrier height for internal rotation has been calculated to be 4.66 Kcal (11). We have observed few higher members in the torsional family in vapour phase spectrum (Table 4.1). However, we have made no attempts to modify the barrier height V_o making use of the additional data, because such calculations are expected to make only a small change in the values given, especially in view of the large differences in V_o calculated for the vapour and liquid phase frequencies (11).

The Out-Of-Plane Wagging Mode: This mode has been assigned by resolving the band near 1000 cm^{-1} into an A-type and C-type contour. From the considerations of PR separation and I_Q/I_{Total} (intensity of Q branch/intensity of whole band; Cf. Chapter VI) of 1000 cm^{-1} band, one C-type band was suspected to occur at 1003.5 cm^{-1} along with the ring breathing mode. It has been confirmed by solid phase studies, where it is observed as a separate band (Table 4.1 and Section M).

The -CHO Rocking Mode: Taking a simple model and assuming that the force constants for wagging and rocking modes are not much different, the rocking mode should fall at lower frequency than wagging mode (58). The band observed at 650.0 cm^{-1}

(mean of the two Q branches - Table 4.1) with B-type contour has been assigned to the CHO wagging mode (Cf. Figure 4.5).

The -CHO valence Angle Deformation: A strong band at 1386.6 cm^{-1} in the vapour phase infrared spectrum with a polarized Raman shift in liquid phase at 1391 cm^{-1} has been assigned to this mode. The A-type contour with expected PR separation observed for this band suggests that during this vibration major change in the dipole moment lies along the axis of minimum moment of inertia. So no hybridization is indicated in the band contour. The overtone of this mode exhibits Fermi resonance with aldehydic CH stretching mode.

The CO Stretching Mode: The strong and broad band at 1727 cm^{-1} in vapour phase infrared has been assigned to this mode. The broadness of the band may be due to the combination bands falling in this region viz. (16b+3) at 1735.3 cm^{-1}, 8a+torsion at 1721 cm^{-1} etc. This frequency is sensitive to the change of state though not as much as OH bands in phenol (Cf. Chapter V). The CO stretch frequency falls at 1696 cm^{-1} in liquid phase at room temperature and further drops to 1691 cm^{-1} in the crystalline state at LNT. Its overtone observed at 3432.5 cm^{-1} supports the view of triplet-singlet fluorescence spectra out of the three different possibilities discussed by Stockburger (44) (Cf. Section M).

The CH Stretching Mode: The moderately strong pair of bands at 2731 and 2811 cm^{-1} are due to the Fermi interaction of the overtone of HCO angle deformation vibration with the aldehydic CH stretching mode (Cf. Figure 4.6). Using the formula 1.41 we

have calculated the unperturbed separation from, (i) the observed intensity ratio 1.031:1 of 2811 and 2731 cm^{-1} bands and (ii) their observed separation $\Delta = 80\ cm^{-1}$. The value of δ (unperturbed separation) comes to be 1.18 cm^{-1}. So the calculated unperturbed positions of the fundamental and overtone bands are 2770 and 2772 cm^{-1}, respectively.

K. RELATIVE INTENSITIES

The intensities (peak height x full width at half the height of the band) of the fundamental vibrational bands normalized relative to the strongest band taken as 100, in each spectrum, are given in Figure 4.6. The vibrations belonging to different species have been shown differently in the figure. The intensity in the infrared spectra of BzH is mainly shared by the CHO group vibrations amongst which the CO stretch is the most intense. However, the X-sensitive a_1 and the out-of-plane b_1 modes of the C_6H_5C- group also have fairly good contribution of the total intensity. In the Raman spectrum the intensity is primarily distributed in the decreasing order among CO, CC, CH stretching and the ring breathing modes.

The most intense band in the infrared spectra of PhCl in all the three phases has been 10b at 740 cm^{-1} and in its Raman spectrum the ring breathing mode at 1000 cm^{-1} was the strongest (Cf. Chapter III). But in BzH the most intense band is CO stretch both in the Raman and infrared spectra. Thus it could be inferred that the maximum changes both in polarizability and dipole moment take place in CO stretching vibration.

L. COMBINATIONS AND OVERTONES

The assignments of all the observed infrared combination bands in all the three phases have been given in Table 4.1. However, the observed overtones have been collected in Table 4.6. From these observations w_e and $w_e x_e$ have been deduced by the method suggested earlier in the case of chlorobenzene and $w_e x_e$ is found to be positive for many bands. Maximum anharmonicity (22 cm^{-1}) is observed in the CO stretching vibration.

M. CORRELATION WITH ELECTRONIC SPECTRA

There have been several studies in electronic absorption and emission spectra of BzH vapour in the past (41-44). The characteristic pattern observed in emission and $n \rightarrow \pi^*$ absorption spectra are shown in Figure 4.7 after Stockburger (44). Robinson (42) explained the first interval of 1735 cm^{-1} as the first vibrational difference between v = 0 and v = 1 level of CO stretching mode. Stockburger (44) has argued that there are three possibilities as illustrated in Figure 4.8 which could give rise to the characteristic pattern mentioned above. On the basis of detailed studies in fluorescence, Stockburger (44) favoured the scheme (c) given in Figure 4.8. Our vapour phase infrared studies clearly show that the first CO stretching interval is 1727 cm^{-1} in the ground state followed by another interval of 1705.5 cm^{-1} (obtained from the observed value of the overtone at 3432.5 cm^{-1}). These observations are fully consistent with the absorption band positions in the electronic spectrum shown in Figure 4.7 and thus unambiguously support the triplet-singlet emission hypothesis of Stockburger (44) for the fluorescence spectrum of BzH.

N. SOLID PHASE (LNT) STUDIES

The solid phase infrared spectral data have also been given in Table 4.1 to compare it with that of liquid and vapour phase data. The sharpening of bands, in the solid phase, occurs in all the bands with respect to the gaseous phase obviously due to disappearance of rotational structure. Typical band widths have been collected in Table 4.7. In the vapour phase there is no significant difference in the half band width from those of PhCl, where as in the solid phase we have not found bands as sharp as those of PhCl.

Small changes in peak positions are observed in most of the vibrational modes. Hydrogen bonding may not be regarded as any potential source of such shifts in the BzH molecule.

The weak appearance of forbidden a_2 bands (Cf. Section I) is obviously due to relaxation of C_{2v} symmetry selection rules in the solid state for the C_6H_5C - group vibrations.

Most of the bands did split into two components, although it has not always been possible to clearly distinguish the two peaks in the bands with large half width. The typical splittings vary in the range 1.6 to 3.3 cm^{-1} and have been shown for few cases in Table 4.8. The splittings cannot be due to site symmetry because there are no degenerate vibrations in BzH molecule. No specific conclusions can be drawn regarding the factor group splittings as there are no data available on the crystal structure of the compound. So no definite information could be obtained from our data on splitting of the bands. Lattice vibrations although do not lie in the range studied by us, but their combinations are observed as shown in Table 4.1.

O. THERMODYNAMIC PROPERTIES

The thermodynamic properties for benzaldehyde vapour have been computed (Cf. Chapter I Sec. L) for the first time using (a) the precise vapour phase fundamental frequencies for the compound (listed in Tables 4.2 - 4.5), (b) the three moments of inertia from the rotational constants determined by Kojima et al. (5,6), (c) the reduced moment of inertia for internal rotation (11) (which can be calculated from the molecular geometry given in section D) and (d) the symmetry numbers 1 for over all rotation and 2 for internal rotation. The thermodynamic quantities have been found for different temperatures in the range 200°K to 1000°K for 1 mole of perfect gas at 1 atmosphere pressure. The gas imperfection correction has been applied using the reported values (59) of critical temperature and pressure. The restricted rotation has been taken into account and its contribution has been evaluated from the tables of Pitzer and Gwinn (60) by interpolation. The corrected quantities are listed in Table 4.9.

The values listed in columns 3 and 5 of Table 4.9 together with those (61) for C (graphite), H_2 (gas), O_2(gas) and the estimated heat of formation of BzH (gas) i.e. -15.45 Kcal/mole* have been used to calculate ΔHf°_T, ΔGf°_T and $\log_{10} K_p$ for the reaction:

---

*Gibbs energy of formation ΔGf°_T of BzH (gas) at 298°K is -1.07 Kcal/mole and change in entropy for the formation of BzH (gas) at 298°K i.e. ΔSf°_T = -48.222 cal/mole °K. Using these values in the relation

$$\Delta Hf^{\circ}_T = \Delta Gf^{\circ}_T - T\ \Delta Sf^{\circ}_T$$

the value of ΔHf°_T is found to be -15.45 Kcal/mole at 298°K.

$$7C \text{ (graphite)} + 3H_2 \text{ (gas)} + \frac{1}{2} O_2 \text{ (gas)} = C_6H_5CHO \text{ (gas)}$$

From the approximate value of liquid state entropy (62), of BzH, the gaseous state value has been estimated by using heat of vapourization. So we do not expect exact agreement between the estimated vapour phase entropy 82.47 cal/mole ^{o}K and the computed value from the spectroscopic data 78.71 cal/mole ^{o}K.

P. REFERENCES

1. F.A.L. Anet and M. Ahmad, J. Am. Chem. Soc., 86, 119 (1964).

2. N. Steinberger and G.K. Fraenkel, J. Chem. Phys., 40, 723 (1964)

3. N.K. Ray and P.T. Narasimhan, Theoret. Chim. Acta (Berl.), 8, 306 (1967).

4. C.R. Quade, Disser. Abstract, 23, 1750 (1962).

5. T. Kojima, C.R. Quade and C.C. Lin, Bull. Am. Phys. Soc., 7, 44 (1962); as given in "Landolt-Barnstein Molecular Constants from Microwave Spectroscopy" by B. Starck, Springer-Verlag Berlin (1967).

6. T. Kojima, Private communication (Aug. '69) to Dr. H.D. Bist in which the rotational constants in the rotational states were given for the lower level (C = 1204.7, B = 1564.3 and A = 5235.2 Mc/sec and also for the higher level (C=1206.5, B = 1564.9 and A = 5213.9 Mc/sec.).

7. J.H.S. Green, W. Kynaston and H.A. Gebbie, Nature, 195, 595 (1962)

8. P. Delorme and J. Lecomte, Compt. Rend; 256, 3272 (1963).

9. J.H.S. Green, W. Kynaston and H.A. Gebbie, Spectrochim. Acta, 19, 807 (1963).

10. W.G. Fateley, I. Matsubara and R.E. Witkowski, Spectrochim. Acta, 20, 1461 (1964).

11. W.G. Fateley, R.K. Harris, F.A. Miller and R.E. Witkowski, Spectrochim. Acta, 21, 231 (1965).

12. P. Delorme, J. Chim. Phys., 61, 1439 (1964).

13. H.G. Silver and J.L. Wood, Trans. Faraday Soc., 60, 5 (1964).

14. J.M. Lebas, J. Chim. Phys. 59, 1072 (1962).

15. W.R. McWhinnie and R.C. Poller, Spectrochim. Acta, 22, 501 (1966).

16. C. Garrigou-Lagrange, N. Claverie, J.M. Lebas and M.L. Josien, J. Chim. Phys. 58, 559 (1961).

17. S. Chattopadhyay and J. Jha, Ind. J. Phys., 42, 610 (1968), and also see references cited therein.

18. J.L. Mateos, M.J. Cerecer and R. Celina, Bol. Inst. Quin Univ., Nacl. Auton. Mex., 12 (1960).

19. G.E. Lewis, Austra. J. Chem. 17, 814 (1964).

20. D. Heinert and A.E. Martell, J. Am. Chem. Soc., 81, 3933 (1959).

21. M.G.K. Pillai, K. Ramaswamy and S.G. Gnanadesikan, Austra. J. Chem. 19, 1089 (1966).

22. M.L. Josien and J.M. Lebas, Bull. Soc. Chim. France, 53 (1956).

23. M.L. Josien and J.M. Lebas, Compt. Rend. 240, 181 (1955).

24. M.L. Josien and J.M. Lebas, Bull. Soc. Chim. France, 57, 62 (1956).

25. A. Pozefisky and N.D. Coggeshall, Anal. Chem., 23, 1611 (1951).

26. S. Pinchas; Anal. Chem. 27, 2 (1955), 29, 334 (1957).

27. D.F. Eggers and W.E. Lingren, Anal. Chem. 28, 1328 (1956).

28. E.L. Saier, R.L. Cousins and M.R. Basila J. Phys. Chem. 66, 232 (1962).

29. R.M. Powers, J.L. Harper and H. Tai, Anal. Chem. 32, 1287 (1960).

30. E. Herz, L. Kahovec and K.W.F. Kohlrausch. Montash Chem. 74, 253 (1943).

31. A.D. Walsh, Trans. Faraday Soc. 42, 62 (1946).

32. F. Almasy, J.Chimie Phys. 30, 528, 634, (1933).

33. S. Imanishi, J. Chem. Phys. 19, 389 (1951).

34. S. Imanishi, K. Semba, M. Ito and T. Anno, Bull. Chem. Soc. Japan, 25, 150 (1952).

35. S.N. Garg, J. Sci. Research B.H.U. 2, 153 (1951-52).

36. A.K. Chandra, J. Am. Chem. Soc. 83, 4177 (1961).

37. Y. Konda, R. Shimoda, H. Shimoda, H. Kaseda and T. Matsumura, Spectrochim. Acta, 20A, 1387 (1964).

38. P.E. Stevenson, J. Mol. Spectry 15, 220 (1965).

39. K. Kimura and S. Nagakura, Theoret. Chim. Acta, 3, 164 (1965).

40. K. Inuzuka and T. Yokota, Bull. Chem. Soc. Japan, 38, 1055 (1965).

41. R.K. Asundi, B. Bhattacharya and N.A. Narasimham, Curr. Science, 21, 273 (1952).

42. G.W. Robinson, J. Chem. Phys. 22, 1384 (1954).

43. S.N. Garg and I.S. Singh, J. Sci Research B.H.U. 9, 61 (1958).

44. M. Stockburger, Z. Physik Chem. (Frankfurt) 31, 350 (1962).

45. E.B. Wilson, Jr., Phys. Rev. 45, 706 (1934).

46. E.A. Braude in E.A. Braude and F.C. Nachod, "Determination of Organic Structuresby Physical Methods". Academic Press, Inc. New York, N.Y. 1955, pp. 172.

47. G.W. Wheland, "Resonance in Organic Chemistry" John Wiley and Sons, Inc. New York, N.Y. (1955) pp. 99, and 108.

48. B.P. Stoicheff, Can. J. Phys. 32, 339 (1954).

49. H.D. Bist, J.C.D. Brand and D.R. Williams, J. Mol. Spectry 24, 402 (1967).

50. A.L. Verma and H.D. Bist, Chem. Physics Letters 4, 577 (1970).

51. G. Herzberg, "Molecular Spectra and Molecular Structure", Part II , D. Van Nostrand Co. Inc., New York (1945).

52. D.H. Whiffen, J. Chem. Soc., 1350 (1956).

53. W.S. Wilcox, C.V. Stephenson and W.C. Coburn Jr. WADD Technical Report 1960, (WADD-TR, 60-333), Spectrochim Acta 17, 933 (1961).

54. J.H.S. Green, W. Kynaston and A.S. Lindsay, Spectrochim. Acta 17, 486 (1961).

55. J.H.S. Green, Spectrochim.Acta 17, 607 (1961).

56. S.C. Sirkar and P.K. Bishui, Indian J. Phys. 42, 1 (1968).

57. H.D. Bist, V.N. Sarin, A. Ojha and Y.S. Jain, Spectrochim. Acta , 26A, 841-47 (1970) and references cited therein.

58. V.S. Tomar, H.D. Bist and D.P. Khandelwal, App. Spectroscopy Nov. - Dec. issue (1970).

59. F. Glaser and H. Ruland, Chem. Ingr. Tech. 29, 772 (1957).

60. K.S. Pitzer and W.D. Gwinn, J. Chem. Phys. 10, 428 (1942).

61. D.R. Stull, I. Carr, J. Chao, T.E. Dergazarian, L.A. du Plessis, R.E. Jostad, S. Levine, F.L. Oetting, R.V. Petrella, H. Prophet and G.C. Sinke, JANAF, "Thermochemical Tables" Clearing house for Federal Scientific and Technical Information, Springfield, Va, (1966).

62. D.R. Stull E.F. Westrum, Jr. and G.C. Sinke, "The Chemical Thermodynamics of Organic Compounds", John Wiley & Sons, Inc., New York, 1969 pp 191.

TABLE 4.1

Infrared absorption spectra of Benzaldehyde in solid (LNT), liquid (25°C) and vapour (22°C) phases and Raman spectrum with polarization data in liquid phase

INFRARED BAND POSITIONS IN cm^{-1}						Raman shifts in cm^{-1} with polarization data		Assignments
Solid (LNT)		Liquid (25°C)		Vapour (22°C)				
1		2		3		4		5
				3439.0 R				
				3432.5 Q	(20)*			2(CO stretch)
				3428.0 P				
3406.0	(27)*							2(1700)
3380.0	(35)							2(CO stretch)
3195.0	(33)	3191.0	(15)*			3193		2(8a)
				3185.0 R				
3170.0	(27)	3165	(13)	3179.0 Q	(17)	3174		2(8b)
				3173.5 P				
				3118.0 R				
3104.4	(1)	3095.5	(4)	3110.0 Q	(17)	3095	sh	CO stretch + CH bend (CHO) or 20a Fundamental
				3103.0 P				
				3087.0 R				
3086.5	(19)	3087.1	(9)	3082.8 Q	(44)			20b, Fundamental
				3078.2 P				
				3068.0 R				
3062.8	(30)	3064.6	(21)	(3062.0)** Q	vw	3064	(55) Pol.	2, Fundamental
				3058 P				
				3046.9 R				
3038.3	(22)	3031.5	(19)	(3041) Q	(38)	3049	hp	7b, Fundamenta
				3036.6 P				
3014.0	(7)	3012	(6)			3011	(4)	13, Fundamenta
				2990.0		2975	(16)	CH bend (CHO) 8a
				2955.0				19b+19a
2906.5	(1)			2920.0				2(19b)
				2856.0 R				
2854.9	(36)	2845	(16)	(2850) Q	(3)	2853	(1)	19b+CH bend (CHO)
				2843.0 P				
				2822.0				
2827.7	(55)	2816.8	(48)	2811.0	(70)	2821		Composite band 8a+7a and 2(CH bend) (CHO
				2800.0				

Contd. ...

1	2	3	4	5
		2735.0 R		
2745.4 (48)	2732.0 (29)	(2731) Q (62)	2740 (9)	CH stretch (CHO), Fundamental
		2724.5 P		
		2700.0 R		
2697.3 (8)	2691.0 (6)	(2694) Q (24)		7a + 19a
		2690 P		
	2617.0 (6)	2624.0 vw	2609 (1)	2(14)
2594.0 vw	2590.0 vw	2593.0 vw		1 + 8b
2512.0 vw	2507.0 vw	2510.0 vw		18a + 19a
2472.0 vw	2473.0 vw			?
		2408 R		
2405.1 (5)	2400.0 vw	(2404) Q vw		17b + 19a
		2400 P		
2376.0 w	2363.0 w	2370.0 (5)		2(9b)(solid)
	2321.0 w	2325.0 (4)		10b + 8b
2270.0 vw	2266.0 vw			7a + 15
2238.0 (1)	2238.0 vw	2236.0 vw		(CHO) rocking 8b
		2165.0 vw		10a + 14
2140.0 (2)	2136.0 vw			12a + 14
		2033.0 R		
2030.6 (6)	2027.0 (4)	2027.0 Q		1 + 18a
		2021.0 P		
1988.0 (10)	1983.0 (5)	1985.0 (1)		17b + 15
	1975.0 sh	1971.0 (2)		4 + 3
		1956.0		?
1918.0 (10)	1922.0 (3)	1912.0 w		6b + 3
		1896.0 R		
	1901.8 (4)	(1891) Q (5)		15 + 12
		1886.0 P		
1849.4 (6)				?
		1824.0 R		
1834.5 (10)	1824.5 (5)	1818.0 Q (8)		6b + 9b
		1812.0 P		
1700 sh	1706.0 w	1706.0 w		2(10a)
1691.0 (100)	1696.0 (100)	1727.0 (100)	1698.0 (100)P	CO stretch Fundamental
1671.4 sh	1682.0 sh			8a + Lattice vibration (74 cm^{-1})
		1655.5 R		
1656.6 (32)	1653.0 (19)	1650.0 Q (15)	1652 (12)	2(12)
		1645.0 P		

Contd. ...

1	2	3	4	5
1649.0 sh	1648.0 (19)			
1605.5 sh				1+CHO rocking
		1614.4 R		6a+9a
1597.7 (54)	1597.7 (32)	1610.0 Q (27)	1595 (83) Pol.	8a, Fundamental
		1604.0 P		
		1596.3 R		
1585.6 (26)	1585.8 (24)	1590.8 Q (33)	1583	8b, Fundamental
		1586.0 P		
	1561.2 sh			
	1534.2 (3)		1539	10b + 12
1494.7 (3)	1493.0 (1)	1489.0 (1)	1491 (2) Pol.	4 + 10a
1481.4 (1)	1474.8 sh			19a, Fundamental
1460.3				2(10b) ?
				Valence angle deformation (CHO) + lattice vib.
		1464.0 R		
1456.1 (16)	1455.7 (14)	(1460) (21)	1456 (3) Pol.	19b, Fundamental
		1455.0 P		
1431.2 (1)	1421.8			
1395.3 sh				18b + 9b
		1391.5 R		
1392.5 (31)	1391.0 (14)	1386.6 Q (15)	1391 (3) Pol.	Valence angle deformation (CHO)
				Fundamental
1338.2				
1343.4 (8)	1337.8 (4)	1338.6 (1)		CHO rocking + 4
		1317.4 R		
1313.5	1310 (15)	1313.0 Q (32)	1313 (1) Pol.	14, Fundamental
1311.8 (31)		1307.0 P		and 7a + Torsion
		1287.6 R		
1295.6 (26)	1286.7 (15)	1285.0 Q (9)		3, Fundamental
		1283.0		
		1278.0 P		
1266.9 (17)		1260.0 vw		6a + 12
1263.6				
		1229.5 R		
1254.5 vw	1241.5 sh	(1225)		18b + 12
		1220.0 P		
		1207.0 R		
1206.6 (41)	1203.0 (33)	1202.0 Q (57)	1201 (33) Pol.	7a, Fundamental
		1196.0 P		
1188.5 vw				9b, Fundamental
		1172.0 R		
1167.2 (48)	1168.2 (25)	1167.0 Q (37)	1166 (30) Pol.	9a, Fundamental
		1161.7 P		

Table 4.1 contd. ...

1	2	3	4
		1144.4 R	
1145.5 sh	1141.5 sh	1137.5 Q vw	1145 16b + 4
		1132.6 P	
		1105.0 R	
1104.2 (5)	1103.0 (5)	(1098) vw	Torsion + 17a
		1093.0 P	
		1075.0 R	
1072.8 (14)	1072.0 (6)	(1071) (5)	1071 15, Fundamental
		1066.8 P	
		1030.0 R	
1022.4 (13)	1022.5 (4)	1024.8 Q (10)	1023 (7) Pol. 18a, Fundamental
		1019.5 P	
		1009.0	
1011.0 (9)	1006.5 (5)	1003.5	CHO wagging, Fundamental
999.8 (10)	1000.5 (3)	1002.6 (5)	1000 (48) Pol? 1 ring, Fundamenta
980.3 (3)	980.3 sh		989 17a, Fundamental
	(973.0)[a] vw	960.0 vw	5, Fundamental
		925.0 R	
928.3 (8)	921.6 (4)	918.0 Q (2)	17b, Fundamental
		910.0 P	
904.6 (1)	900.6 vw	904.8 w	
		870.0 vw	2(6a)
857.1 (11)	848.2 sh		850 10a, Fundamental
		830.7 R	
829.0 (56)	826.5 (24)	825.3 Q (47)	826 (13) Pol. 12, Fundamental
		820.0 P	
822.9 sh			Torsion + 4
		810.0 R	
815.6 hp	810.5 sh	804.0 Q	804 2 (16a)
		798.0 P	
787.8 vw	789.8 (17)	785.0	Torsion + 4
761.7 sh			Lattice vib. + 4
		747.0 R	
749.7 (72)	749.0 (55)	739.5 Q (73)	747 (1) 10b, Fundamental
		732.0 P	
707.5 w			
717.5 w	714.2 (11)		?
		695.6 (16)	2(16a) - Torsion

Contd. ...

1	2	3	4	5
689.9 (37)	690.3 (29)	696.0 R 688.0 Q (46) 682.0 P	687	4, Fundamental
651.6 (30)	651.5 (25)	655.8 R 651.2 Q (33) 648.9 Q 644.8 P	649 (6) Pol.	CHO rocking, Fundamental
611.3 (5)	612.4 (4)	634.0 R (630.0) w 626.0 P	613 (11)	6b, Fundamental
550.7 w	554.5 vw 509.5 sh	548.7 (1) 514.0 (1)		Torsion + 16b Torsion + 16a
453.7 (33)	452.2 (11)	456.9 R 449.1 Q (16) 441.8 P	(441)[c]	16b, Fundamental
438.6 (6)	439.0 sh		437 (13) Pol.	6a, Fundamental
407.2 (4)	403.2 (1)		404	16a, Fundamental
		340.9 w		Torsion + 18b
		325 w		3xTorsion
	262.0 sh	249.6		?
	(237)[b]	236 vw	236 (7)	18b, Fundamental
	(223)[b]	?	228 (10)	11, Fundamental
		223.4 R 215.7 Q vw 209.6 P		2xTorsion
	(133)	111[d]	129	Torsion, Fundamental

'a','b','c','d' Values taken from Garrigou-Lagrange et al. (16), Herz et al. and Imanishi (30,33), Chattopadhyay et al. (17) and Fateley et al (10) respectively.

* Number in parentheses indicates the intensity of the band on arbitrary scale.

** Frequency in parentheses is the position of the dip between P and R branches of a B-type band.

sh,hp,w,vw and Pol denote shoulder, hump, weak, very weak and polarized Raman shift respectively.

TABLE 4.2

Totally symmetric 'a_1' fundamental frequencies (in cm^{-1}) of C_6H_5C-group in Benzaldehyde

Mode and approximate description $a_1(a')$ Class	BENZALDEHYDE					C_6H_5COCl[a]	$C_6H_5NO_2$[b]
	IR Vapour phase			Raman shift with polarization data		IR-LIQUID	IR-VAPOUR
	Frequency	Contour	PR Separation			Frequency	Frequency
20a, CH stretch	3110.0	A*	15.0	3095		3095	3096
2 CH stretch	3062.0	?	10.0	3064	P**	3072	3081
13, CH stretch	3011.0			3011			
8a, CC stretch	1610.0	A	10.4	1596	P	1595	1603
19a, CC stretch	1489.0			1491	P	1485	1475
7a, X-sensitive	1202.0	A	11.0	1204	P	1202	1107
9a, CH bend	1167.0	A	10.3	1170	P	1173	1174
18a, CH bend	1024.8	A	10.5	1023	P	1027	1020
1 ring	1002.6	A	11.5	1000	P	1001	1002
12, X-sensitive	825.3	A	10.7	826	P	672	852
6a, X-sensitive				437	P	312	397

'a' and 'b' Values are taken from references (17,54).

*A denotes A-type band contour.

**P denotes polarized Raman shift.

TABLE 4.3

Non totally symmetric 'b_2' fundamental frequencies (in cm^{-1}) of C_6H_5C-group in Benzaldehyde

Mode $b_2(a')$ class	Approximate description	C_6H_5CHO IR Vapour Phase Frequency	Contour	PR Separation	Raman shift with polarization data		C_6H_5COCl[a] IR-LIQUID Frequency	$C_6H_5NO_2$[b] IR-VAPOUR Frequency
20b	CH stretch	3082.8	B*	8.8	-	-	-	-
7b	CH stretch	3041.0	B	10.3	-	-	3030	3068
8b	CC stretch	1590.8	?	10.3	1583	D**	1581	1585
19b	CC stretch	1460.0	B	9.0	1459	P	1452	1412
14	CC stretch	1313.0	A	10.4	1313	P	1314	1316
3	CH bend	1204.0	B	9.6	-	-	1240	1307
9b	CH bend	(1188.5)[c]	-	-	-	-	1161	1161
15	CH bend	1071.0	B	8.2	-	-	1075	1069
6b	ring	630.0	B	8.0	614	D	617	612
18b	X-sensitive	233.8	-	-	(237)[d]	D	197	252

'a' and 'b' - Values taken from references (17,54)

'c' - Value from solid phase spectrum (Cf. Table 4.1)

'd' - Value taken from references (30,33)

* - A denotes A-type band contour, B denotes B-type contour

** - P and D denote polarized and depolarized Raman shifts respectively

TABLE 4.4

Out-of-plane Fundamental frequencies of $'b_1'$ and $'a_2'$ species of C_6H_5C-group in Benzaldehyde

Mode	Approximate description	C_6H_5CHO					C_6H_5COCl[a]	$C_6H_5NO_2$[b]
		IR Vapour Phase			Raman shift with polarization data		IR-LIQUID	IR-VAPOUR
		Frequency	Contour	PR Separation			Frequency	Frequency
$b_1(a'')$ class								
5	CH bend	(373.0)†	-	-	-	-	973	990
17b	CH bend	918.0	C*	15.0	-	-	873	935
10b	CH bend	729.5	C	15.0	747	-	-	794
4	CC Twist	688.0	C	14.0	687	-	-	704
16b	X-sensitive	449.1	C	15.0	441	?	-	420
11	X-sensitive	223.4	C	13.5	228	D**	163	176
$a_2(a'')$ class		Solid phase		Liquid phase				
17a	CH bend	980.3		980.3	989	-	988	977
10a	CH bend	857.1		848.2	850	-	840	837
16a	CC twist	407.2		403.2	404	-	415	397

'a' and 'b' - Values are taken from the references (17,54)

* - C denotes C-type band contour

** - D denotes depolarized Raman shifts

† Value taken from the reference (16)

TABLE 4.5

Fundamental vibrational frequencies (in cm^{-1}) of a' and a'' species of -CHO group in Benzaldehyde

Approximate description	C_6H_5CHO IR Vapour Phase Frequency	Contour	PR Separation	Raman shift with polarization data		C_6H_5COCl[a] IR-LIQUID Frequency	$C_6H_5NO_2$[b] IR-VAPOUR Frequency
a' species							
CH stretch	2731.0	B*	10.5	2740	-	772	-
CO stretch	1727.0	?	-	1698	P**	1735	1351
HCO Valence angle deformation	1386.6	A	10.2	1391	P	1427	677
CHO rocking	650.0	B	11.0	649	P	505	420
a'' species							
CHO wagging	1003.5	-	-	-	-	932	532
CHO torsion	(111)[c]	-	-	(130)	D	163	176
Antisymmetric stretch NO_2	-	-	-	-	-	-	1527

'a' and 'b': Values are taken from the references (17,54)

* : A and B denote A-type and B-type band contours

** : P and D denote polarized and depolarized Raman shifts respectively

'c' Vapour phase value is from reference (10) and liquid phase value is from reference (9)

TABLE 4.6

Observed and calculated values (in cm^{-1}) of the overtones of some vibrational fundamentals of benzaldehyde in vapour phase

Mode	Observed		Calculated		
	Fundamental	Overtone	Harmonic value of overtone	$2w_e x_e$	w_e
CO stretch	1727	3432.5	3454.0	21.5	1748.5
CO stretch (Solid)	1691(a)	3380(a)	3382.0	2.0	1693
8b	1590.8	3179.0	3181.6	2.6	1593.4
19b	1460	2920.0	2920.0	0.0	1460
9b	1188.5(a)	2376.0(a)	2377.0	1.0	1189.5
10a	857.1(a)	1700	1714.2	14.2	867.2
12	825.3	1650.0	1650.6	0.6	825.9
6a	437(c)	870.0	874.0	4.0	441.0
16a	404(c)				
	403.2(b)	810.5	806.4	-4.1	407.3
	407.2(a)	815.6	814.4	-1.2	408.4
Torsion (-CHO)	111(d)	215.7	222.0	6.3	117.3
	3(Torsion) =	325	333.0	8.0	119.0

(a) Peak position in solid phase
(b) Peak position in liquid phase
(c) Position of Raman shift
(d) Value taken from Ref. (10)

TABLE 4.7

Typical half band width (in cm^{-1}) of some bands in infrared absorption spectrum of Benzaldehyde in the vapour, liquid and solid phases

Mode	Vapour at 22°C		Liquid at 25°C		Solid (LNT)	
	Frequency	Half width	Frequency	Half width	Frequency	Half width
16b	449.1	21	452.2	10.0	453.7	10.0
CHO rocking	651.2	25	651.5	15.5	651.6	7.7
18a	1024.8	16.6	1022.5	5.5	1022.4	6.4
15	1071.0	24	1072.0	7.5	1072.8	6.4
14	1313.0	23	1310.0	10.0	1311.8	8.9
8b	1590.8	25	1585.8	10.0	1585.6	5.7

TABLE 4.8

Observed splitting of bands in the infrared spectrum of Benzaldehyde in solid phase (LNT)

Frequency cm^{-1}	Splitting cm^{-1}	Assignment
1395.3 1392.5	2.8	Valence angle deformation of COH
1313.5 1311.8	1.7	14, Fundamental
1266.9 1263.6	3.3	6a + 12 (Weak)
1169.4 1167.2	2.2	9a, Fundamental
1074.4 1072.8	1.6	15, Fundamental
751.7 749.7	2.0	10b, Fundamental
692.4 689.9	2.5	4, Fundamental
455.6 453.7	1.9	16b, Fundamental

TABLE 4.9

The molal thermodynamic properties of benzaldehyde in the ideal gas-state

$T^{\circ}K$	C_p°	$\frac{H^{\circ}-H_o^{\circ}}{T}$	$-\frac{(G^{\circ}-H_o^{\circ})}{T}$	S°	ΔHf_T°	ΔGf_T°	$\text{Log}_{10} K_p$
	in cal/Mole $^{\circ}K$				in Kcal/Mole		
200	23.93	11.09	56.52	67.61	-14.44	-5.23	5.715
298.16	27.40	15.28	63.43	78.71	-15.55	-0.96	0.704
400	35.30	19.38	68.80	88.18	-16.60	4.08	-2.229
500	42.05	23.26	73.66	96.92	-17.40	9.28	-4.057
600	47.54	26.87	78.25	105.12	-18.04	14.65	-5.336
700	51.94	30.15	82.66	112.81	-18.56	20.15	-6.291
800	55.52	33.10	86.90	120.00	-18.88	25.66	-7.010
900	58.47	35.76	90.95	126.71	-19.13	31.26	-7.591
1000	60.93	38.15	94.86	133.01	-19.26	36.87	-8.058

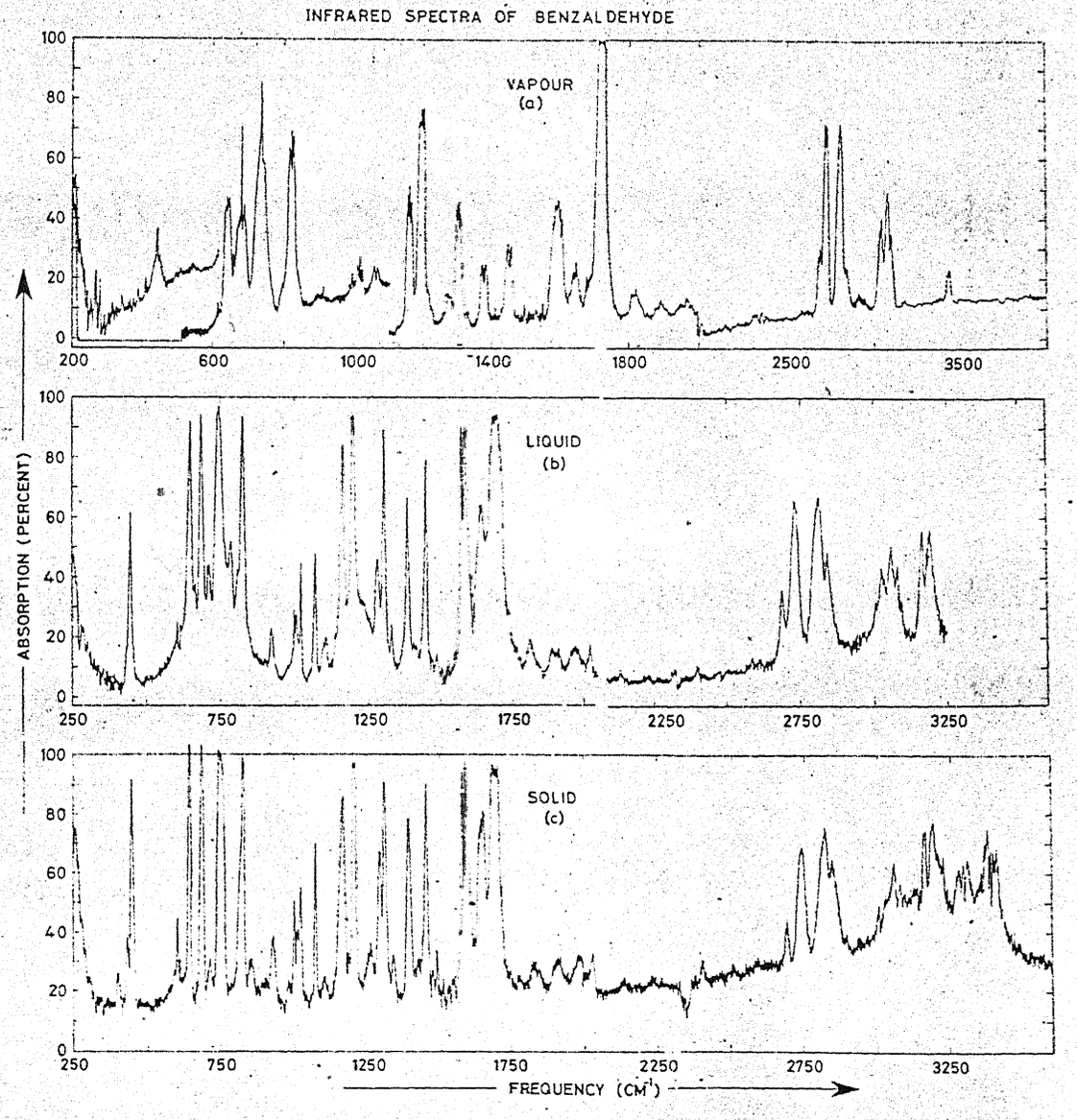

Fig. 4.1 The infrared spectra of benzaldehyde vapour (with 1.25 meter path and at ~ 1 mm pressure), liquid (0.025 mm cell) and solid (at liquid nitrogen temperature).

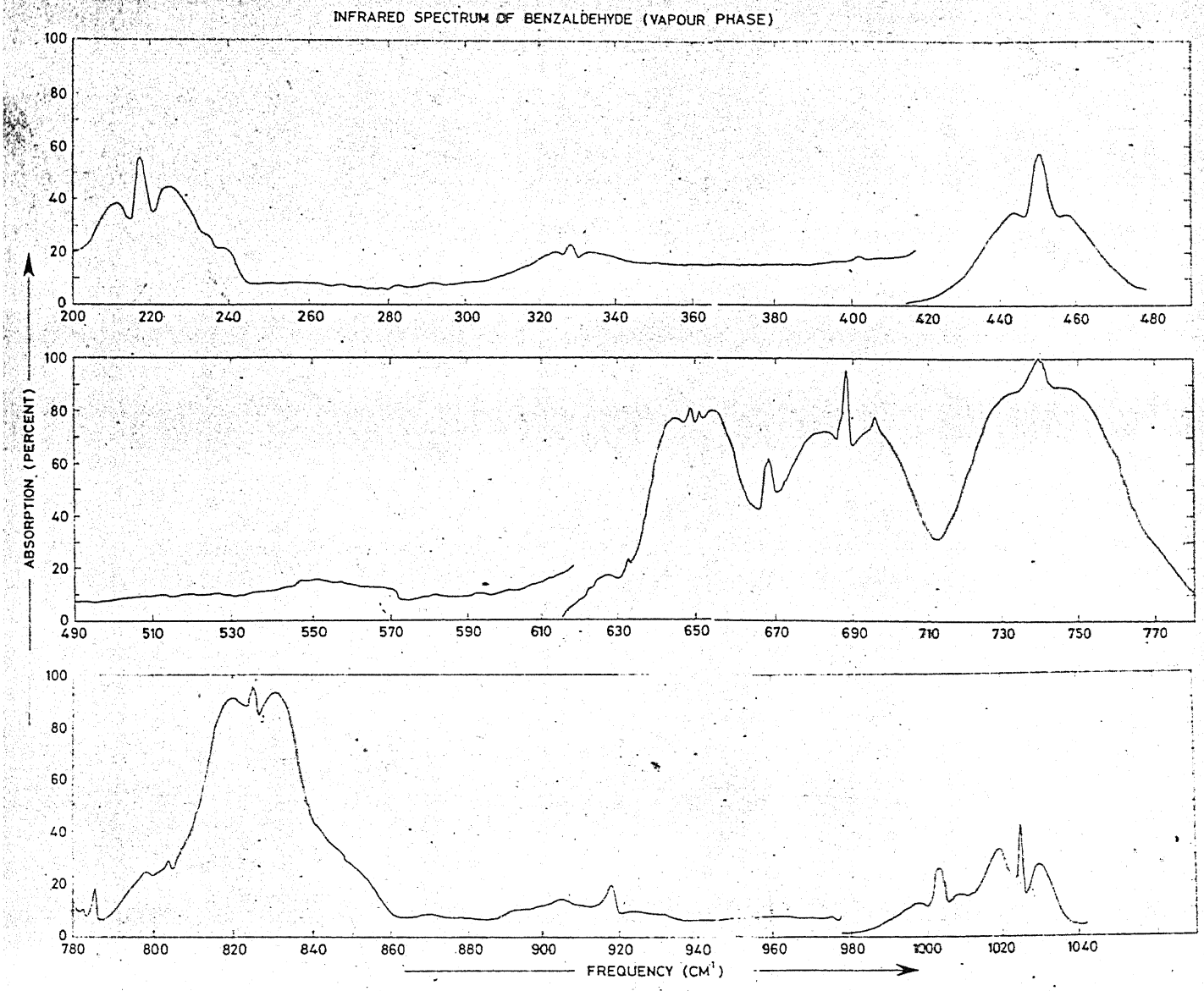

Fig. 4.2A The infrared spectrum of benzaldehyde in the vapour phase (with 5 meter path and at ~ 1 mm pressure) for range 200 - 1040 cm^{-1}

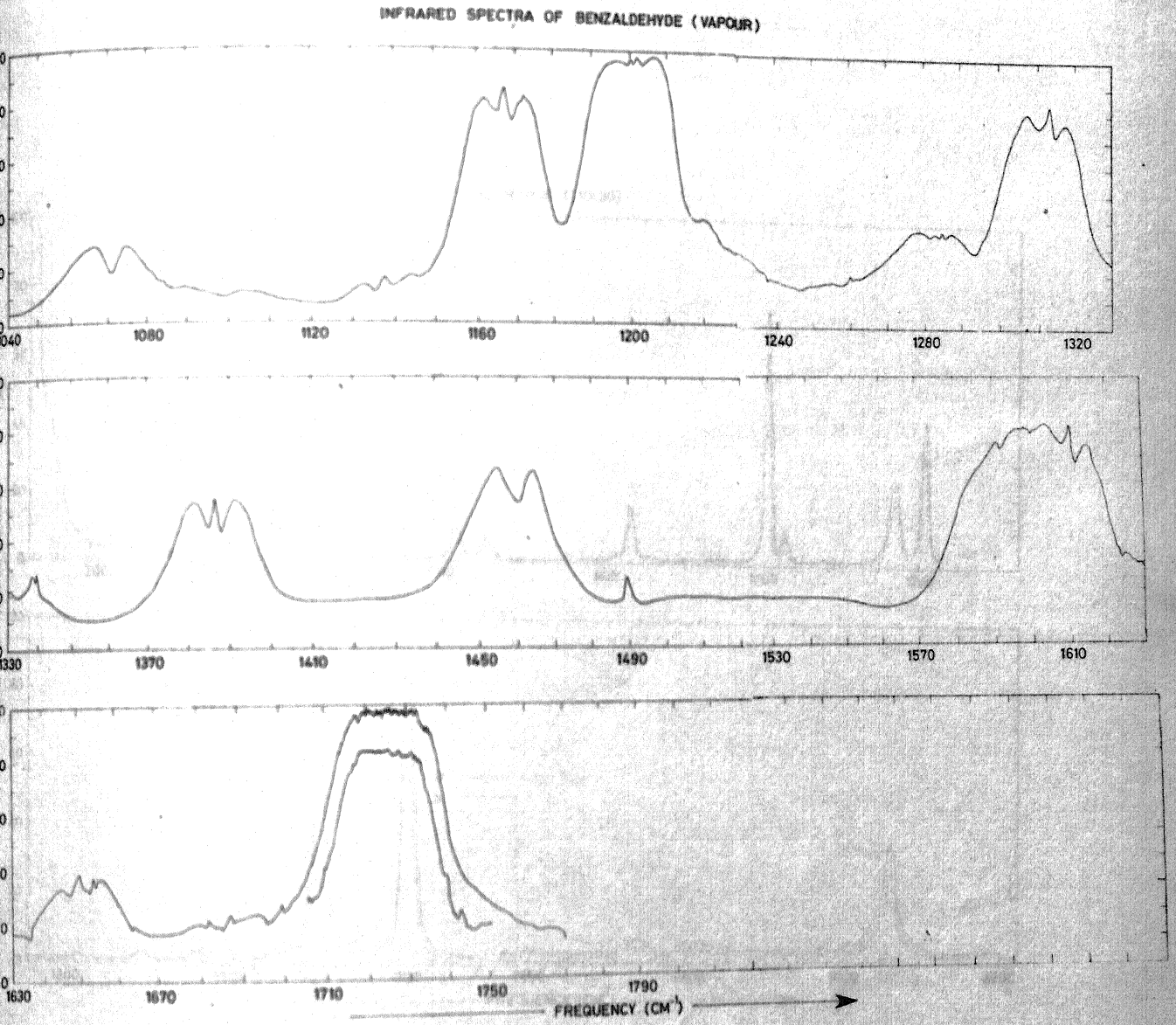

Fig. 4.2B The infrared spectrum of benzaldehyde in the vapour phase (with 5 meter path and at ~ 1 mm pressure) for range (1040-1800 cm^{-1}). Insert curve at 1700 cm^{-1} has been recorded with 1.25 meter path and at ~ 1 mm pressure.

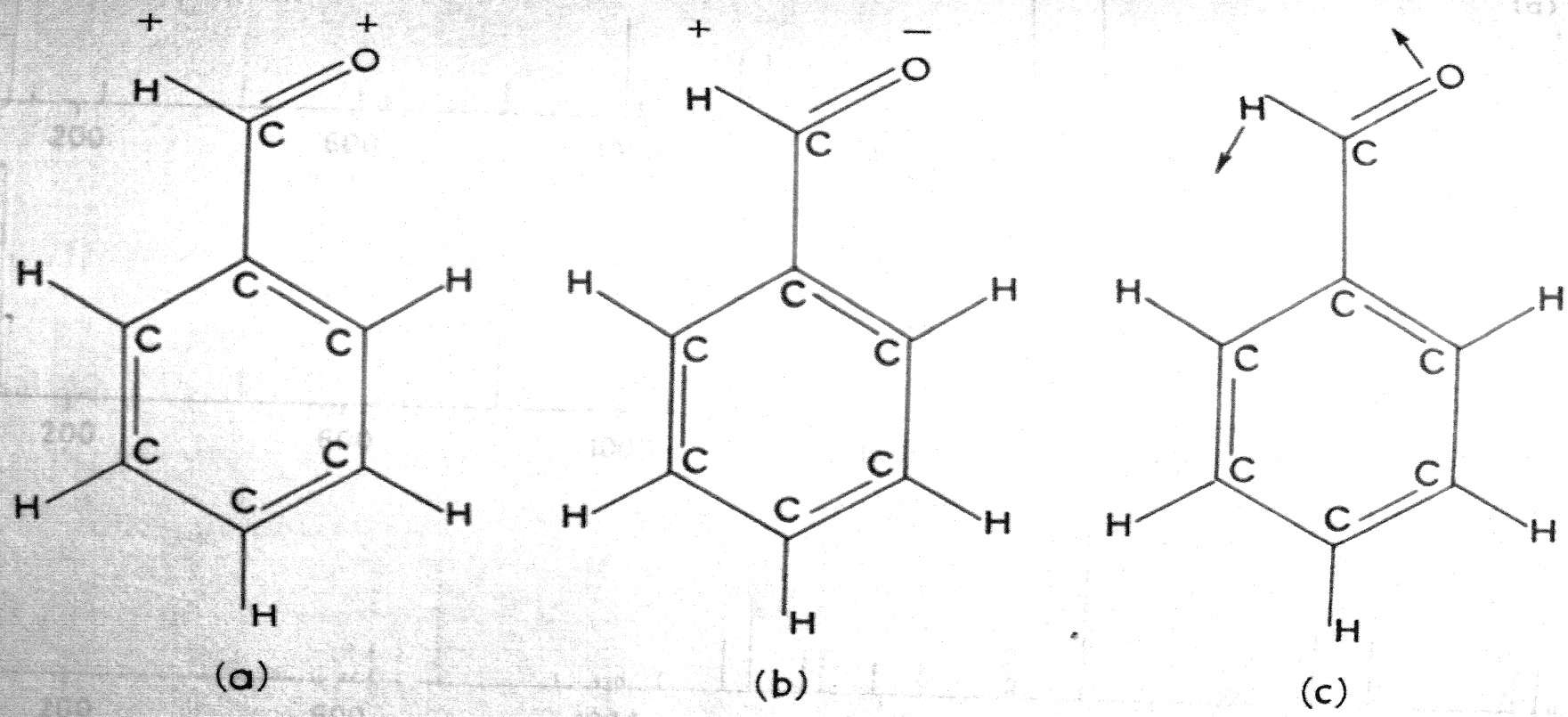

Fig. 4.5 – The Wagging (a), Twisting (b), and Rocking (c) vibrations of – CHO group in Benzaldehyde. The + and – signs represent motion above and below the plane of the paper respectively.

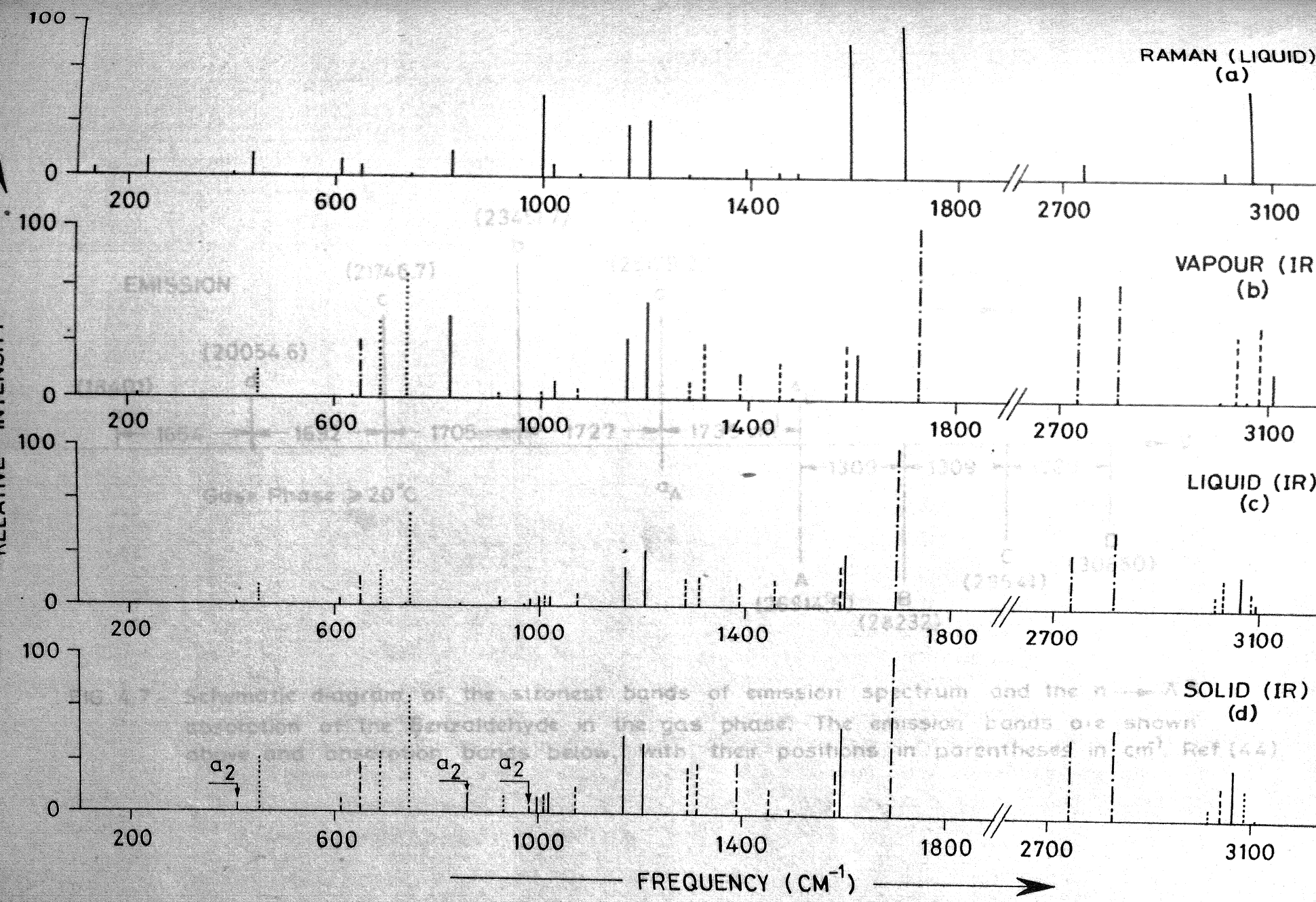
RAMAN (LIQUID)
(a)
VAPOUR (IR
(b)
LIQUID (IR)
(c)
SOLID (IR)
(d)
100
0
200
600
1000
1400
1800
2700
3100
a_2
a_2
a_2
FREQUENCY (CM^{-1})
Species ——, b_2 Species – – – – –, b_1 Species ·····, CHO Group —·—·—· Raman shifts ——

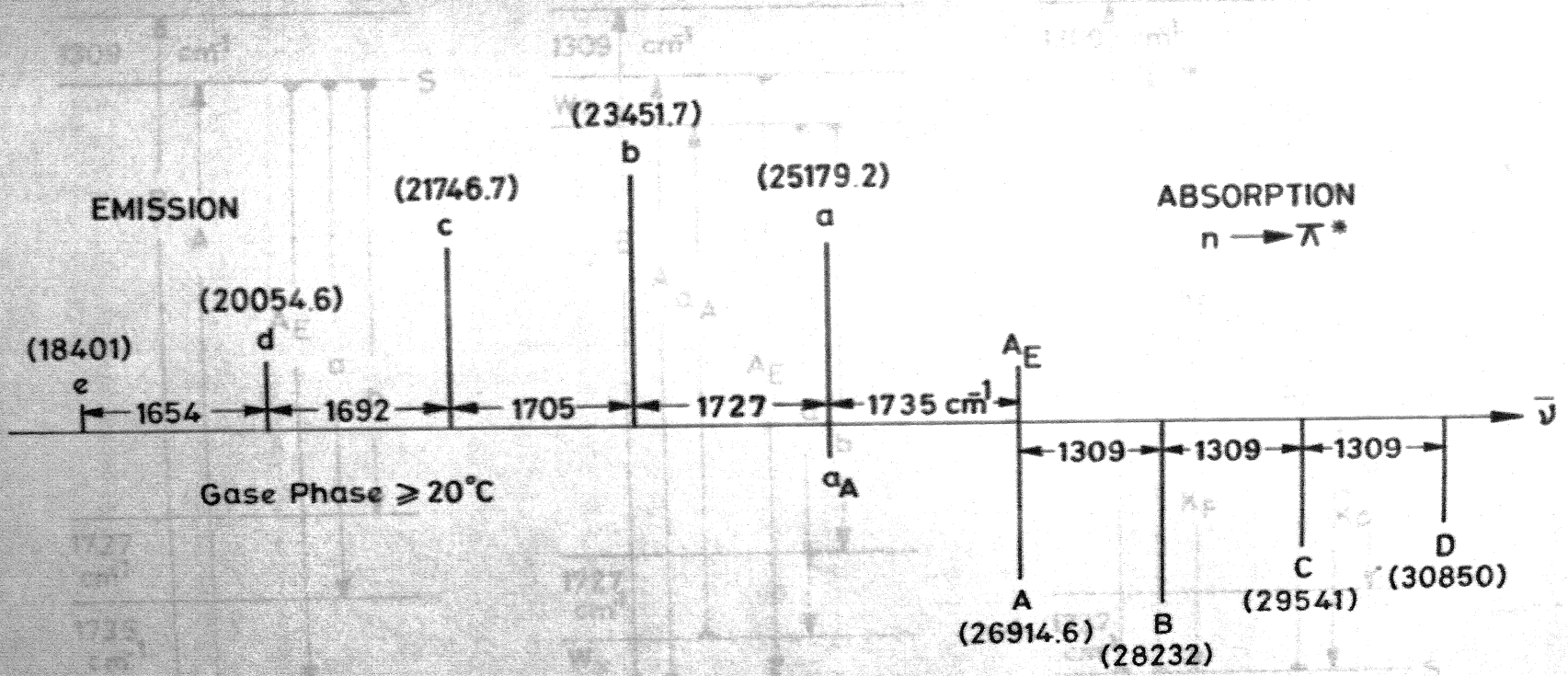

FIG. 4.7 - Schematic diagram of the stronest bands of emission spectrum and the $n \longrightarrow \pi^*$ absorption of the Benzaldehyde in the gas phase. The emission bands are shown above and absorption bands below, with their positions in parentheses in cm^{-1}. Ref.(44)

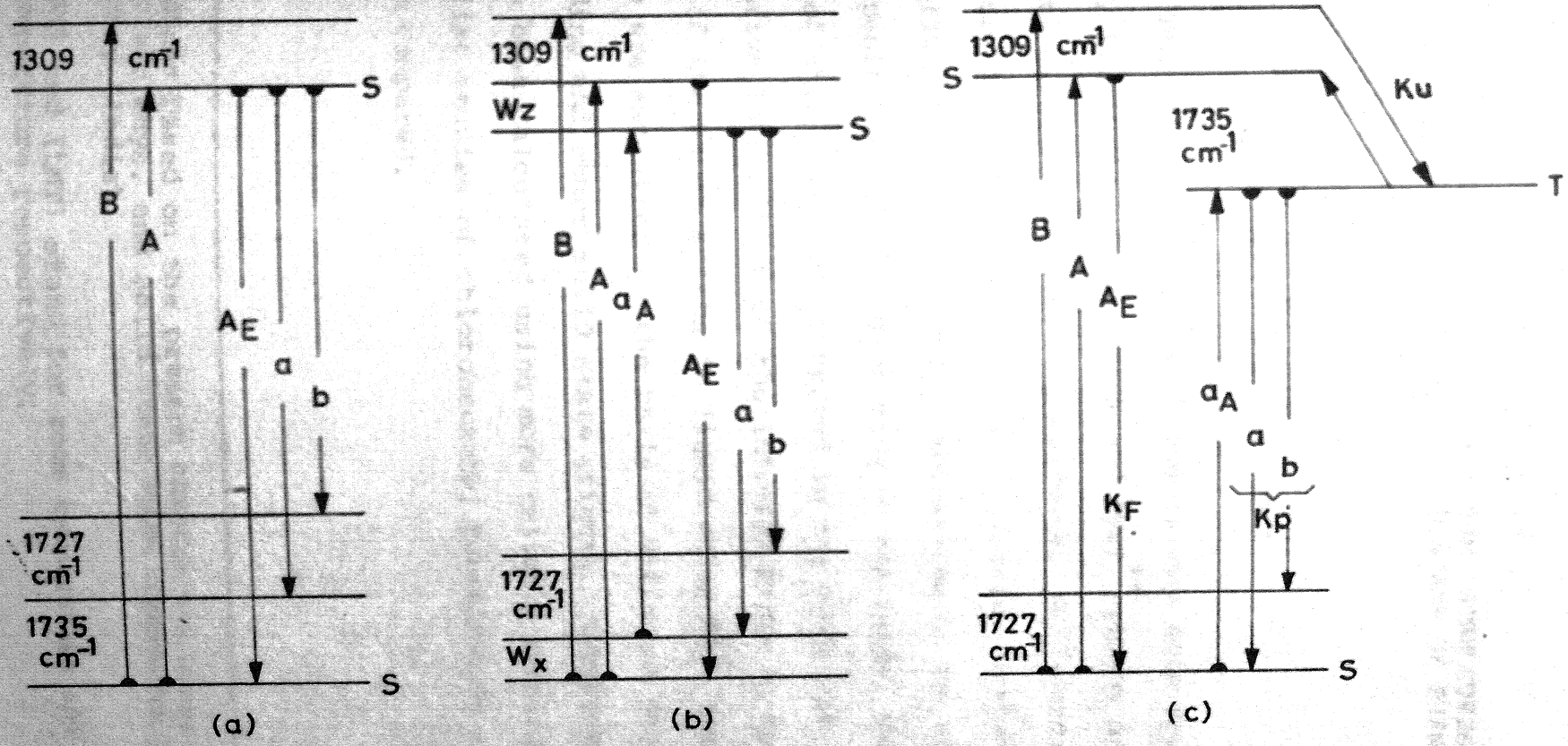

Fig. 4.8 - (a) Emission and $\eta \longrightarrow \pi^*$ absorption of some allowed arrangment of electronic transitions. (b) Emission and $\eta \longrightarrow \pi^*$ obsorption are arranged for some forbidden electronic transitions ($W_x + W_z = 1735\ cm^{-1}$). (c) the emission corresponding to transition from the lowest triplet state to the ground state singlet and $\eta \longrightarrow \pi^*$ absorption of some singlet singlet transitions. Ref. (44)

CHAPTER V

SPECTRAL CORRELATION WITH STRUCTURES IN VAPOUR, LIQUID AND SOLID STATE OF PHENOL*

ABSTRACT

The infrared spectra of phenol have been recorded in vapour (RT), liquid (RT), solid (RT and LNT)** phases and also of its solution in non-interacting solvents. Differential changes in OH stretching and deformation frequencies, occurrence of ring forbidden bands and binary combinations in the range 2000-3000 cm^{-1}, sharpening and shifting of many of the bands, and splitting in few of them have been observed in the condensed phases. The relative intensities of the infrared bands in different phases and of the Raman shifts in liquid phase have been plotted. The data are explained on the basis of different degrees of hydrogen bonding and other solid state effects. Thermodynamic quantities have been calculated using more reliable spectroscopic data. Similar studies of chlorobenzene, benzaldehyde and phenol have been compared.

---

*A paper based on the present chapter has appeared in Proc. Nuclear Phys. and Solid State Phys. Symposium 3, 252 (1968) Bombay (India)

**(RT) and (LNT) stand for room temperature and liquid nitrogen temperature respectively.

A. INTRODUCTION

Recently, the hydrogen bonded systems have attained considerable importance. The systems are interesting to molecular physicists and chemists for purely academic reasons since the structures of compounds like phenol in vapour liquid and solid phases still have not been completely unravelled. From the practical application point of view it would be of immense importance to understand the physics of the system in which a dimer bond formed from a building unit becomes stronger when it forms a trimer, tetramer or polymer. Direct structural studies are basic to the understanding of such problems. Infrared spectral analysis has also been one of the powerful tools for fixing the molecular symmetries and molecular parameters, especially when used in conjunction with the other techniques for obtaining the molecular structure (1,2).

Bist, Brand and coworkers (3-8) have presented an extensive vibrational and vibronic analysis for phenol in vapour phase. This has led to a reasonably correct geometry for the molecule in the ground state $^{1}A_1$ consistent with the microwave studies (9-10). Attempts (8) have also been made to establish the molecular geometry for the first singlet excited state $^{1}B_2$ on the basis of rotational contour analysis. Subsequently Brand and coworkers (11) have reported the force constant calculations for the out-of-plane vibrational modes of phenol both in its $^{1}A_1$ and $^{1}B_2$ states. Similar attempts for determining the force constants for planar vibrational modes are in progress in this laboratory (12).

In this chapter we have attempted to correlate the infrared data of phenol with its structures in vapour and solid states as

determined by other methods (8,10,13). We have also discussed few other salient infrared spectral features in different states of the compound and also given the revised and reliable thermodynamic quantities calculated from the spectroscopic results.

B. EXPERIMENTAL

Phenol (Merck, A.R. Grade) was vacuum distilled many times (as described in detail in Chapter II) till a clear crystalline material was obtained. The vapour phase spectra were recorded on Perkin Elmer-621 spectrophotometer fitted with a frequency marker; accuracy of data being better than $\pm$ .5 cm^{-1} for sharp peaks. Solutions (in non-interacting solvents), melt and solid (RT and LNT) phase spectra were scanned on Perkin Elmer-521, and Carl Zeiss UR-10 spectrophotometers; the accuracy being limited to $\pm$ 2 cm^{-1} in some regions of the spectrum. For studies at LNT, the material was vacuum deposited (and allowed to crystallize by annealing) on the cold finger of the low temperature cell (Cf. Chapter II). The Raman spectrum of phenol (in CCl_4 solution) were recorded on Cary-81.

C. MOLECULAR GEOMETRY IN VAPOUR AND SOLID STATES

An isolated phenol molecule is planar in its equilibrium configuration as suggested by OH and OD stretching and bending A/B hybrid infrared band contours (Cf. Chapter VI), and the low value of inertial defect observed in the microwave studies (9,10). The phenyl group possesses an axis of symmetry as indicated by the vibrational behaviour of the phenyl ring modes.

In addition, microwave studies of at least seven isotopically labelled compounds would be necessary to obtain the minimum of fourteen structural parameters leading to the determination of reasonably correct geometry of an isolated phenol molecule. If one makes further assumptions that the CH bonds are of equal length and located along C-C-C angle bisectors, and also that the CC bonds are all equivalent; then one needs only six parameters to determine its geometry. Forest and Dailey (10), on the basis of microwave analysis extended the work to four different isotopic molecules of phenol viz. $C_6H_5{}^{18}OH$, C_6D_5OH, C_6D_5OD and C_6H_5OH, and have been able to obtain fairly reasonable ring parameters, as shown in column 2 of Table 5.1, but the COH group geometry is only partially satisfactory.

X-ray studies (13) have shown that phenol molecules are connected by spiral hydrogen bonds into an endless chain along 'a' direction, and two such chains, each having three molecules (Cf. Figure 5.1) lie in the unit cell. Taking the CC bond distances determined by Scheringer (13) in phenol, assuming the CH bond distance as given by Stoicheff (14) for benzene and knowing the experimental data on torsional family of OH group in three of the isotopic molecules of phenol, Brand and coworkers (6) were able to determine the geometry of COH fragment as given in column 3 of Table 5.1. These values of the COH fragment compare reasonably well with those for methanol as given by Venkateswarlu and Gordy (15) later modified by Swalen (16). Using these data the molecular geometry of isolated phenol molecule has been depicted in Figure 5.2. The

coordinates of various atoms are also given for a better understanding of the structure.

The structure in the molten state or in solution is expected to be intermediate to above two structures i.e. for vapour and solid state phenol. The infrared spectra of phenol in different phases support this view.

D. INFRARED SPECTRA IN VAPOUR, SOLUTION, LIQUID AND SOLID PHASES

We have given the characteristic infrared spectra of phenol (different phases) in Figures 5.3 - 5.5, which exhibit variations with the changes in the physical states of the sample. The variations are in the band positions, half band widths and relative intensities. Further, appearance of new bands in the condensed phases and splitting of the bands in the crystalline state are also observed.

Phenol involves hydrogen bonding. So in condensed phase the intermolecular interaction becomes very significant. This causes the change in the whole character of the infrared spectrum on going from vapour to the state of aggregation. The most marked changes have been observed for OH group frequencies which are directly involved in the hydrogen bonding and smaller changes in others where a significant amount of the character of OH vibrations are present. These changes are of two types (i) shift in the peak positions and (ii) changes in the half band widths.

(i) Shifts: The data listed in Table 5.2 can be explained on the general model of hydrogen bond formation to different degrees under the specific experimental conditions. The out-of-plane OH vibration (the OH torsion) shows frequency rise by about 45%

in solid phase. Although out-of-plane torsional modes have been observed only in a few cases and not many correlations exist in literature, in water molecule upward shift by 25% of the frequency value is known to occur in going from liquid to crystalline form (17) at -170°C. Our data for OH stretching vibration agree with the observations of Bellamy and Pace (18) for different degrees of associations. A decrease of OH stretch from 3656 cm^{-1} to 3220 cm^{-1} at LNT supports the X-ray hypothesis of endless chains of phenol molecules in solid state. The decrease in CO bond frequency with increasing hydrogen bonding is as expected. Further, no major shift has been observed in case of benzene skeletal vibrations viz. 4,10b,12,17b,1,18a and 15 (Cf. Table 5.3). The low lying vibrations have a trend of upward shift but not always, so nothing can be said with certainty about the effect of association of molecules on the peak positions.

ii) Half Band Widths: The half band widths in the vapour phase spectrum recorded at low pressure (≃.27 mm) have been found to be in the range 19 to 26 cm^{-1} with well resolved band envelopes (Table 5.4). In the liquid and solution phases the vibrational bands possess a comparatively simpler form consisting of a single maximum at appropriate vibrational frequency with the absence of rotational structure; thus for distinct bands the reduced half band widths have been found of the order of 6 cm^{-1} in dilute solution and 6-10 cm^{-1} in the liquid phase. This difference may be due to the extensive hydrogen bonding in the liquid state.

It is evident from Table 5.4 that the vibrations having significant contributions from OH group show larger half band

widths than usual. This half band width is reduced by lowering the temperature. In case of sharp clean bands the half band widths are of the order of 3 to 4 cm^{-1} in solid phase at LNT (Table 5.4).

In condensed phase unusually large half band widths have been found in case of OH stretching and OH bending modes. These are due to the formation of polymers and also due to overlap by other bands.

E. RELATIVE INTENSITIES

It is difficult to make satisfactory quantitative estimates of the intensity changes with change of phase because in large number of cases the bands overlap to such an extent, that although their peaks are clearly resolved, considerable uncertainty is involved in deducing their individual intensities; further, atmospheric water absorptions are involved below 400 cm^{-1} and in OH stretching and bending regions. So in a semi-quantitative way, the relative intensities of the fundamental vibrational frequencies of phenol have been obtained by multiplying the peak height with the band width at half the height of the band on an arbitrary scale. Taking the maximum number thus obtained as 100 others are estimated and are listed in Table 5.3 and plotted in Figure 5.7.

In the Raman spectrum the major part of the intensity is distributed in the decreasing order among CH (stretch), ring breathing X-sensitive and out-of-plane ring bending modes, while in the infrared vapour phase spectrum most of intensity

is shared in the descending order by OH(bend), CO(stretch), OH(torsion), 10b(CH bend) and 19a(CC stretch). In the spectra of condensed phases OH bend always remains strongest followed by 10b while others like 7a,9a,18a,18b and the torsional vibrational modes show considerable decrease in their intensities in the solid phase at LNT (Cf. Table 5.3 and Figure 5.7).

In the condensed phase, reliable intensity measurements could not be made for OH stretch (hydrogen bonded) because it appears as a broad band in the wide range of frequencies and is also overlapped by other bands. Hence the total estimated area under the absorption band (on an arbitrary scale) is depicted in Figure 5.7 by dotted rectangle.

It is evident from Figure 5.7 that the strong Raman bands are not strong in infrared and vice versa. In infrared spectra the vibrational modes 8a and 8b, and 19a and 19b interchange intensities among themselves i.e. 8a with 8b and 19a with 19b, in going from vapour to condensed phases.

The changes in intensities, especially in X-sensitive and OH modes can broadly be attributed to the intermolecular association.

F. SOLID PHASE SPECTRA

For recording the solid phase infrared spectra of phenol at LNT and at RT two different methods of sample preparation were used. For low temperature spectrum the usual method described in section B was used. For recording the spectrum at room temperature the vacuum distilled phenol was dissolved in carbontetrachloride (AnalaR grade) dried over night on P_2O_5

in a desiccator. This solution was poured over a CsBr plate and evaporated till a suitable crystalline film was deposited. This was covered by another plate of CsBr and then the spectrum was recorded.

Splitting of Bands: Phenol molecule belongs to Cs point group, so it does not have any degenerate vibration. In the crystalline state, therefore there could not be site symmetry splitting of the infrared bands. The observed splitting of bands may be due to factor group splitting. From the X-ray study (13) the crystal structure of phenol has been found to have monoclinic symmetry of space group C_2^2 with six molecules per unit cell. These are arranged in two infinite screw like chains each having three molecules in the unit cell as shown in Figure 5.1. This suggests that each vibration should split into six, but we have observed splitting into two only in a few bands (Cf. Figure 5.6 and Table 5.5) where the separation is in the range of 5 to 6 cm^{-1}. This may suggest that the two chains of phenol molecules do not influence each other in the unit cell; therefore, out of the three expected components of each band one is obscured probably due to resolution of the instrument.

All of the bands found splitted at LNT (Cf. Figure 5.6 and Table 5.5), have not shown splitting at RT; obviously this may be due to lowering of temperature.

Appearance of New Bands: The modes of vibrations belonging to a_2 species which are forbidden in vapour phase infrared, have been observed as weak bands in the solid phase shown in

Table 5.3 and Figures 5.3-5.5. This suggests that the symmetry of the free molecule is altered in the bonded form in solid phase. Mode 3 has not been observed in the vapour phase spectrum but appeared in the solid state at 1292 cm^{-1} which shows a considerable shift from its position at 1277 cm^{-1} estimated from UV spectra (7). Some combinations shown in Table 5.7 have not been observed in vapour but are observed in solid phase at LNT. Further, bands in the range 2000-3000 cm^{-1} have been observed in phenol-h_6 only and that too in condensed phases. They are discussed in the next section.

G. OVERTONES AND BINARY COMBINATIONS

Overtones: The observed overtones of the fundamental vibrations have been collected in Table 5.6. The anharmonicities and corrected frequencies have been listed in columns 6 and 7. A striking feature is that the anharmonicities are negative and small for all the bands except for OH torsion.

Binary Combinations: The prominent vapour and solid (LNT) phase bands have been listed with their assignments in Table 5.7. Many of these combinations involve out-of-plane or bending modes of the phenyl ring. All the combinations are not common to the vapour and solid phase spectra. The number of combinations in the solid phase is larger than in the vapour phase.

The combinations in the region 1650-2000 cm^{-1}, normally, are five in number in the low resolution spectrum, but in high resolution spectrum the number is more. These combinations are of CH bending modes and also appear in the spectrum

of phenol-d_1. The combinations in the region 2000-3000 cm^{-1} are observed in the liquid and the solid phases and also in solution provided it is not very dilute. Seven of these bands are the combinations of OH bend and other ring vibrational modes, hence could not be observed in the spectra of phenol-d_1. The combinations at 2510, 2440 and 2405 cm^{-1} may be due to monomer species as they have been observed in the vapour phase and in dilute solutions spectra. So far difference bands are concerned, as expected, none of them could be observed in the solid phase (LNT).

H. THERMODYNAMIC PROPERTIES

With the availability of precise values of vapour phase fundamental vibrational frequencies of phenol, the barrier height for free rotation of OH group (7,8) and the moments of inertia (10), it is worthwhile to recalculate the thermodynamic quantities and compare them with the earlier results (21) reported on the basis of solution phase spectral data and speculated geometry of the molecule. Using the usual methods in statistical mechanics (Cf. Chapter I Section L) the thermodynamic quantities have been calculated for 1 mol of gas at 1 atmosphere pressure in the temperature range 200 to 1000°K and corrected for gas imperfection and restricted rotation. The symmetry numbers are 'one' for over all rotation and 'two' for internal rotation. The thermodynamic functions thus computed have been listed in Table 5.8a.

From the quantities given in columns 3 and 5 of Table 5.8a together with those (23) for C(graphite), H_2 (gas), and O_2(gas)

and the experimental values of heat of formation of phenol gas (22) the values of ΔHf^{o}_{T}, ΔGf^{o}_{T} and $\log_{10} K_p$ have been calculated for the reaction

$$6C(\text{graphite}) + 3H_2(\text{gas}) + \tfrac{1}{2} O_2(\text{gas}) = C_6H_5OH(\text{gas})$$

In comparison to the entropy calculated by Green (21) the present value is found to be in better agreement with the experimental (Cf. Table 5.8b) value. Therefore it seems that there is no major error in the assignment and the geometry of the molecule used; and the quantities listed in Table 5.8a are probably correct within $\pm$ .1.

I. COMPARISON OF THE RESULTS OF PhCl, BzH AND PhOH

The results obtained from the infrared and the Raman studies of these molecules have been compared below:

Geometry: In all these molecules the substituent acts like a point mass centered on the main axis so the vibrations pertaining to the benzene ring behave as belonging to C_{2v} symmetry. Only the vibrations belonging to or involving significant contribution of the substituent show the exact symmetry of the molecule. In the condensed phases the point group symmetry is lowered in all cases studied. So the transitions, forbidden under C_{2v} symmetry for a free molecule, become allowed and are observed in the solid phase (LNT) spectrum. Further, combinations of lattice vibrations with internal modes, and the splitting of some bands, in each compound, have been observed.

Shifts in Band Positions: No relationship could be established between the shifts in the benzene ring vibrations and the electronegativity and/or reduced mass of the substituent in the molecules studied.

The shifts in the frequencies pertaining to the substituent in passing from vapour phase to solid phase are far greater in PhOH (evidently, due to extensive hydrogen bonding effects) than in BzH and PhCl; the OH torsion frequency increases by ≈45%, the OH bending mode increases by ≈ 5% and OH stretching frequency decreases by≈12%. In contrast, the CO frequency in BzH changes by ≈ 2%. Further, in general most of the vibrations below 400 cm^{-1} are found to increase and those with higher frequencies decrease on going from vapour to the condensed phases.

Intensities: In the infrared spectra both in the vapour and the solid (LNT) phases the strongest bands belong to the same normal mode of vibration. (However, the OH stretching mode in phenol shows abnormal broadening in condensed phase spectra). The CH out-of-plane bending mode at 740 cm^{-1} in PhCl, CO stretching mode in BzH and OH bending mode in PhOH are the strongest bands in the infrared vapour phase spectra.

In the Raman spectra the strongest bands are: ring breathing mode in PhCl; CO stretching mode in BzH; and CH stretching modes in PhOH. It may be inferred from these observations that the intensity distribution among different vibrations does not follow any rule both in infrared and Raman

spectra; it simply depends on the nature and the type of the substituent in the benzene ring.

The CO stretching mode in BzH is the only vibration, in these molecules, which shows maximum change in the dipole-moment and polarizability simultaneously.

Infrared Vapour Phase Band Contours: In the vapour phase infrared spectra of these molecules: the bands of CHO group in BzH and all the b_2 class vibrations of PhOH are of A/B hybrid nature and; the remaining vibrations of BzH and PhOH, and all the vibrations of PhCl are observed with distinct A-, B- and C-type band envelopes. The PR separations in A-, B- and C-type band contours and the I_Q/I_{Total} (for A and C-type contours) are nearly same for PhCl and BzH, but both these values are higher for PhOH compared to the values of PhCl and BzH. These differences may be due to (a) the larger asymmetry of PhOH in comparison to PhCl and BzH and (b) the direction of the change of dipole moment with respect to the axis of intermediate moment of inertia.

Half Intensity Band Width: The vapour phase half band widths of clean infrared bands of PhCl and BzH are $\sim$ 20 cm^{-1} and PhOH is $\sim$26 cm^{-1}. In solid phase at LNT the half band widths of the infrared bands are reduced to $\sim$ 2 cm^{-1} in PhCl, 6 cm^{-1} in BzH and $\sim$ 3 to 6 cm^{-1} in PhOH. The values of liquid phase half band widths, in the three molecules, have been found to lie between vapour and solid phase values. The different values of half band widths in the vapour phase spectra are

associated with the differences in the rotational constants and asymmetry parameters (Cf. Table 6.2) for the molecules and in the condensed phases are due to the different types of associations in these molecules.

Isotope Effects: The X-sensitive modes have been found to split into two in the infrared spectra of PhCl due to the natural abundance of chlorine isotopes ^{35}Cl and ^{37}Cl in the ratio 3:1. However, no conclusive evidence for the separate bands due to the natural abundance of ^{13}C and ^{12}C could be found in any of the compounds.

Overtones: The anharmonicities have been calculated for those fundamental vibrations, whose overtones have been observed. It has been found that the anharmonicities lie between -3 and 13.6 cm^{-1} in PhCl, between -4.1 & 21.5 cm^{-1} in BzH and between -4 and 30 cm^{-1} in PhOH. No reason could be assigned for these findings.

Combinations: Each of the 5 strong characteristic infrared bands of monosubstituted benzenes in the range 1650-2000 cm^{-1} has been found to be made of more than one closely situated combinations resulting in a complex structure under high resolution.

In the condensed phases of PhOH only some strong infrared bands have been observed in the region 2000-3000 cm^{-1} which happen to be the combinations of OH bending mode and the ring vibrations.

The out-of-plane bending fundamentals and inplane bending modes are primarily responsible for most of the observed binary combinations in these molecules.

J. REFERENCES

1. J.C.D. Brand and J.C. Speakman: "Molecular Structure, The Physical Approach", Edward Arnold (Publishers) Ltd., London, (1960).

2. P.J. Wheatley: "The Determination of Molecular Structure", The Clarendon Press, Oxford, (1959).

3. H.D. Bist, J.C.D. Brand and D.R. Williams: J. Mol. Spectry. 21, 76 (1966).

4. H.D. Bist and D.R. Williams: Bull. Am. Phys. Soc. 11 (6), 826 (1966).

5. J.C.D. Brand and H.D. Bist: Symp. Mol. Structure and Spectroscopy, Columbus, Ohio 26 (1966).

6. J.C.D. Brand and H.D. Bist: Proc. of the International Conference on Spectroscopy 1, 264 (1967).

7. H.D. Bist, J.C.D. Brand and D.R. Williams, J. Mol. Spectry. 24, 402 (1967).

8. H.D. Bist, J.C.D. Brand and D.R. Williams, J. Mol. Spectry. 24, 413 (1967).

9. T. Kojima; J. Phys. Soc. Japan 15, 284 (1960).

10. H. Forest and B.P. Dailey: J. Chem. Soc. 45, 1736 (1966).

11. J.C.D. Brand, S. Califano and D.R. Williams, J. Mol. Spectry 26, 398 (1968).

12. V.S. Tomar, H.D. Bist and V.D. Gupta; (To be published).

13. von. C. Scheringer, Z. Krist. 119, 273 (1963).

14. B.P. Stoicheff, Canadian J. Phys. 32, 339 (1954).

15. P. Venkateswarlu and W. Gordy, J. Chem. Phys. 23, 1200 (1955).

16. J.D. Swalen, J. Chem. Phys. 23, 1739 (1955).

17. G.C. Pimental and A.L. McClellan: "The Hydrogen Bond", Freeman and Co., Reinhold, N.Y., (1960), pp 125.

18. L.J. Bellamy and R.J. Pace: Spectrochim Acta 22, 525 (1966).

19. R.J. Jakobsen and J.B. Brasch: Spectrochim. Acta 21, 1753 (1965).

20. S.G.W. Ginn and J.L. Wood, Spectrochim. Acta 23, 611 (1967).

21. J.H.S. Green, J. Chem. Soc. 2236 (1961).

22. D.R. Stull, E.F. Westrum, Jr. and G.C. Sinke, "The Chemical Thermodynamics of Organic Compounds", pp. 454, John Wiley and Sons, Inc. New York,(1969).

23. D.R. Stull, I. Carr, J. Chao, T.E. Dergazarian, L.A. du Plessis, R.E. Jostad, S. Levine, F.L. Oetting, R.V. Peterlla, H. Prophet, and G.C. Sinke, JANAF "Thermochemical Tables", Clearinghouse for Federal Scientific and Technical Information, Springfield, Va,(1966).

TABLE 5.1

Structural parameters of phenol in vapour phase

Parameter[a]	Vapour phase	
	Microwave[b]	Infrared[c]
C-C	1.3954 ± .0002	1.396
C-H	1.082 ± .001	1.084
O-H	0.944 ± .009	0.944
C-O	1.379 ± .001	1.3615
∠COH	105.04 ± .35	114.7[d]
		114.2[e]
∠φ	-11.17 ± .50	5.4[d]
		5.0[e]

'a' The bond distances are in Å units and angles in degrees.

'b' Best structure given by Forest and Dailey (10).

'c' Results calculated by Bist et al. (8)

'd' Value for the pair of compounds C_6H_5OH and C_6H_5OD.

'e' Value for the pair of compounds $C_6H_5{}^{18}OH$ and C_6H_5OD.

TABLE 5.2

Important structure sensitive infrared bands (in cm^{-1}) in phenol

Vibrations	Vapour at RT[a]	Solutions			Solid	
		Monomer	Dimer	Higher polymer	RT	LNT
OH stretch	3656	3611[b]	3481[b]	3352[b]	3220	3220[c] 3200[c] 3400[c]
OH bend (ip)	1176	1179	1185	1224	1224	1237
CC stretch	1343	1341	1351	1380	1380	1376
OH bend (oop)	309	320	-	-	453	465 457
O---O stretch	-	-	-	150[d]	176	175[c] 135[c]
O---O bend (oop)	-	-	-	-	-	88.45[c] 92.49[c]
CO stretch	1261	1253	1252	1250	1252	1252
X-sensitive	244 (Raman)	-	-	-	255	267

'a','b','c' and 'd' are the values taken from references Bist et al. (7), Bellamy et al. (18), Jakobson et al. (19) and Ginn and Wood (20) respectively.

(ip), (oop), (RT) and LNT) denote inplane, out-of-plane, room temperature and liquid nitrogen temperature respectively.

TABLE 5.3

Fundamental vibrations (in cm^{-1}) of phenol from the infrared (different phases) and the Raman (solution in CCl_4) spectra

Mode and approximate description	INFRARED								RAMAN	
	Vapour† (RT)		solution in CCl_4 (RT)†		Liquid (≃ 45°C)		Solid (LNT)†		Solution in CCl_4	
a' (a_1)										
OH stretch	3656	(36)*	3600	(18)*	3365		3220			
20a, CH stretch	3087	(17)	3090		3078		3085			
2, CH stretch	3063	(22)							3066	(100)
13, CH stretch	3027		3012	(4)						
8a, CC stretch	1603	(34)	1593	(52)	1593	(33)*	1594	(34)*	1598	(23)
19a, CC stretch	1501	(73)	1494	(42)	1495	(24)	1497	(15)		
7a, CO stretch	1261	(85)	1252	(48)	1253	(15)	1252	sh	1253	(24)
OH bend	1176	(100)	1177	(100)	1224	(100)	1237	(100)		
9a, CH bend	1168	(53)	1167	(5)	1168	(12)	1166	(3)	1169	(18)
18a, CH bend	1025	(52)	1022	(7)	1023	(4)	1022	(5)	1024	(22)
1, ring	999	(4)	996	(5)	1000	(4)	998	(1)	999	(100)
12, X-sensitive	823	(46)	823	(6)	823	(5)	820	(12)	826	(28)
6a, X-sensitive	526	(16)	522	(2)	526	(2)	531	(10)	534	(15)
a' (b_2)										
20b, CH stretch	3070		3070	(7)	3048	(8)	3050	sh		
7b, CH stretch	3049		3038	(16)	3028	(3)	3027	sh		
8b, CC stretch	1610	(46)	1603	(26)	1601	(12)	1603	(10)	1609	(8)
19b, CC stretch	1472	(38)	1468	(20)	1468	(34)	1473	(33)		
14, CC stretch	1343	(48)	1340	(21)	1358	(17)	1375	(24)		

Contd. ...

1	2		3		4		5		6
3, CH bend					1290	(2)	1292	(2)	
9b, CH bend	1150	(37)	1150	(24)	1150	(16)	1150	(3)	1157
15, CH bend	1070	(16)	1068	(14)	1071	(11)	1071	(8)	1076
6b, ring	619		618		619		612	(3)	618
18b, X-sensitive	403	(23)	405	(7)	406	(1)	411	(1)	
a'' (a_2)									
17a, CH bend	(995.2)**				978	vw	982	(1)	
10a, CH bend	(817.2)				811	(12)	813	(16)	813
16a, CC twist	(408.5)				417	vw	417	(1)	
a'' (b_1)									
5, CH bend	973		970		957	vw	965	(2)	968
17b, CH bend	881	(4)	881	(8)	890	(10)	888	(7)	
10b, CH bend	751	(92)	751	(61)	752	(33)	754	(73)	761
4, CC twist	686	(13)	688	(28)	690	(15)	690	(11)	
16b, X-sensitive	503	(27)	501	(15)	502	(8)	498	(16)	503
Torsion	309	(91)	319	(5)	343		457	(10)	
11 X-sensitive							267		244

*Number in parentheses indicates the relative intensity of the band.

**Frequencies in the parentheses are from electronic spectra Ref. (8).

†(RT) and (LNT) stand for room temperature and liquid nitrogen temperature respectively.

sh and vw denote shoulder and very weak intensity respectively.

†Vapour phase data are same as reported in reference (7).

TABLE 5.4

Typical half band widths of some bands in the infrared absorption spectrum (in cm^{-1}) of Phenol in different phases

Mode	Vapour		Solution in CS_2		Liquid		Solid (R.T.)		Solid (LNT)	
	Frequency	Half width	Frequency	Half width	Frequency	Half width	Frequency	Half width	Frequency	Half width
ν OH	3656	29	3600	50	3365	350	3330	350	3220	350
14	1343	26	1340	6	1358	(overlap)	1370	(overlap)	1375	20 (overlap)
	1326	26	1328	6	1316	10	1311	8	1314	6
9b	1150	24	1150	7	1150	10	1150	7	1150	4
15	1070	21	1068	7	1071	13	1070	10	1071	6
18a	1025	19	1022	6	1023	9	1023	8	1022	7
1	999	21	996	5	1000	6	997	6	998	3
17a					978	7	979	4	982	3
17b	881	24	881	12	890	14	890	14	888	4
4	686	19	688	7	692	9	690	10	690	6
6a	526	25	522	4	526	9.5	528	7	531	5
18b	403	26	406	6	406	5.5	409		411	4

Gap indicates that the band is either very weak or could not be observed.

'ν' stands for bond stretching mode.

TABLE 5.5

Infrared bands of phenol (in cm^{-1}) which show splitting in the crystalline phase at liquid nitrogen temperature (LNT) and room temperature (RT)

Mode and approximate description	Vapour (RT) (cm^{-1})	Solid (RT) (cm^{-1})	Solid (LNT) (cm^{-1})	Splitting in bands (at LNT)
19b, CC stretch	1472	1476 1471	1478 1473	5
9a, CH bend	1168	1166	1172 1166	6
18a, CH bend	1025	1023	1027 1022	5
10b, CH bend	751	751	754 748	6
16b, X-sensitive	503	499	503 497	6
Torsion 'OH'	309	460 457	462 457	5

TABLE 5.6

Observed and calculated values (in cm^{-1}) of the overtones of some fundamental vibrations of phenol

Mode	OBSERVED			CALCULATED		
	Frequency (cm^{-1})	Phase	Overtone (cm^{-1})	Harmonic value of overtone	$2w_e x_e$ (cm^{-1})	w_e (cm^{-1})
OH bend	1237	solid	2474	2474	0	1237
9b	1150	solid	2302	2300	-2	1148
5	965	solid	1933	1930	-3	962
17b	888	solid	1777	1776	-1	887
17b	881	vapour	1763	1762	-1	880
10a	811	liquid	1623	1622	-1	810
10b	754	solid	1510	1508	-2	752
10b	751	vapour	1505	1502	-3	748
16b	503	vapour	1009	1006	-3	500
18b	403	vapour	809	806	-3	400
Torsion	309 [a]	vapour	588	618	30	339
11	(244.5) [a]	vapour	493	489	-4	240.5
O---O stretch	(135) [b]	solid	272	270	-2	133

'a' Value taken from the Raman spectra.

'b' Value taken from Jacobson et al. (19).

TABLE 5.7

Infrared binary combinations of phenol

Frequency in cm^{-1}	Assignments					
2960	2OH bend	+	16b,	2 X 1237	+ 498	= 2972
2840	OH bend	+	8b,	1237	+ 1603	= 2840
2720	OH bend	+	19a,	1237	+ 1497	= 2734
2606	OH bend	+	14,	1237	+ 1375	= 2612
(2510)*	OH bend	+	14,	1176	+ 1343	= 2519
2474	2OH bend,			2 X 1237		= 2474
(2440)	OH bend	+	3,	1176	+ 1277	= 2453
2412	8b	+	10a,	1603	+ 813	= 2416
(2405)	14	+	15,	1343	+ 1070	= 2413
2302	2 X 9b,			2 X 1150		= 2300
2172	9b	+	18a,	1150	+ 1022	= 2172
2028	9b	+	17b,	1150	+ 888	= 2038
1977	1	+	17a,	998	+ 982	= 1980
1954	19a	+	T**,	1497	+ 456	= 1953
1933	2 X 5,			2 X 965		= 1930
(1931)	OH bend	+	10b,	1176	+ 751	= 1927
(1925)	8b	+	T,	1610	+ 309	= 1919
1847	17b	+	5,	888	+ 965	= 1853
(1830)	18a	+	10a,	1025	+ 817	= 1842
1803	17a	+	12,	982	+ 823	= 1805
1777	2 X17b,			2 X 888		= 1776
(1765)	2 X17b,			2 X 881		= 1762
1710	12	+	17b	823	+ 888	= 1711
(1690)	15	+	6b,	1070	+ 619	= 1689
1547	17b	+	10b,	888	+ 754	= 1542
1390	17b	+	16b,	888	+ 498	= 1386
(1326)	2	+	16b,	823	+ 503	= 1326
(1197)	17b	+	T,	881	+ 309	= 1190
1135	5	+	OO Str.	965	+ 175	= 1140
(1102)	14	−	11,	1343	− 244	= 1099
(1057)	10b	+	T,	751	+ 309	= 1060
1050	O---O(oop.b)†		5		88 + 965	= 1053
(951)	7a	−	T,	1261	− 309	= 952
(904)	16b	+	18b,	503	+ 403	= 906
838	O---O(oop.b)	+	10b,	754	+ 88	= 842
(827)	6a	+	T,	526	+ 309	= 835
795	6a	+	11,	531	+ 267	= 798
(588)	2,(Torsion)			2(309)		= 618
(469)	5	−	16b,	973	− 503	= 470
(278)	6a	−	11,	526	− 244	= 282

† * (oop.b) stands for out-of-plane bend (Cf. Table 5.2). Values in parentheses are vapour phase frequencies.
** T stands for OH Torsion. Str. stands for O---O stretch.

TABLE 5.8a

The molal thermodynamic properties of phenol in the ideal gas state

$T^{\circ}K$	C_p°	$(H^{\circ}-H_o^{\circ})/T$	$-(G^{\circ}-H_o^{\circ})/T$	S°	ΔHf_T°	ΔGf_T°	$Log_{10} K_p$
	Cal/mole $^{\circ}K$				K cal/mole		
200	17.71	10.10	54.83	64.93	-21.82	-12.21	13.342
298.16	24.94	13.75	60.17	73.92	-23.03	-7.41	5.431
400	32.52	17.58	64.89	82.47	-24.09	-1.97	+1.076
500	38.71	21.21	69.26	90.47	-24.88	3.65	-1.595
600	43.60	24.59	73.41	98.00	-25.49	9.40	-3.424
700	47.51	27.59	77.43	105.02	-25.96	15.26	-4.764
800	50.68	30.26	81.33	111.59	-26.34	21.15	-5.775
900	53.32	32.68	85.04	117.72	-26.60	27.09	-6.578
1000	55.55	34.85	88.60	123.45	-26.76	33.08	-7.229

TABLE 5.8b

Vapour phase entropy of phenol at 298.16$^{\circ}K$

Calorimetric	73.81 $\pm$ .64	cal/mole $^{\circ}K$
Spectroscopic (present)	73.92	cal/mole $^{\circ}K$
Spectroscopic (Ref. 21)	75.43	Cal/mole $^{\circ}K$

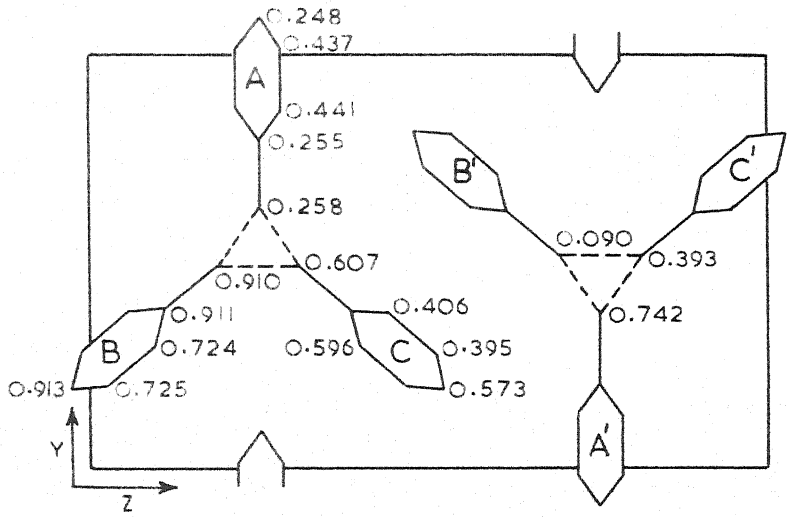

Fig. 5.1 Projection in the direction of 'a' axis. The hydrogen atoms are left out for the sake of clarity. The numbers given are x-parameters. (After reference 13)

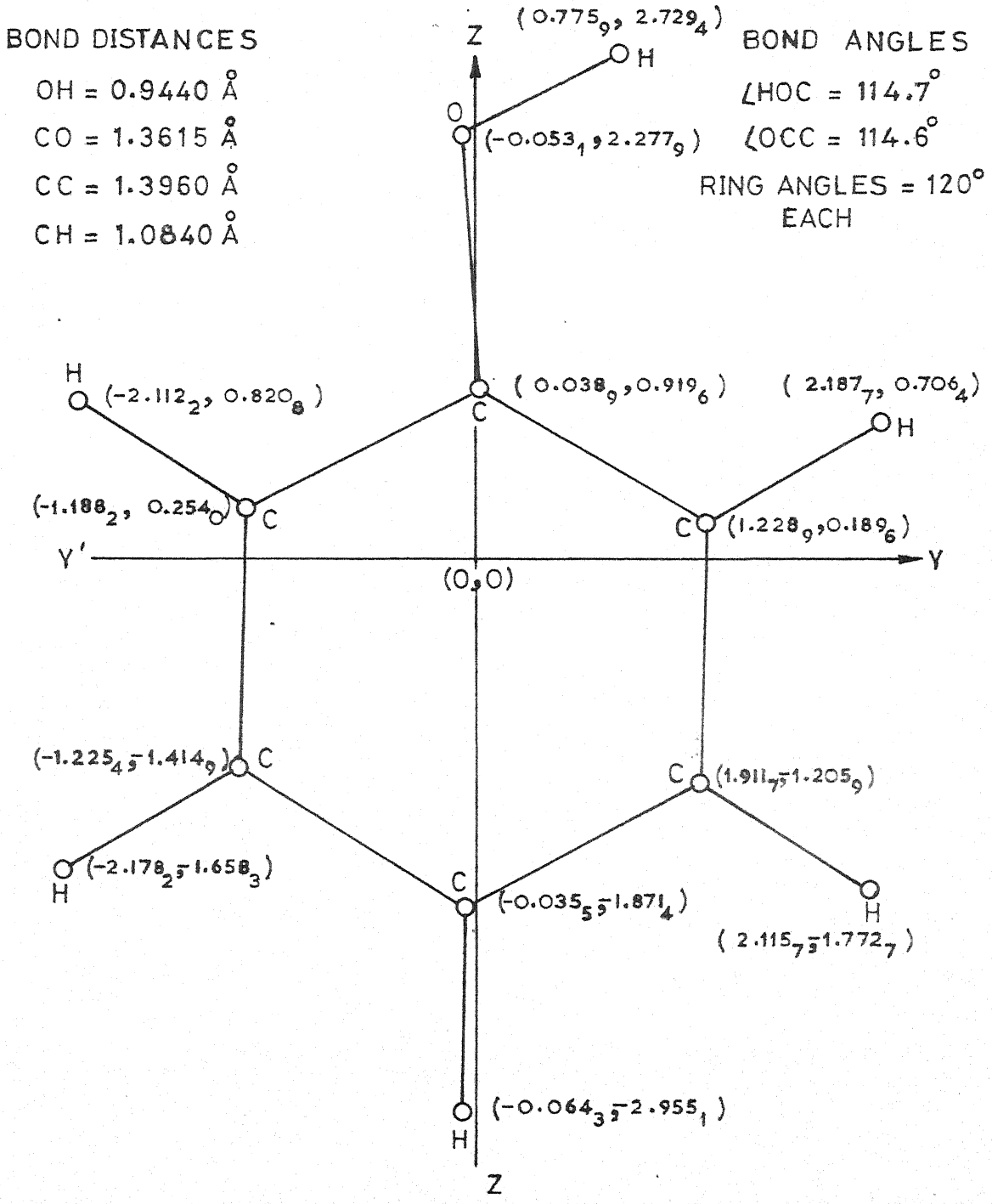

FIG. 5.2 VAPOUR PHASE GEOMETRY OF PHENOL IN ITS GROUND STATE. NUMBERS IN PARENTHESES DENOTE Y, Z COORDINATES (IN Å UNITS) OF THE ATOMS WITH RESPECT TO THE ORIGIN (0,0) THE CENTER OF MASS OF THE MOLECULE.

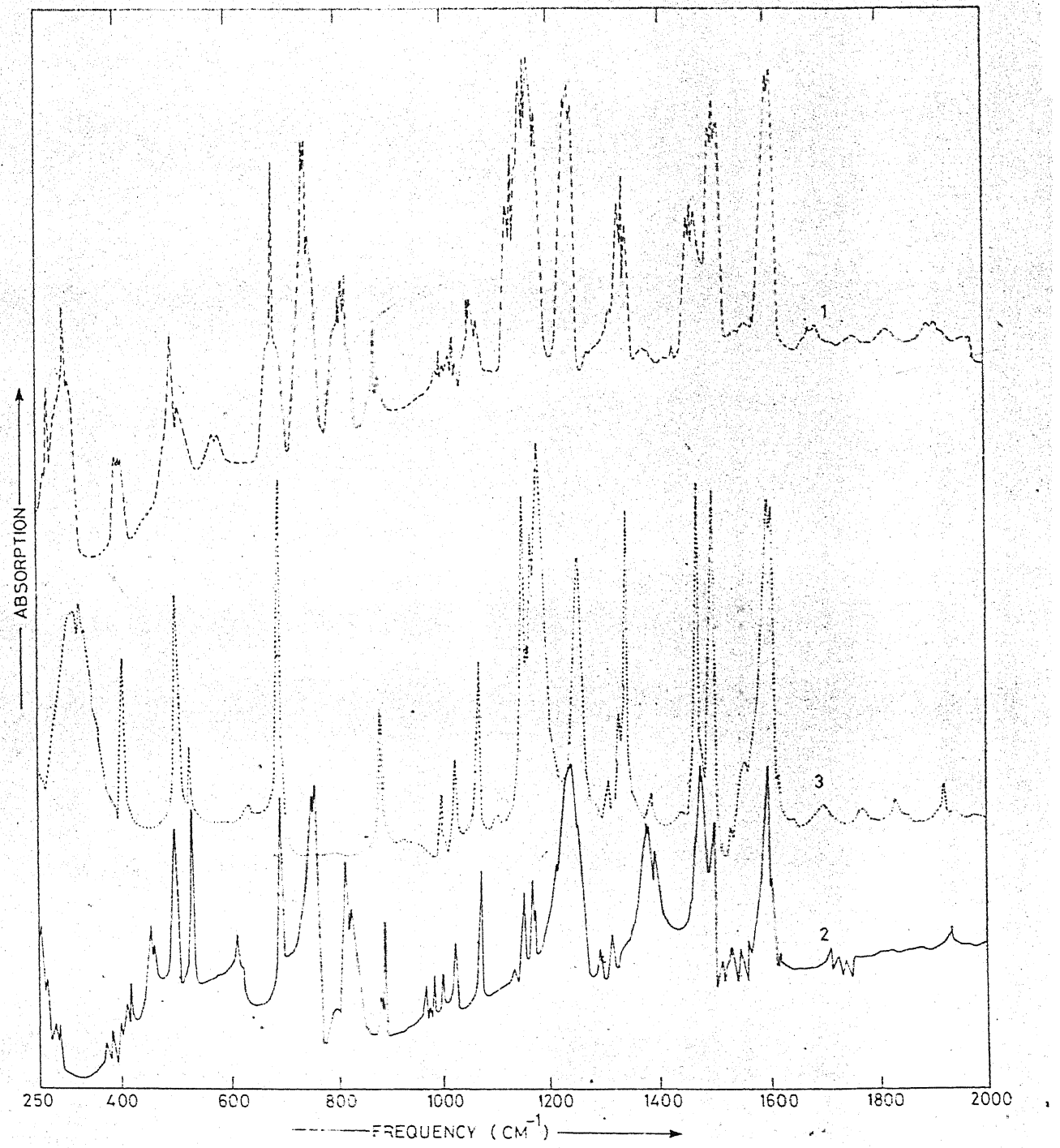

Fig. 5.3: The infrared spectra of Phenol-h_6 in the range 250-2000 cm^{-1}; (1) ---- Vapour phase (recorded on P-E 621); (2) —— Solid phase (liquid nitrogen temperature); (3) ... Very dilute solution in CCl_4. (2 and 3 recorded on P-E 521).

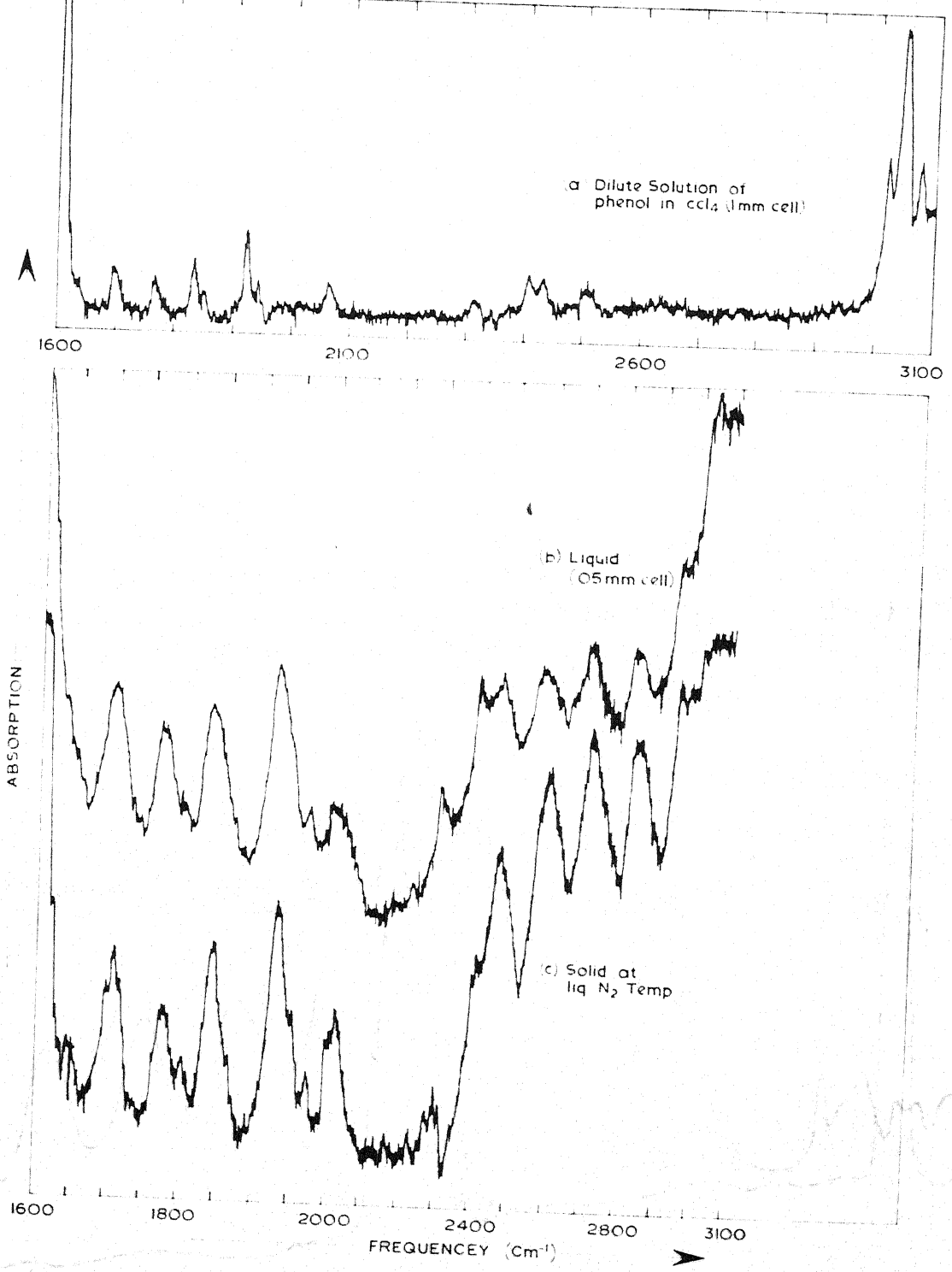

Fig. 5.4: The infrared spectra of Phenol-h_6 in the range 1600-3100 cm^{-1}; (a) Solution in CCl_4 using 1 mm thick cell ; (b) Liquid phase using .05 mm cell; (c) Solid phase at liquid nitrogen temperature (Recorded on P-E 521).

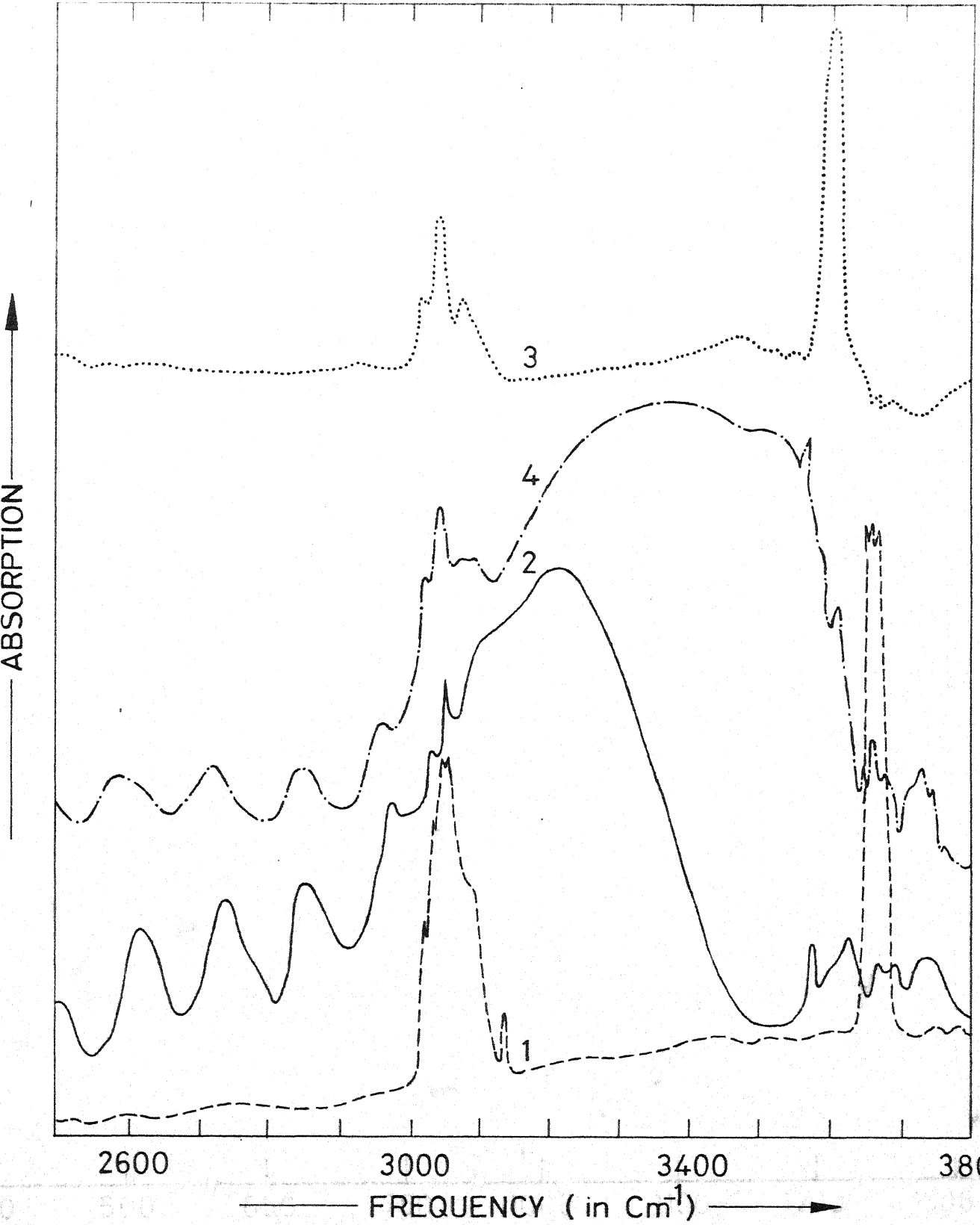

5.5- Infrared spectra of Phenol - h_6 in the range 2500 - 3800 Cm
1.- - - - - - - - Vapour (Recorded on P.E.621), 2- ——— So
(Liq. N_2 Temp.), 3- ..... Very dilute solution in ccl_4 a
4- —·—·— Liquid. (2.3 and 4 Recorded on Carl zeiss UR-1

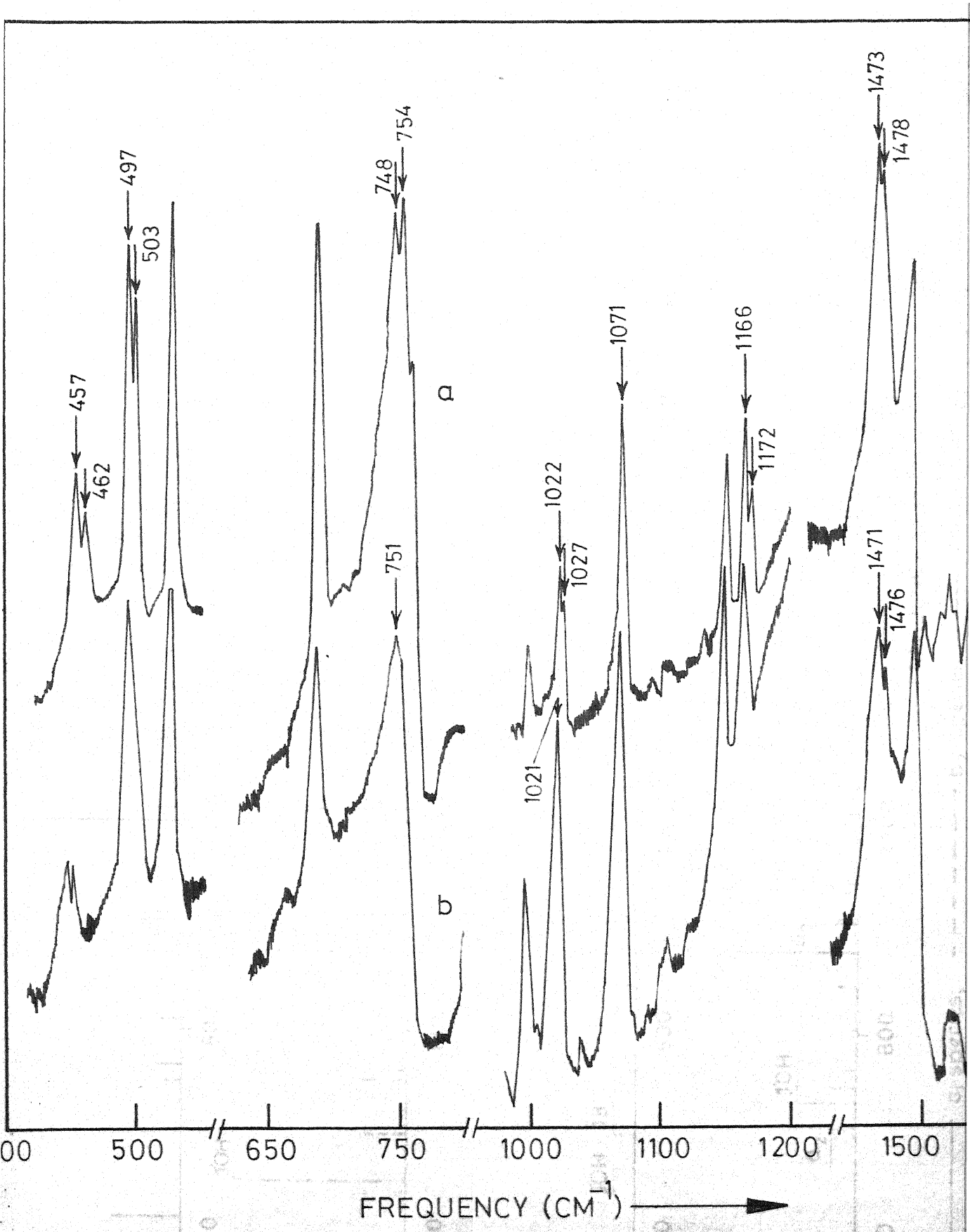

Fig. 5.6 Infrared bands (with their peak positions in cm^{-1}) of phenol-h_6 which sh splitting in the crystalline phase (a) at liquid nitrogen temperature (b) room temperature (cf. table 5.5)

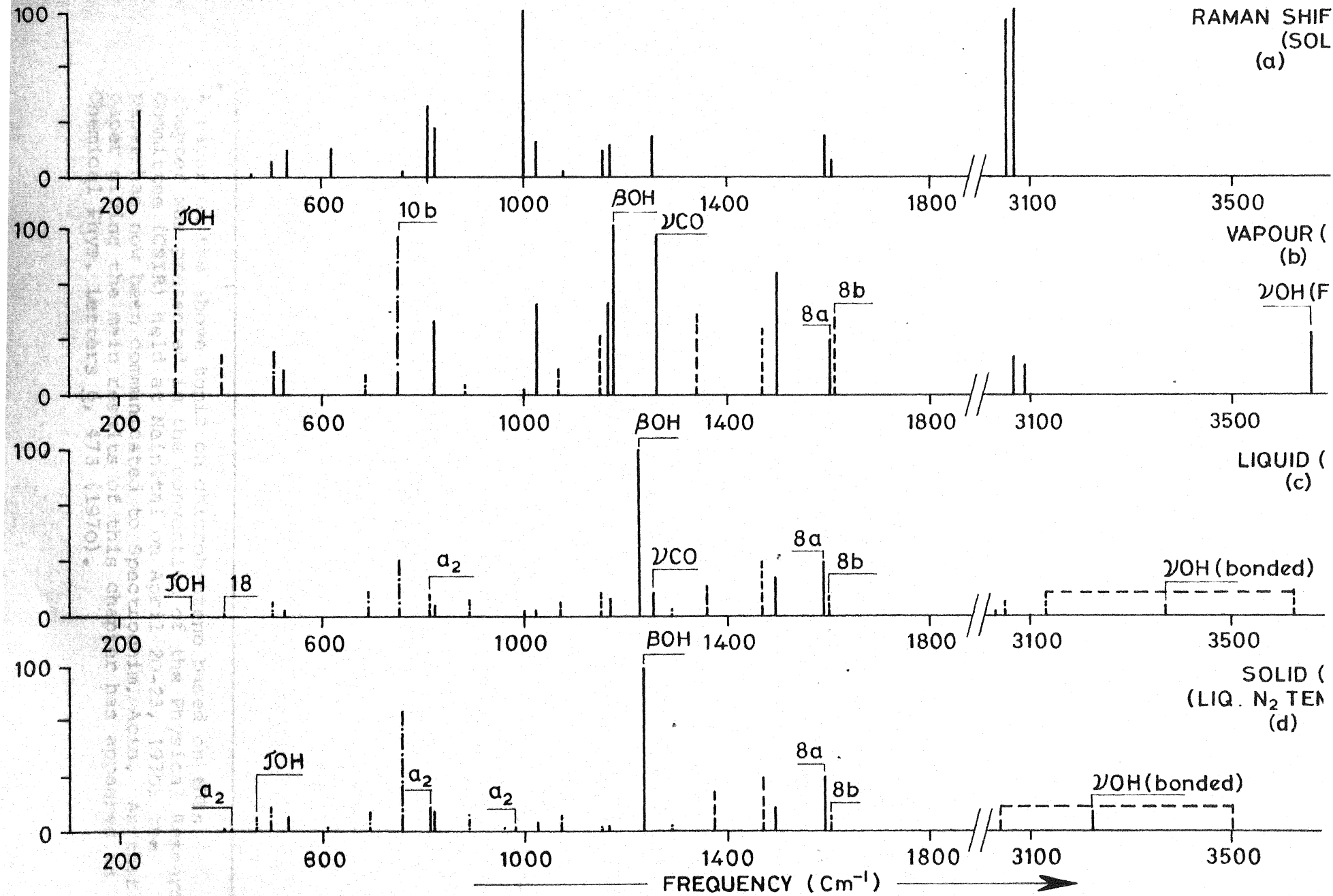
100
0
200
600
1000
1400
1800
3100
3500
RAMAN SHIF
(SOL
(a)
γOH
10b
βOH
νCO
8a
8b
VAPOUR (
(b)
νOH (F
LIQUID (
(c)
18
a2
νOH (bonded)
SOLID (
(LIQ. N2 TEN
(d)
FREQUENCY (Cm-1)
b2 species
b1 species,
Raman sh

CHAPTER VI

PR SEPARATIONS AND RELATIVE 'Q' BRANCH INTENSITIES IN INFRARED BAND CONTOURS OF MONOSUBSTITUTED BENZENES*

ABSTRACT

PR separations in band envelopes of typical A-, B- and C-type and hybrid bands and relative intensity of Q branch with respect to that of the whole band for typical A- and C-type bands have been measured in the spectra of some monosubstituted benzenes. The observed values are compared with those computed from available molecular parameters using the existing semi-empirical theory. General applicability of the infrared band contour method for deducing the molecular parameters is critically examined.

---

* A paper on the above topic on chlorobenzene based on this chapter was presented in the convention of the Physical Research Committee (CSIR) held at Nainital on April 20-23, 1970; the paper has now been communicated to Spectrochim. Acta. Another paper giving the main results of this chapter has appeared in Chemical Phys. Letters 6, 473 (1970).

ellipsoid (MF). The ME is an ellipsoid with the principal axes a, b and c such that

$$a = 2(I_A)^{-\frac{1}{2}},\ b = 2(I_B)^{-\frac{1}{2}} \text{ and } c = 2(I_C)^{-\frac{1}{2}}$$

Thus a is the 'major', b the 'intermediate' and c the 'minor' axis of inertia (1).

For linear and prolate symmetric top molecules a band is referred to as parallel (||) or perpendicular ($\perp$) when it corresponds to a dipole change parallel or normal to the unique (major) a-axis of inertia. For oblate symmetric top molecules a band is referred to as parallel or perpendicular depending on whether it corresponds to electrical oscillations parallel or perpendicular to the unique (minor) c-axis of inertia. However, for asymmetrical top molecules, the letters A-type, B-type and C-type are used to qualify the bands, denoting that the transition dipole moments are parallel to the a, b and c axis respectively.

C. THE BAND STRUCTURE

PQR means that the band consists of three branches with the P branch ($\Delta J = -1$) on the low-frequency side and the R branch ($\Delta J = +1$) on the high frequency side of the Q branch ($\Delta J = 0$). PQQR means that the band structure with four maxima is seen. By PR separation we mean the interval (in cm^{-1}) between the intensity maxima of P and R branches.

D. THEORETICAL STATUS

(i) Linear Molecules: For a linear molecule the PR separation, δ, in a vibration-rotation vapour phase band contour at $T^{o}K$ is given by (2):

$$\Delta\nu_{PR} \equiv \delta = (8BkT/hc)^{\frac{1}{2}} \qquad (6.1)$$

where B is the rotational constant and other symbols have their usual meanings. In the derivation of this formula the change of rotational constants in different vibrational states, the centrifugal distortion effects and the complications resulting from Coriolis interaction have been neglected; and it has also been assumed that the intensity of rotational transition is primarily governed by the product of the statistical weight and the Maxwell-Boltzmann distribution function for the particular energy level from which the absorption is taking place (2).

(ii) Symmetric Top Molecules: For symmetric top molecules Gerhard and Dennison (3) deduced an expression for PR separation in parellel bands which can be represented as:

$$\Delta\nu_{PR}(||) = S(\beta) \cdot \delta \qquad (6.2)$$

where parameter β was defined as

$$\beta = (A/B) - 1 \quad \text{or} \quad (C/B) - 1 \qquad (6.3)$$

for prolate or oblate molecules respectively and the function $S(\beta)$ was given by an empirical relation

$$\log_{10} S(\beta) = \frac{0.721}{(\beta + 4)^{1.13}} \qquad (6.4)$$

which was found to hold good within 0.5% for β in the range $-.5$ to $+100$. They also deduced an expression for the ratio I_Q/I_{Total} in the parallel type bands given by:

$$\frac{I_Q}{I_{Total}} = \frac{\log_e\left[\beta^{\frac{1}{2}} + (1+\beta)^{\frac{1}{2}}\right] - \left[\beta/(1+\beta)\right]^{\frac{1}{2}}}{\beta\left[\beta/(1+\beta)\right]^{\frac{1}{2}}} \qquad (6.5)$$

for $\beta > 0$, a case in which we will be interested as our molecules are all near prolate symmetric tops. Thus I_Q/I_{Total} was a function of parameter 'β' alone. It tends to $\sim$0.5 for disc shaped molecules ($\beta = -\frac{1}{2}$), $\sim$0.33 for a spherical top molecule ($\beta = 0$), and falls to 0 for a linear molecule ($\beta = \infty$).

For the perpendicular bands in symmetric top molecules Gerhard and Dennison deduced expressions for intensity in terms of frequency for the different branches, from which actual band contours were deduced for a few specific values of β but no general formulae for $\Delta\nu_{PR}$ or for I_Q/I_{Total} were given. The notable conclusions for ($\perp$) bands were (i) the Q branch got stronger with β increasing from $-$ 0.5 to $\sim$ 1, beyond which the bands rapidly ceased to show PQR structure, and (ii) $\Delta\nu_{PR}$ decreased monotonously with increasing β .

(iii) Asymmetric Top Molecules: For the asymmetric top molecules the energy level scheme becomes more complex (4), being expressed (for a near prolate molecule) by

$$F(J,\tau) = \overline{B}\ J(J+1) + (A - \overline{B}).E_\tau\ (\kappa) \qquad (6.6)$$

where $\overline{B}$ is defined by:

$$\overline{B} = \tfrac{1}{2}\ (B + C) \qquad (6.7)$$

and the asymmetry parameter κ is defined by:

$$\kappa = \frac{B - \frac{1}{2}(A + C)}{\frac{1}{2}(A - C)} \qquad (6.8)$$

and $E_\tau\ (\kappa)$ represents the (2J + 1) solutions of a determinantal equation first given by Wang (5). Badger and Zumwalt (6) showed that since large J values were involved in the heavy molecules

one could obtain approximate solutions for the (2J + 1) values of $F(J,\tau)$ in terms of κ and another parameter $\ell = (A-C)/B$, and then use Gerhard and Dennison's procedure to obtain band contours. However, general formulae neither for the band contours nor for the PR separations were given; only the contours were drawn for A-, B- and C-type bands for 8 sets of κ and ℓ combinations in a limited range. Use has also been made of computer programmes to obtain the band contours for limited range of κ and ℓ, in the neighbourhood of estimated values, and then to use interpolation. Hollas (7) has found that band contours can be considerably influenced by the differences between rotational constants of ground and upper vibrational states, and therefore any programme must take care of this fact. Franks and Innes (8) have demonstrated the use of this method to deduce, κ from measured I_Q/I_{Total} in favourable cases.

For both parallel and perpendicular type bands of the prolate and oblate asymmetric top molecules, Seth-Paul et. al. (9-12) have proposed general sets of empirical expressions for PR separations applicable in various ranges of κ and ℓ. In effect, for parallel bands of near prolate symmetric tops they used expression (6.2) in the form

$$\Delta\nu_{PR}\, A(||) = S(\bar{\beta}).\bar{\delta} \qquad (6.9)$$

where $\bar{\delta}$ and $S(\bar{\beta})$ are obtained on replacing B by $\bar{B}$ in the expressio for δ and $S(\beta)$ respectively*.

---

* Actually Seth-Paul et.al. (9) have used the harmonic mean of B and C as $\bar{B}$ instead of the arithmetic mean. The results however would not differ appreciably unless the differences between B and C is fairly large (13-14).

For B(⊥) and C(⊥) bands in the range $\frac{3}{4} < \ell < 3$ (a case of interest in the present study) Seth-Paul and Dijkstra's (9) expressions may be put in the form

$$\Delta\nu_{PR}\ B(\perp) = \bar{\delta} \tag{6.10}$$

and

$$\Delta\nu_{PR}\ C(\perp) = \frac{3}{2}\ S(\bar{\beta}).\ \bar{\delta} \tag{6.11}$$

Expressions are not available for the ratio I_Q/I_{Total} for bands of asymmetric top molecules. We therefore propose to extend the application of relation (6.5) to asymmetric top molecules just by replacing β with $\bar{\beta}$.

(iv) Hybrid Bands: For PR separation in hybrid bands Seth-Paul and De Meyer (11) have proposed a formula which is equivalent to

$$\Delta\nu_{PR}\ (\alpha\beta) = \frac{\Delta\nu\,(A)\ \cos\alpha + \Delta\nu\,(B)\ \cos\beta}{\cos\alpha + \cos\beta} \tag{6.12}$$

where α and β are the angles between the oscillating dipole and the a and b axes of the molecule, and $\Delta\nu\,(A)$ and $\Delta\nu\,(B)$ are the PR separations for pure A-type and pure B-type bands, respectively.

However, this is again an empirical formula. The uncertainties in measurement of $\Delta\nu_{PR}$ values (in hybrid bands in particular are so large that relation (6.12) can at best be used to check hybrid character but not for deducing the direction of dipole oscillation within a narrow range. In fact we find that a simple rule-of-three formula like

$$\Delta\nu_{PR}\ (\alpha\beta) = \frac{\alpha\,\Delta\nu\,(A) + \beta\,\Delta\nu\,(B)}{\alpha + \beta} \tag{6.13}$$

gives as good a fit as the formula (6.12) in almost all cases.

In this chapter we have reported the band contours, the PR separations, and the relative Q-branch intensities in some distinct vibration rotation band envelopes of benzaldehyde, chlorobenzene, phenol $-d_5$, phenol $-d_1$ and phenol-h_6 molecules and discussed these results with those computed from the above formulae using rotational parameters available from microwave data (15-19).

E. EXPERIMENTAL

The infrared spectra in the vapour phase were recorded in the 200-4000 cm^{-1} region using a Perkin-Elmer 621 grating spectrophotometer fitted with a frequency marker accessory and equipped with a 10 meter variable path multiple reflection cell with CsI windows. Both the survey runs and high resolution runs were recorded with pressure path products in the ranges 0.1 to 12.0 cm. atm. The strongest bands were recorded with the minimum available path of 1.25 meters from the multiple reflection cell by reducing the pressure available at the ambient temperature ($22^{o}C$) with the help of an adjoining vacuum system. The weakest bands were scanned at normal pressure using the full 10 meter path length. The data presented were obtained after careful adjustment of signal-to-noise ratio and scanning time . The absolute frequency scale, used after calibration, is accurate to $\pm$ 0.5 cm^{-1} below 1600 cm^{-1}, although the inherent breadth of the peaks may limit the accuracy of the reported positions of P and R peaks to as much as $\pm$ 1 cm^{-1}.

The chemicals (AnalaR grade) were triply distilled (Cf. Chapter II) just before recording the spectra.

F. RESULTS

The infrared spectra of chlorobenzene and benzaldehyde molecules have already been given in Figures 3.2 and 4.2 in Chapter III and IV respectively. The complete data for chlorobenzene is tabulated in Appendix 3.1 and that for benzaldehyde in Table 4.1 and the assignments of the observed bands have been discussed in Chapters III and IV respectively.

The high resolution vapour phase infrared spectrum of phenol $-d_5$ is being presented for the first time in Figure 6.1. Although the assignments of the fundamental vibrational modes have been made earlier with the help of the electronic band contour analysis (20-22), but no infrared band contours are available in literature for the phenol $-d_5$.

The infrared spectra for the $-d_1$ and $-h_6$ phenol have been reported earlier (23) and their complete assignments are available (20-22). However, the spectra of these two compounds are given in Figures 6.2 and 6.3 respectively for the sake of completeness.

The relevant details of the bands for $-d_5$, $-d_1$ and $-h_6$ isotopic species of phenol are given in Appendix 6.1.

In the spectra presented, some regions have been skipped as they do not contain any prominent bands.

G. GRAPHICAL RESOLUTION

In some of the bands the band contour is quite distinct and the location of P,Q and R peaks is therefore directly available from the spectrum. However, when two or more bands overlap, the experimental intensity contour has to be resolved. Representative cases of such graphical analysis are given in Figure 6.4 for a

few bands of chlorobenzene. In most cases the characteristic band envelopes and group theoretical considerations are helpful in assignments, and also in decomposition of overlapping bands into A-, B- or C-type. Although these facts are of great assistance in carrying out the analysis, the conclusions in some cases may not be unambiguous. The relative intensity of Q-branch with respect to that of the whole band is yet another aid in the assignment of bands.

H. OBSERVED Q-BRANCH INTENSITY

The ratio 'r' of the Q branch intensity to the total intensity of a band (I_Q/I_{Total}) has been estimated for A- and C-type bands. For this analysis curves were drawn in linear absorbance scale vs. linear frequency scale. The Q branch was separated and using a method analogous to that of Franks and Innes (8) its contribution was deduced giving it a Gaussian shape as shown in Figure 6.5. The areas were measured with a planimeter. Such intensity estimates are subject to considerable uncertainty and the values of 'r' thus estimated may be in error by $\pm$ 30%.

I. THE RE-PLOTTED BANDS

The spectrum of each of the above compound shows a large number of bands all of which could not be examined for their $\Delta\nu_{PR}$ and I_Q/I_{Total} values due either to the complex structure resulting from overtones, binary combinations, Fermi-resonance, hot bands etc., or due to their very feeble intensities - especially in isotopically labelled molecules. For our present purpose we have chosen only those bands of medium intensity which either

exhibit no overlapping with other bands or which could easily be analysed into components (Section G). In the latter case we were guided by the typical band contours of A, B and C-type. The typical replotted bands for benzaldehyde, chlorobenzene, phenol $-d_5$, phenol $-d_1$ and phenol $-h_6$ are given in Figures 6.6, 6.7, 6.8, 6.9 and 6.10 respectively.

Table 6.1 contains the positions of Q peaks. The letters A, B and C infront of the Q positions indicate the type of band based on earlier assignments in phenol and its isotopic species (20-23), in chlorobenzene (24-25 and Cf. Chapter III) and in benzaldehyde (Cf. Chapter IV).

For pure B-type bands the Q positions were obtained from the positions of minimum between the P and R branches. The Q positions given in Table 6.1 are claimed to be accurate within $\pm$ 0.2 cm^{-1} (14

PR Separations: The P and R maxima are rather broad and hence measurement of PR separation has larger uncertainty. However, in the distinct bands chosen by us the $\Delta\nu_{PR}$ values (given in column 2 of Table 6.1) were reproducible within $\pm$ 0.8 cm^{-1} for A- and B-type bands and within $\pm$ 1.5 cm^{-1} for C- type bands.

Using the rotational constants given in Table 6.2 the PR separations in A-, B- and C-type bands have been calculated using the formulae 6.9, 6.10 and 6.11 respectively. Although the ambient temperature was 295°K, we have used T = 300°K in these calculations. However, as the temperature inside the infrared cells is always a few degrees higher and also in view of the other larger limitations of accuracy this approximation seems justified. The calculated values of $\Delta\nu_{PR}$ B($\perp$) and $\Delta\nu_{PR}$ A($\parallel$)

6.4 (iv). In contrast to this, the contours of bands at 416.8 cm^{-1} and 559.1 cm^{-1} would not qualify them to be listed as A-type (Cf. Figure 3.2B). But these contours are different from B- and C-type also. Nevertheless, we have listed these bands as of A-type in view of their established vibrational assignments (24). The origin of this difference in the shape of contour is not clear.

The values of $\Delta\nu_{PR}$ in the 20 bands of A(||) type (Cf. Appendix 3.1) range from 9.8 to 11.0 cm^{-1}; (13 of them are listed in Table 6.1) the computed value being 10.6 cm^{-1}. In view of uncertainty of about $\pm$ 1 cm^{-1} due to breadth of P and R peaks even in clean bands the agreement is satisfactory. This does not however mean that we would be justified in using formula (6.9) freely for all asymmetric top molecules. In fact, chlorobenzene happens to be quite close to a prolate symmetric top molecule with κ = -.845 and hence the symmetric top formulae may be applicable to a fairly good extent. The same remark may be applicable for other monosubstituted benzenes discussed in this chapter.

PQ and QR Separations in A-Type Bands: For the seven A(||) bands which appear very distinctly the PQ and QR separations are given in Table 6.3. It is found that PQ separation is consistently greater than QR separation in all these bands, the ratio being $\sim$1.3. Among the remaining 13 bands (Cf. Appendix 3.1) only in four QR separation is greater than PQ separation. Considering that these latter bands have considerable overlapping with other neighbouring bands it may be inferred that in the A(||)

bands of chlorobenzene the PQ separation is larger than the QR separation. Whether this is a general feature of all asymmetric tops, and whether the ratio ($\Delta\nu_{PQ}$)/($\Delta\nu_{QR}$) has simple correlation with the asymmetry parameter needs closer examination. In fact drastic approximations are involved in deducing the theoretical expressions given above. The change in rotational constants between various vibrational states and the centrifugal distortion effects will have additional important roles to play in modifying the envelopes of different bands of the same class in a given molecule (7).

PR Separations in B($\perp$) and C($\perp$) Type Bands: The typical shapes of B($\perp$) and C($\perp$) band contours in the spectrum of chlorobenzene, are represented by the bands at 1448.0 cm^{-1} (Cf. Figure 3.2B) and 740.6 cm^{-1} (Cf. Figure 6.7) respectively. In the B($\perp$) bands there is no Q-branch and the dip between P and R branches is quite characteristic. In the C($\perp$) bands the Q-branch is prominent and, while the R-branch shows a distinct peak the P branch appears only as a shoulder to the Q-branch. This knowledge about the characteristic shapes has been used to identify the bands at 684.6 and 902.3 cm^{-1} as C($\perp$) bands (Cf. Figure 3.2A); although, their R peaks are lost due to overlap by other bands. Similarly, the spectrum in the range 350-380 cm^{-1} is analysed into two B-type bands, as shown in Figure 6.4 (i).

The PR separations in the 10 bands of B-type (Cf. Appendix 3.1) are experimentally found to range from 9.4 to 11.6 cm^{-1}, whereas the value computed by using equation (6.10) comes to 8.84 cm^{-1}. This discrepancy is well outside the range of

experimental error (Seth-Paul and Dijkstra's (9-10) expressions for $\bar{B}$ and $\bar{\beta}$ give the computed value as 8.77 cm^{-1}). In fact even the range of variation of experimental value from 9.4 to 11.6 cm^{-1} may not be wholly on account of uncertainty in location of the band peaks. It is notable that as in A(||) bands, in B($\perp$) bands also the PQ separation comes out greater than QR separations in all cases except in one band at 1296.3 cm^{-1} (Cf. Appendix 3.1).

For C($\perp$) bands evaluation of PR separation is subject to large uncertainty because the P branch appears only as a shoulder, and in most of the observed bands in this spectrum the R-branch is overlapped by other bands. For three of the C-type bands we could obtain estimates of $\Delta\nu_{PR}$ as $\sim$15 cm^{-1}, whereas computed value comes to 15.9 cm^{-1}.

K. BAND CONTOURS IN BENZALDEHYDE AND PHENOL

It is clear from Table 6.1 that for most of the A- and B-type contours the calculated and observed PR separations agree within the experimental limitations. In some cases the divergence is, however, large and one must either reexamine the assignment or look for hybridization effects. Those of the A- and B- type bands which show large divergence in PR separations have been marked with an asterisk (*) in Table 6.1. On examining their detailed assignments (20-25) we find that many of these bands pertain to localized modes, in which the change in the direction of dipolemoment are neither parallel to A nor to B axis; and the deviations of $\Delta\nu_{PR}$ values would largely be explained by considering the AB hybridization effects (11). We have calculated the

PR separation for the well established (20-25) hybrid bands using our simple formula given by equation 6.13 and listed the values in Table 6.4. The good fit between the observed and calculated PR separations provides an additional evidence for their correct assignments.

The $\Delta\nu_{PR}$ deviations in non-localized modes could be used to estimate the direction of the change in effective dipole moment.

Present study also indicates that in some cases where the $\Delta\nu_{PR}$ value of a band assigned as B-type is close to that expected for an A-type band, the older assignment (23) would need to be reexamined. The band at 1021 cm^{-1} in C_6D_5OH falls in this last category (23).

L. RATIO I_Q/I_{Total}

The observed I_Q/I_{Total} ratio 'r' (Cf. section H) for all those bands which exhibit a Q branch is given in column 4 of Table 6.1. Using the modified (Section D(iii)) formula of Gerhard and Dennison (3) for parallel type bands, the calculated values of this ratio for all the molecules are given in column 10 of Table 6.2. The ratios are also given against the A-type bands alone in columns 5 of Table 6.1. For the A-type bands there is a satisfactory agreement of the observed 'r' values (within the experimental limitations mentioned earlier) with those calculated from modified equation 6.5. Thus, our modification of the expression, suggested by Gerhard and Dennison (3), for the parallel bands of the symmetric top molecules, is justified for

the near symmetric top molecules. However, for the C-type bands no theoretical expressions are available to calculate the ratio 'r' due to the inherent difficulties in exact evaluation of the complex integrations involved in such calculations. Progress in this direction can be made by making some plausible approximations for these calculations, if sufficiently accurate experimental data are available for justifying such assumptions. Our observed values of 'r' for few representative bands are consistent to better than $\pm$ 10%. However, the large inherent uncertainty ($\pm$ 20%) in evaluation of I_Q/I_{Total} would hardly justify the use of such ratio to deduce the asymmetry parameter especially by choosing a solitary band from a complex spectrum (8). We note that the ratio 'r' is larger for C($\perp$) bands as compared to A($\parallel$) bands. Further work will be necessary to draw any definite conclusions from the intensity ratios in the C($\perp$) bands.

M. REFERENCES

1. R.S. Mulliken; J. Chem. Phys. 23, 1997 (1955).
2. G. Herzberg, "Molecular Spectra and Molecular Structure I: Diatomic Molecules", Prentice-Hall, New York (1939).
3. S.L. Gerhard and D.M. Dennison, Phys. Rev., 43, 197 (1933).
4. H.C. Allen and P.C. Cross, "Molecular Vib-Rotors", John Wiley and Sons, Inc., New York 1963.
5. S.C. Wang, Phys. Rev. 34, 243 (1929).
6. R.M. Badger & L.R. Zumwalt, J. Chem. Phys. 6, 711 (1938).
7. J.M. Hollas, Spectrochim. Acta 22, 81 (1966).
8. L.A. Franks and K.K. Innes, J. Chem. Phys. 47, 863 (1967).
9. W.A. Seth-Paul and G. Dijkstra, Spectrochim. Acta. 23A, 2861 (1967).
10. W.A. Seth-Paul, J. Mol. Structure 3, 403 (1969).
11. W.A. Seth-Paul and H. De Meyer, J. Mol. Structure 3, 11 (1969).
12. W.A. Seth Paul and H. De Meyer, Spectrochim. Acta, 25A, 1671 (1969).
13. V.N. Sarin, H.D. Bist and D.P. Khandelwal, Spectrochim. Acta (Communicated) 1970.
14. V.N. Sarin, M.M. Rai, H.D. Bist and D.P. Khandelwal, Chem. Phys. Letters 6, 473 (1970).
15. T. Kojima, C.R. Quade and C.C. Lin, quoted in Landolt Bernstein Numerical Data, group 2, Vol. 4, Springer-Verlag, Berlin (1967). Also T. Kojima Private communication to Dr. H.D. Bist (1969).
16. R.L. Poynter, J. Chem. Phys. 39, 1962 (1963).
17. H. Forest and B.P. Dailey, J. Chem. Phys. 45, 1736 (1966).
18. T. Kojima, Pvt. communication to Dr. H.D. Bist (Jan. 1967).
19. T. Kojima, J. Phys. Soc. Japan 15, 284 (1960).
20. H.D. Bist, J.C.D. Brand and D.R. Williams, J. Mol. Spectry. 21, 76 (1966).

21. H.D. Bist, J.C.D. Brand and D.R. Williams, J. Mol. Spectry, 24, 402 (1967).

22. H.D. Bist, J.C.D. Brand and D.R. Williams, J. Mol. Spectry. 24, 413 (1967).

23. J.C. Evans, Spectrochim. Acta 16, 1382 (1960), and references cited earlier.

24. H.D. Bist, V.N. Sarin, A. Ojha and Y.S. Jain, Spectrochim. Acta, 26A, 841 (1970).

25. Y.S. Jain and H.D. Bist, Spectrochim. Acta (communicated).

TABLE 6.1

The Q-band peaks, observed and calculated PR separations and I_Q/I_{Total} for A(||), B(⊥) and C(⊥) bands of a few near prolate symmetric top molecules

Frequency (cm^{-1})		PR separation (cm^{-1})		I_Q/I_{Total}	
		Obs.	Calc.	Obs.	Calc.
			C_6H_5Cl		
294.8,	B*	10.0	8.8		
416.8,	A	10.4	10.6		0.17
466.9,	C	15	15.9	0.25	
559.1,	A	10.5	10.6		0.17
684.6,	C*	14	15.9	0.25	
706.0,	A	11	10.6	0.16	0.17
740.6,	C	15	15.9	0.23	
806.0,	A	10.6	10.6	0.17	0.17
1003.3,	A	10.4	10.6		0.17
1025.4,	A	10.6	10.6	0.17	0.17
1091.6,	A	10.8	10.6	0.18	0.17
1126.0,	A	10.5	10.6		0.17
1175.5,	A	9.8	10.6	0.16	0.17
1208.0,	A	10.0	10.6	0.17	0.17
1232.0,	A	11.0	10.6	0.19	0.17
(1270.5),	B*	10.0	8.8		
(1296.3),	B*	11.0	8.8		
(1448.0),	B*	10.5	8.8		
1483.5,	A	10.8	10.6	0.18	0.17
1729	B*	9.4	8.8		
3082.0	A	11.0	10.6		0.17
			C_6H_5CHO		
450.3,	C	15	15.9	0.31	
650.0,	B	10.1	8.8		
688.0,	C	14	15.9	0.23	
825.3,	A	10.7	10.6	0.18	0.18
1003.0,	A	10.5	10.6	0.22	0.18
1024.8,	A	10.8	10.6	0.17	0.18
(1071.0),	B	8.4	8.8		
1167.0,	A	10.3	10.6	0.18	0.18
1313.1,	B*	10.0	8.8	0.18	
1386.6,	B*	9.8	8.8	0.18	
(1459.4),	B	8.8	8.8		

Contd. ...

1		2	3	4	5
			C_6H_5OH		
309.6,	C	21	21.2	0.25	
402.9,	B*	13.6	11.1	0.20	
503.0,	C	21.0	21.2	0.23	
526.4,	A	15.0	14.1	0.16	0.22
686.0,	C	19.7	21.2	0.24	
751.2,	C	20.3	21.2	0.25	
809.8,	A	12.2	14.1	0.16	0.22
823.2,	A	13.0	14.1	0.18	0.22
881.2,	C	20.4	21.2	0.25	
998.9,	A	13.7	14.1	0.14	0.22
1025.6,	A*	13.0	14.1	0.19	0.22
1057.0,	A	14.0	14.1	0.18	0.22
1069.5,	B	11.4	11.1	0.15	
1343.5,	B*	13.5	11.1	0.15	
1471.5,	B*	13.3	11.1	0.20	
1501.2,	A	14.5	14.1	0.22	0.22
3655.5,	A*	12.1	14.1	0.25	0.22
			C_6D_5OH		
307.4,	C	19	20.4	0.31	
386.4,	B*	13.8	10.6	0.24	
551.3,	C	19	20.4	0.31	
753.7,	A	13.2	13.6	0.22	0.23
1020.8,	B	13.4	10.6	0.20	
1178.6,	A	12.3	13.6	0.20	0.23
1236.7,	B	10.2	10.6	0.19	
1372.5,	B*	13.1	10.6	0.20	
3656.2,	A	12.0	13.6		0.23
			C_6H_5OD		
686.7,	C	20.4	20.7	0.26	
751.4,	C		20.7	0.22	
917.3,	A*	13.5	13.8	0.19	0.22
1499.6,	A	13.2	13.8	0.20	0.22
2699.8,	A*	12.5	13.8	0.18	0.22

*Indicates the hybrid or overlapped band.
Blank space indicates overlapped or weak band

TABLE 6.2

Rotational Parameters and calculated PR separations at 300°K for the infrared band contours of monosubstituted benzenes

Molecules	A (Mc/Sec.)	B (Mc/Sec.)	C (Mc/Sec.)	$\bar{B}$ (Mc/Sec.)	$\bar{\beta}$	$S(\bar{\beta})$	PR separation (in cm^{-1}) B(⊥)	PR separation (in cm^{-1}) A(∥)	I_Q/I_{Total}
(-0.82135) C_6H_5CHO	5224.6	1564.6	1205.6*[a]	1385	2.772	1.211	8.8	10.6	0.180
(-0.84542)† C_6H_5Cl	5572.950	1576.774	1233.672[b]	1405	3.037	1.201	8.8	10.6	0.173
(-0.46470) C_6D_5OH	4582.77	2422.815	1596.930[c]	2010	1.330	1.285	10.6	13.6	0.232
(-0.59376) C_6H_5OD	5609.25	2528.43	1743.15[d]	2136	1.626	1.266	10.9	13.8	0.216
(-0.57036) C_6H_5OH	5650.450	2619.190	1789.843[e]	2205	1.563	1.270	11.1	14.1	0.222

*The rotational constants A, B and C tabulated here are from microwave data: a - Ref. (15); b - Ref. (16); c - Ref (17); d - Ref. (18) and e (Ref. 19).

†Number in parentheses is the value of asymmetry parameter of the molecule.

TABLE 6.3

PQ and QR separations (in cm^{-1}) in clean A(||)-type bands of chlorobenzene and their ratio

Frequency (in cm^{-1})	Separation		Ratio
	PQ	QR	(PQ)/(QR)
706.0	6.5	4.5	1.44
806.0	6.0	4.6	1.30
1025.4	6.0	4.6	1.30
1091.6	6.2	4.6	1.35
1175.5	5.0	4.8	1.04
1232.0	6.0	5.0	1.20
1483.5	6.5	4.3	1.51

TABLE 6.4

Calculated and observed PR separations of hybrid bands of benzaldehyde and phenol-h_6

Compound	Vibrational mode	Frequency (in cm^{-1})	Angle α*	PR separations of A/B hybrid bands in cm^{-1}		Remarks
				Obs.	Calc.	
C_6H_5CHO (Benzaldehyde)	aldehydic CH stretch	2731	72°	10.5	10.2	
	aldehydic CH bend	1386.6	15°	10.0	9.1	
	CO stretch	1727.0	45°	?	9.7	Contour not resolved
	CHO rocking	650.0	50°	11.0	9.8	overlapped band
C_6H_5OH (Phenol-h_6)	OH stretch	3655.5	62°	12.1	12.6	
	OH bend	1175.7	28°	?	11.5	overlapped band

* For stretching vibrations the change of dipole moment is assumed parallel to the bond, so 'α' is the angle between the bond and the 'z-axis' shown in Figure 4.4 and 5.2. For bending vibrations the change of dipole moment is assumed perpendicular to the bond, so 'α' is the angle between the normal to the bond involved and the 'z-axis' of the molecule.

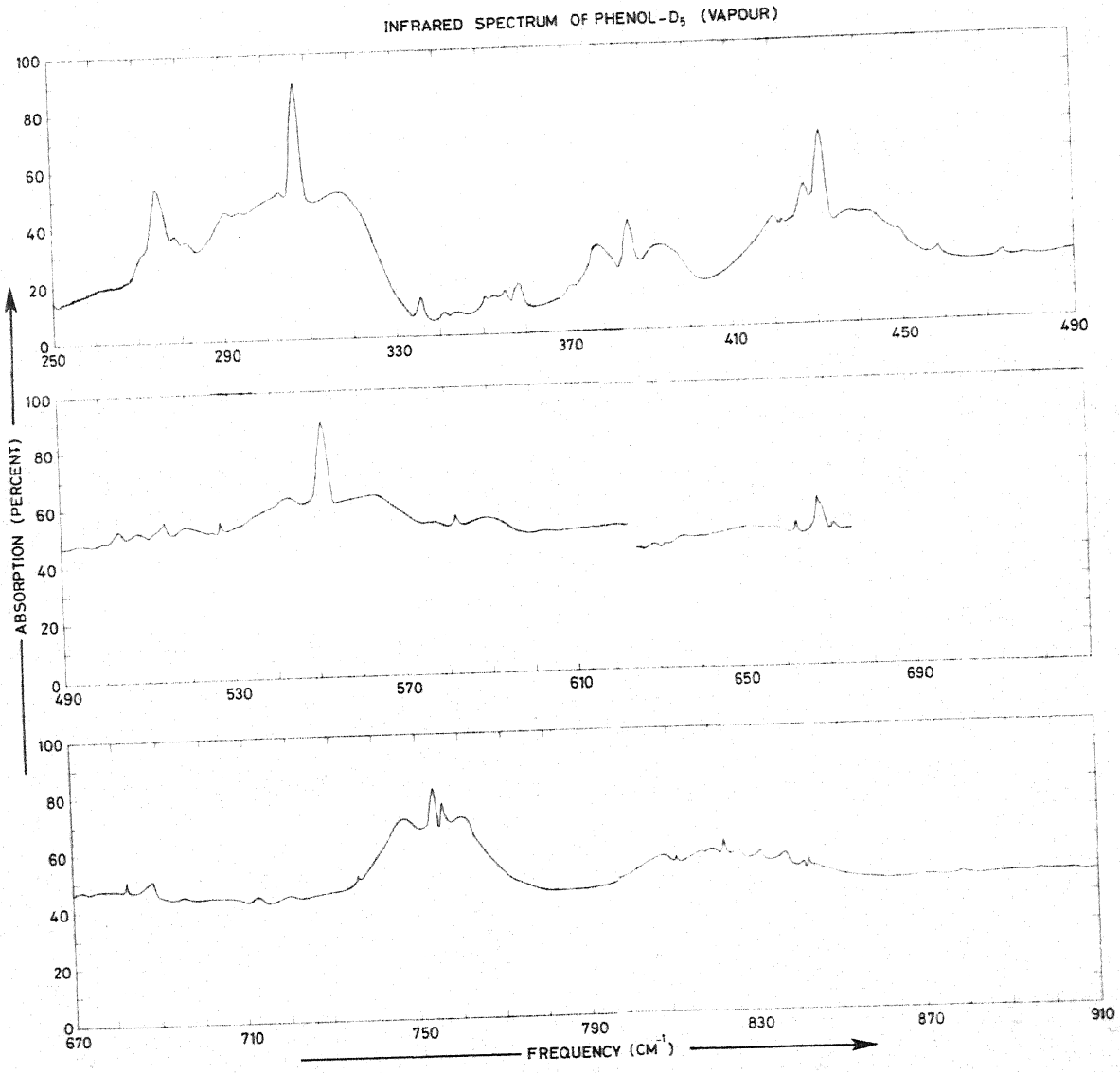

Fig. 6.1A The infrared spectrum of phenol-d_5 in the vapour phase (with 5 meter path and saturated vapour pressure at 22°C) for range 200-910 cm^{-1}.

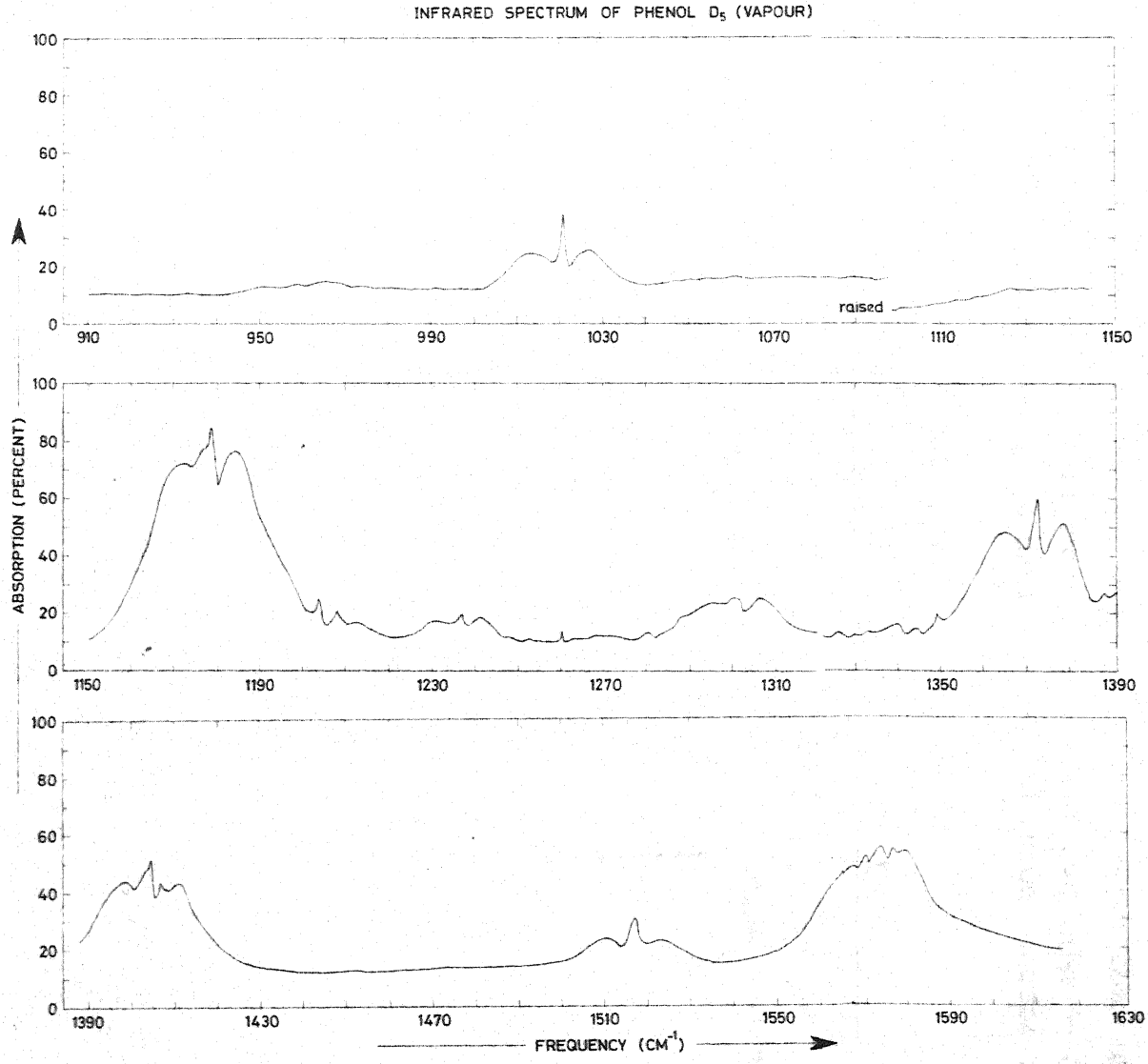

Fig. 6.1B The infrared spectrum of phenol- d_5 in the vapour phase (with 5 meter path and saturated vapour pressure at 22°C) for range 910 - 1700 cm^{-1}.

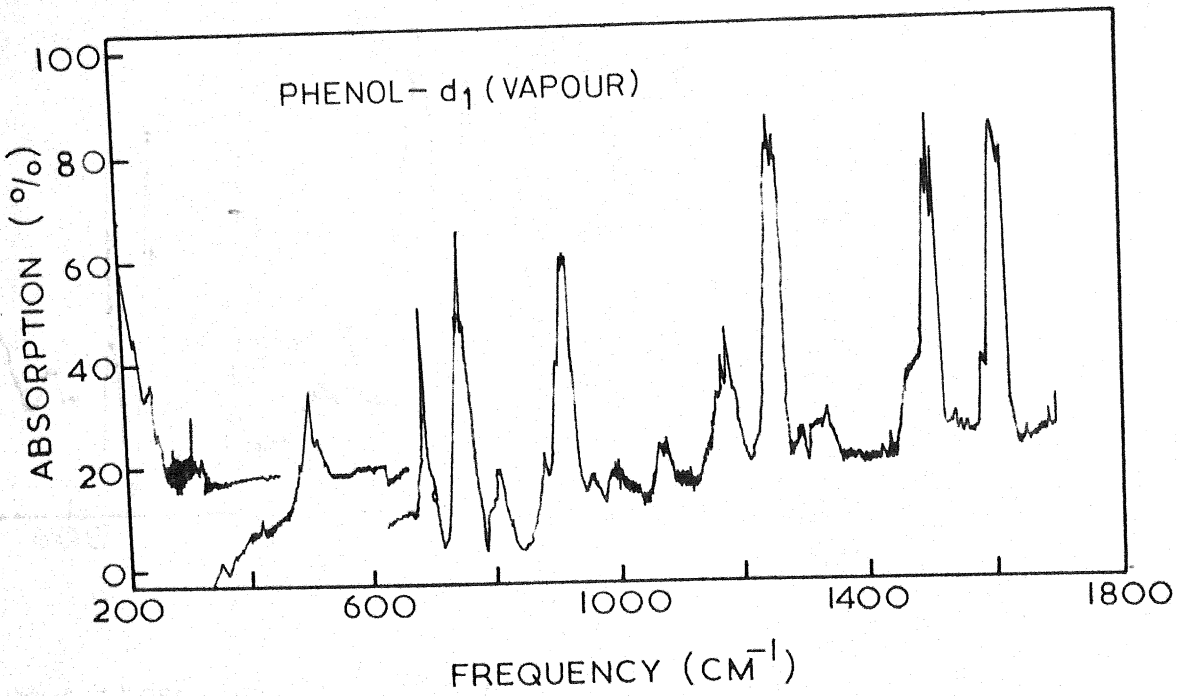

Fig.6.2 The vapour phase infrared spectrum of phenol-d_1 for range 200 —— 1800 Cm^{-1} at ~ 0.3 mm vapour pressure and 5 meter path length.

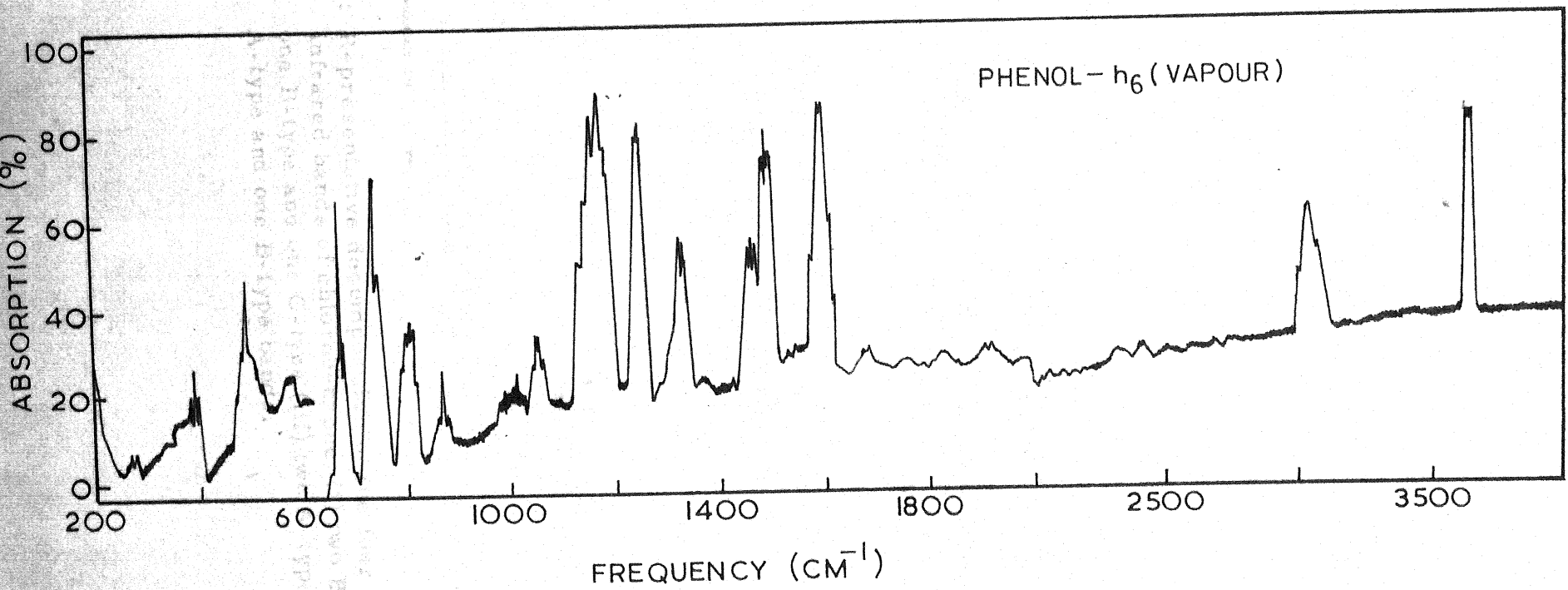

Fig.6.3 The vapour phase infrared spectrum of phenol – h_6 for range 200 — 4000 Cm^{-1}, at 0.272 mm pressure and 5 meter path length.

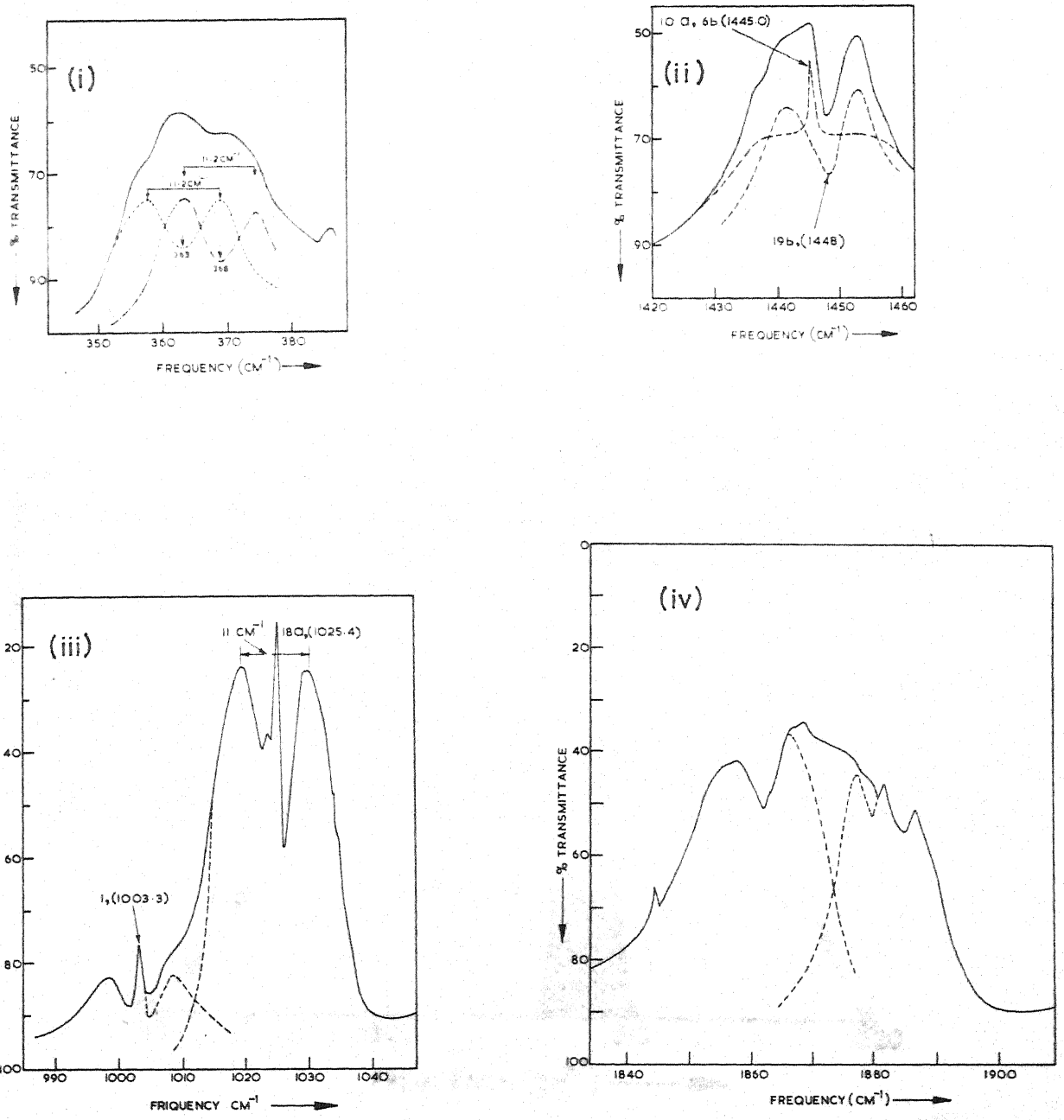

Fig. 6.4: Representative decomposition of the four composite infrared bands of chlorobenzene: (i) two B-type (ii) one B-type and one C-type (iii) two A-type and (iv) one A-type and one B-type bands.

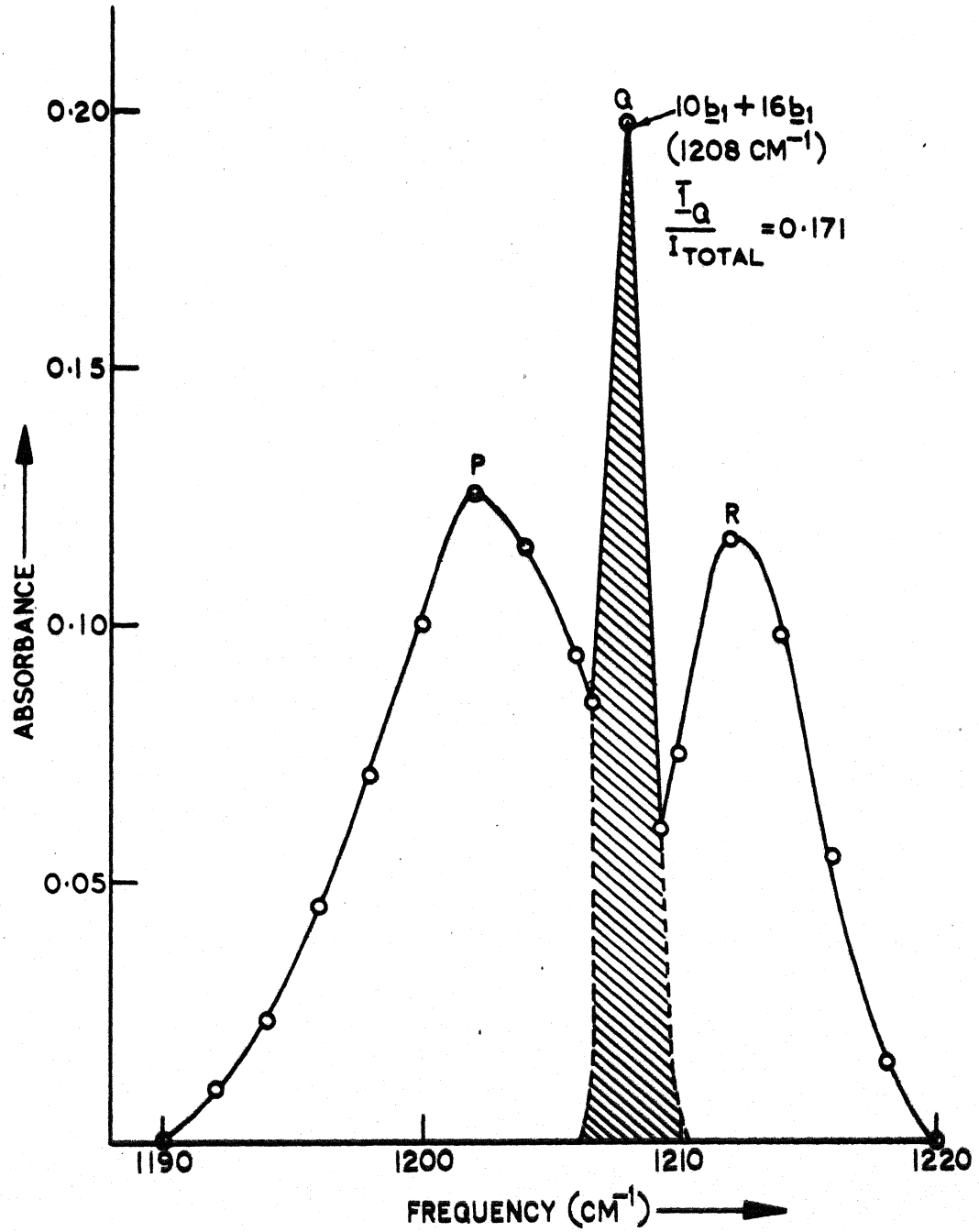

Fig. 6.5: Representative curve for calculating I_Q/I_{Total} in an A-type band. Shaded portion indicates the area attributed to Q branch.

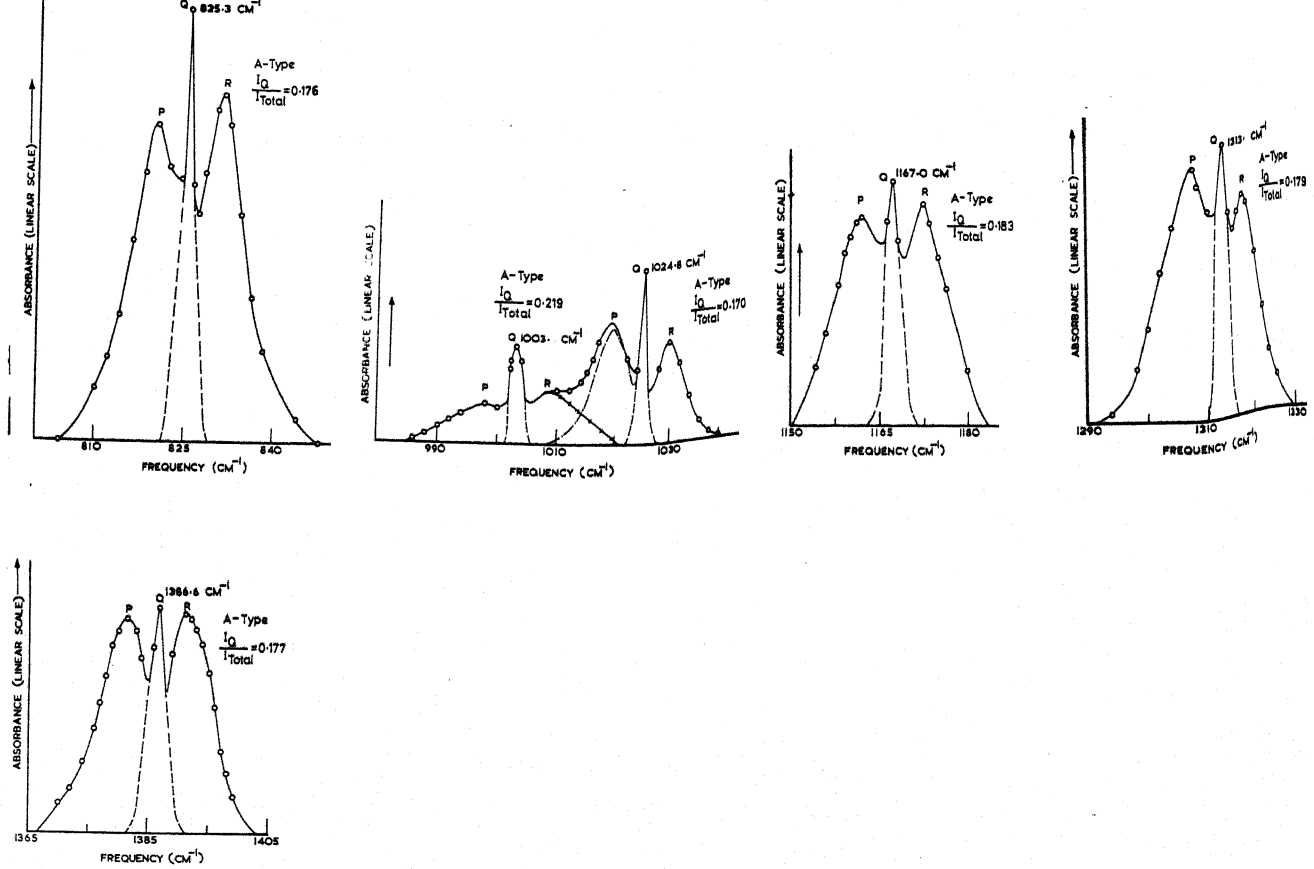

Fig. 6.6: Typical A and C-type infrared bands of benzaldehyd The 648.9 cm^{-1} band is regarded as a B-type band with PQQR structure.

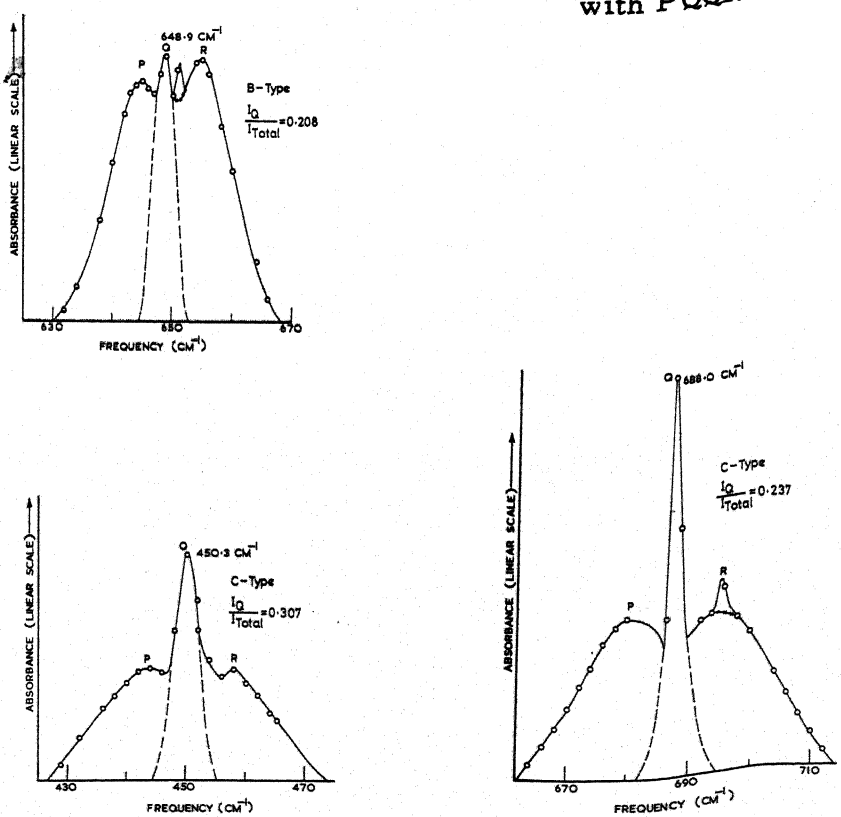

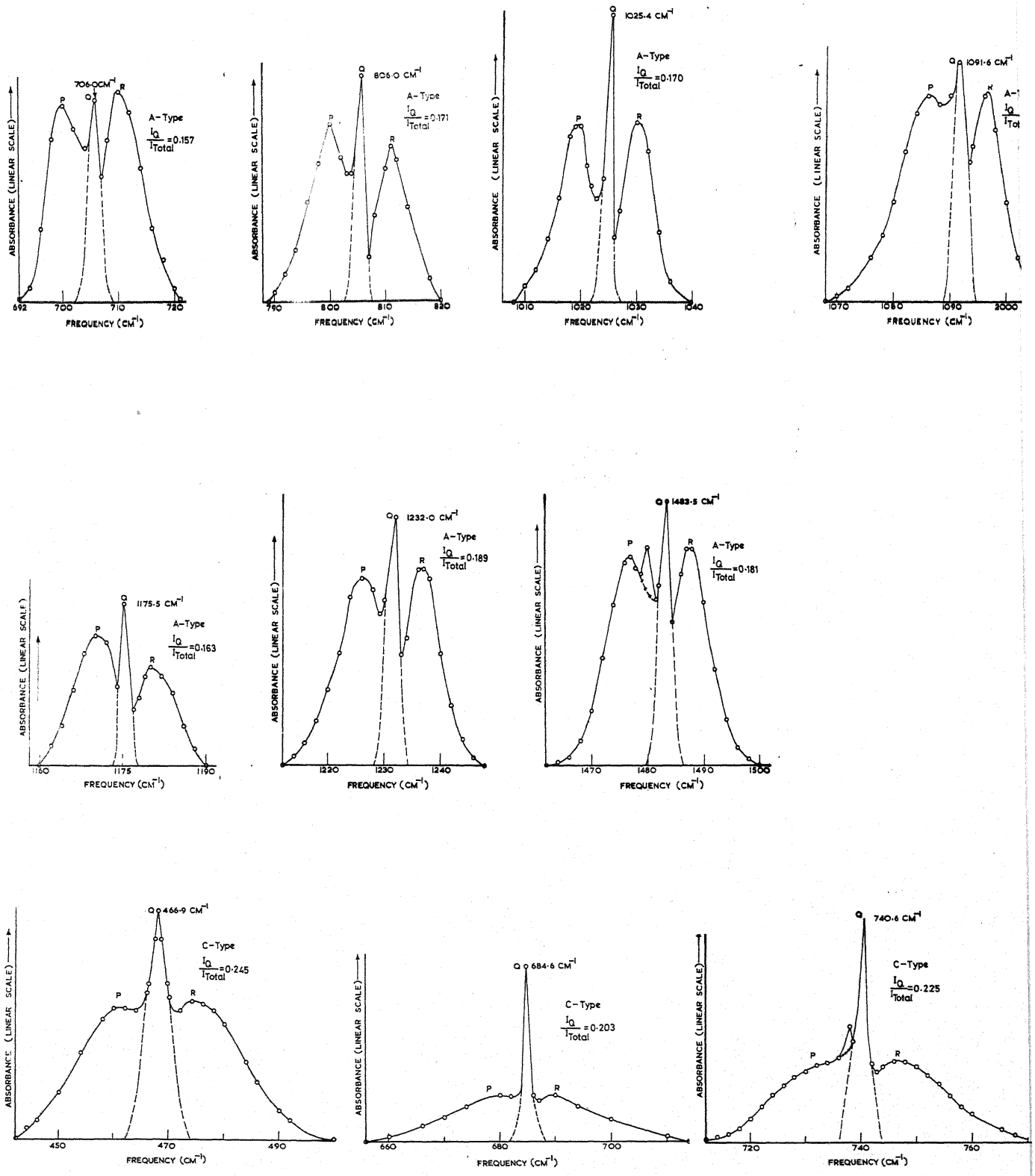

Fig. 6.7: A and C-type infrared bands of chlorobenzene.

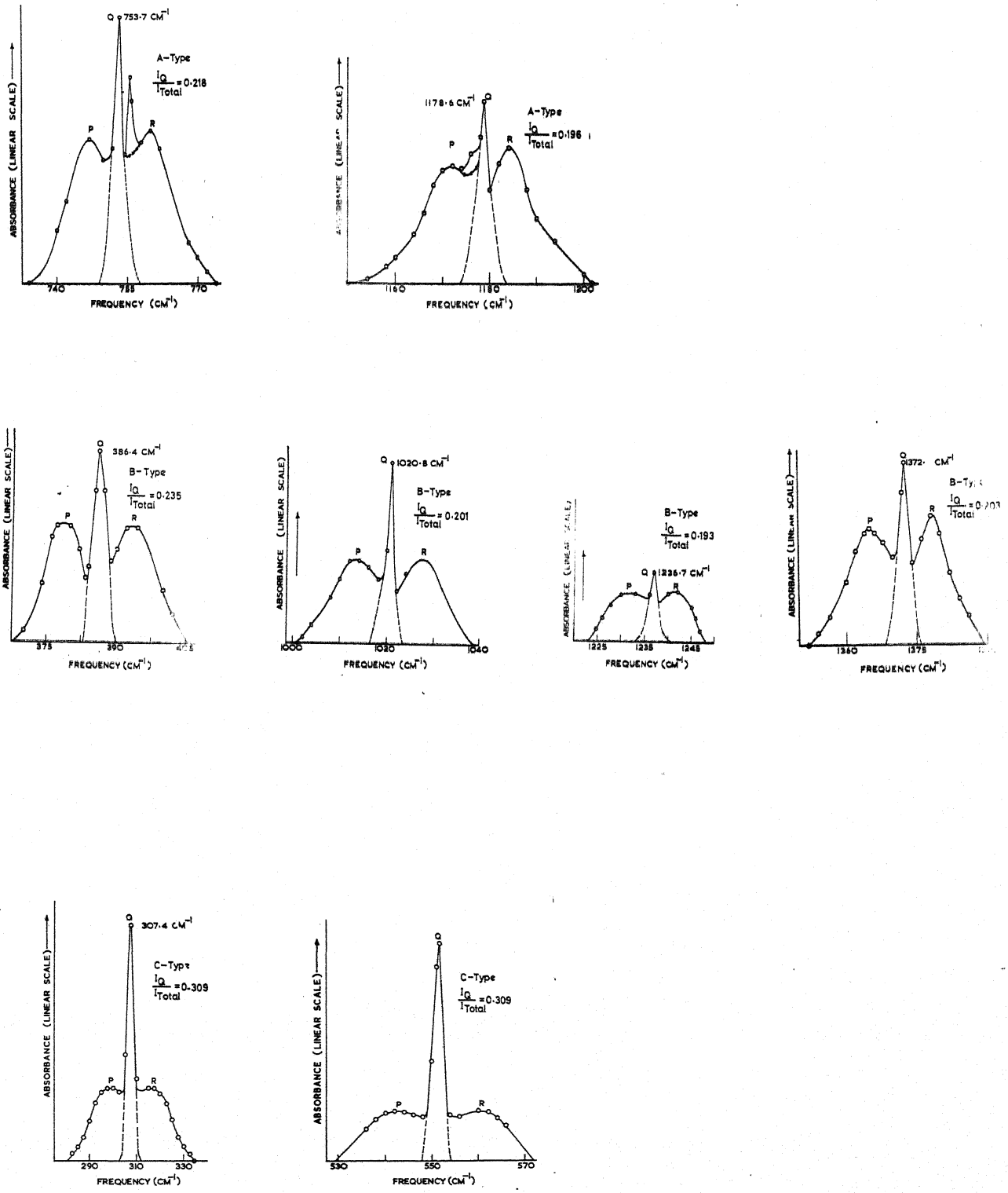

Fig. 6.8: A, B and C-type infrared bands of phenol-d_5.

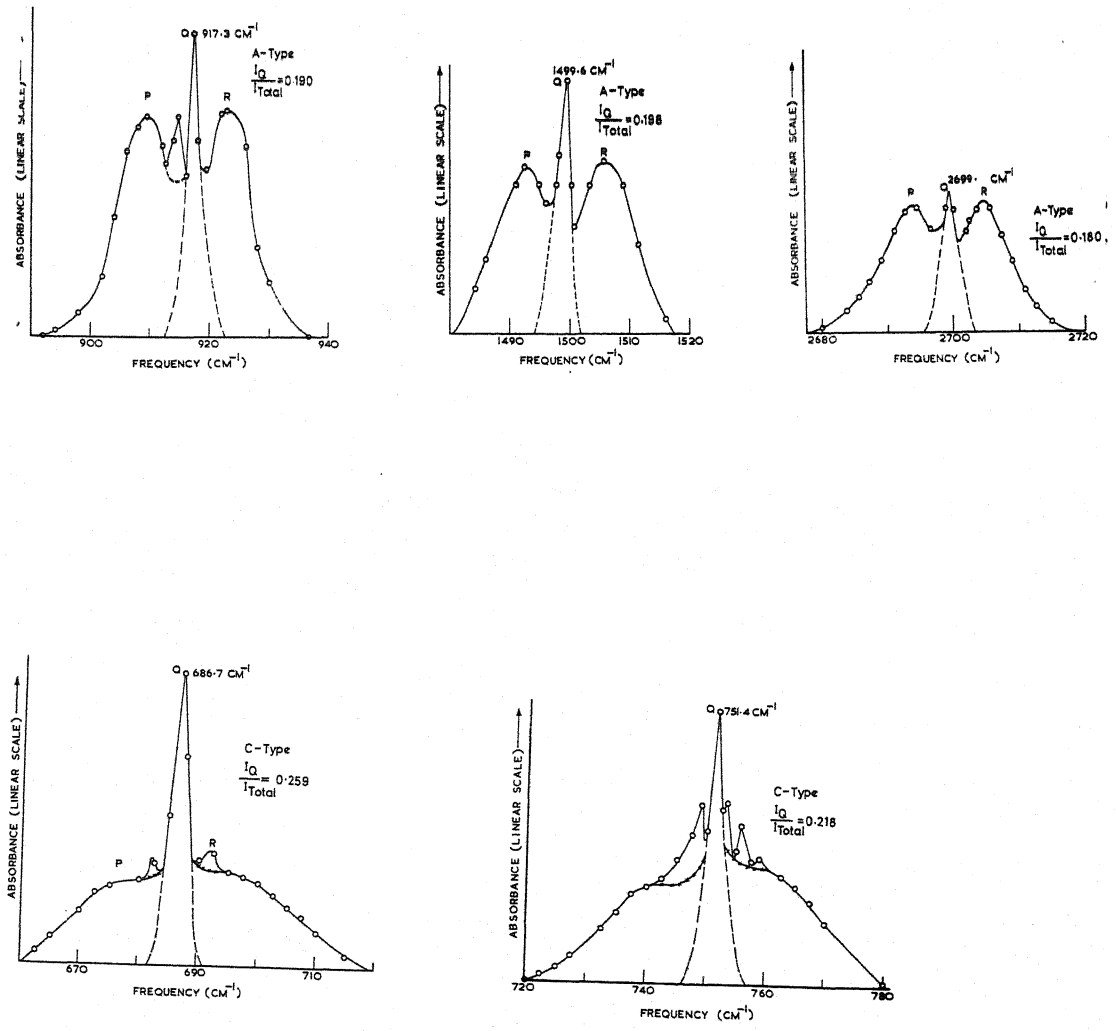

Fig. 6.9: A and C-type infrared bands of phenol-d_1.

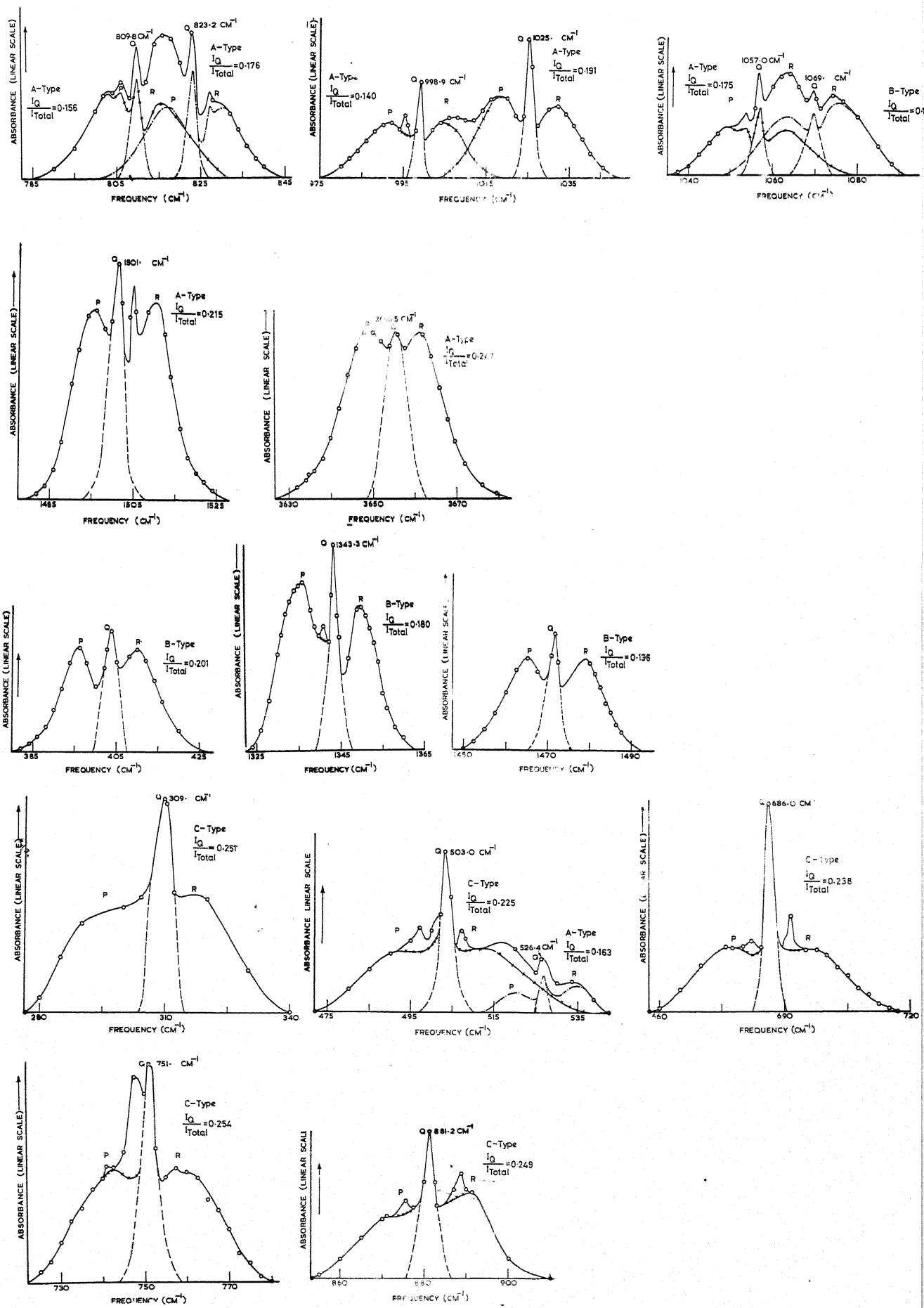

Fig. 6.10: A, B and C-type infrared bands of phenol - h$_6$

APPENDIX 6.1

Vapour phase vibrational frequencies (in cm^{-1}) of $-d_5$, $-d_1$ and $-h_6$ isotopic species of phenol; and the assignments of bands with the peak positions of P,Q and R branches

Phenol-d_5 C_6D_5OH		Phenol-d_1 C_6H_5OD		Phenol-h_6 C_6H_5OH		Remarks
1		2		3		4
274.2						
275.7						OH Torsion (2 ← 1)
299.0	P			297	P	
307.4	Q	246		309.6	Q	C, OH Torsion (1 ← 0)
318	R			321	R	
379.5	P	374.8	P	395.3	P	
386.4	Q	382.5	Q	402.9	Q	B, 18b, X-sensitive
393.3	R	396	R	408.9	R	
		403		462		
		418.7		469		16b-17a
		423.3		473		
420	P	488	P	492	P	
426.7		498		497		
				501		
430.6	Q	503.3	Q	503.5	Q	C, 16b, X-sensitive;
				507.2		overlapped band
439	R	507.4	R	513	R	
		514	P	520	P	
448.5		521.5	Q	526.4	Q	A, 6a, X-sensitive
		527	R	534.5	R	
				581	P	
				588	Q	2 Torsion
				592	R	
(594.9)		618.7		618.7		6b, ring
543	P	676.4	P	676.7	P	
		682.1		682.0		
551.3	Q	686.7	Q	686.0	Q	C, 4, CC Twist, overlapped
		692.3		691.3		band
562.0	R	696.8	R	696.4	R	

Contd. ...

1		2		3		4
681	P	741	P	740.8	P	
		748.5		744.5		
				748.2		
686.5	Q	751.4	Q	751.2	Q	C, 10b, CH bend;overlapped
		753.2		756.8		band
		755.7				
		758.5				
696	R	761	R	761.1	R	
				803.0	P	
				806.0		
				809.8	Q	A, overtone of 18b
				815.2	R	
747.0	P	801	P	817.5	P	
753.7	Q	805.0	Q	823.2	Q	A, 12, X-sensitive
755.8		809.7		827.2		
760.2	R	813.3	R	830.5	R	
806	P	819.6	P			
812	Q	823.0	Q			16b + 18b;(C_6D_5OH)
818	R	828	R			
		873	P	871.0	P	
				875.3		
(720.0)		880.8	Q	881.2	Q	17b, CH bend
				888.6		
		890	R	891.4	R	
				904.4		16b + 18b
		934.2				
		940		950.8		16a + 6a
		959.3	P			
(825.1)		964.4	Q	973.0		5, CH bend
		970	R			
		991	P	991.3	P	
		993.5		995.4		Torsion + 4
960		996.6	Q	998.9	Q	1, ring
		995.5				
		1005.5	R	1006.0	R	
				1050	P	
				1053.7		Overtone of 6a
				1057.0	Q	10b + OH Torsion
				1064	R	

Contd. ...

1	2	3	4
(810.9)	1065 P (1072) 1079 R	1064 P 1069.8 Q 1075.0 R	15, CH bend
		1094 P 1099.5 1102.8 Q 1105 1109 R	16b + 6b ?
(831.2)	1142.4 P 1149.7 Q 1159.0 R	1142.6 P 1149.6 Q 1156.0 R	B**, 9b, CH bend
(879.1)	1161.0 P 1167.6 Q 1173.0 R	1168.4	9a, CH bend
1171.5 P 1178.6 Q 1183.8 R	909.5 P 914.7 917.3 Q 923 R	1170.4 P 1175.7 Q 1183.5 R	OH or OD bend
	1171 P 1175.6 Q ? 1182.6 R	1191.0 P 1197.5 Q 1202 R	4 + 16b; (C_6H_5OH)
	1190.6 P 1197.2 Q 1203.4 1206 R		4 + 16b; (C_6H_5OD)
1231.0 P 1236.7 Q 1241.2 R		1244 P 1251.2 Q 1253.4 R	10b - 16b
1187	1248 P 1257.4 Q 1262 R	1255 P 1261.4 Q 1267.8 R	7a, X-sensitive
1013.4 P 1020.8 Q 1026.8 R		(1277.4)	B, 3, CD bend
		1318.6 1324.6 1326.0 1324	16b + 12

**A,B, and C denote the types of band contour (Cf. Chapter VI).